ACCELERATED GRADIENT METHODS WITH BIASED GRADIENT ESTIMATES: RISK SENSITIVITY, HIGH-PROBABILITY GUARANTEES, AND LARGE DEVIATION BOUNDS

MERT GÜRBÜZBALABAN^{1,3}, YASA SYED¹, NECDET SERHAT AYBAT²

¹Department of Statistics, Rutgers University, Piscataway, NJ, USA
²Department of Industrial Engineering, Pennsylvania State University, University Park, PA, USA
³Department of Management Science & Information Systems, Rutgers University, Piscataway, NJ, USA

Abstract. We study trade-offs between convergence rate and robustness to gradient errors in the context of first-order methods. Our focus is on generalized momentum methods (GMMs)—a broad class that includes Nesterov's accelerated gradient, heavy-ball, and gradient descent methodsfor minimizing smooth strongly convex objectives. We allow stochastic gradient errors that may be adversarial and biased, and quantify robustness of these methods to gradient errors via the risk-sensitive index (RSI) from robust control theory. For quadratic objectives with i.i.d. Gaussian noise, we give closed form expressions for RSI in terms of solutions to 2×2 matrix Riccati equations, revealing a Pareto frontier between RSI and convergence rate over the choice of stepsize and momentum parameters. We then prove a large-deviation principle for time-averaged suboptimality in the large iteration limit and show that the rate function is, up to a scaling, the convex conjugate of the RSI function. We further show that the rate function and RSI are linked to the H_{∞} -norm—a measure of robustness to the worst-case deterministic gradient errors—so that stronger worst-case robustness (smaller H_{∞} -norm) leads to sharper decay of the tail probabilities for the average suboptimality. Beyond quadratics, under potentially biased sub-Gaussian gradient errors, we derive non-asymptotic bounds on a finite-time analogue of the RSI, yielding finite-time high-probability guarantees and non-asymptotic large-deviation bounds for the averaged iterates. In this more general scenario of smooth strongly convex functions, we also observe an analogous trade-off between RSI and convergence-rate bounds. To our knowledge, these are the first non-asymptotic guarantees for GMMs with biased gradients and the first risk-sensitive analysis of GMMs. Finally, we provide numerical experiments on a robust regression problem to illustrate our results.

Keywords. momentum methods, accelerated gradient methods, stochastic optimization, biased stochastic gradients, risk sensitivity, high-probability bounds, robustness to gradient errors

1. Introduction

First-order optimization algorithms form the backbone of modern large-scale optimization, underpinning recent advances across a range of disciplines, including machine learning, signal processing and statistics [1, 2, 3, 4, 5, 6]. These methods are often the preferred computational approach for obtaining low- to medium-accuracy solutions to large-scale problems, owing to their inexpensive iterations and relatively mild dependence on problem dimension and data size.

Traditional analyses of first-order methods assume exact gradient information and focus on characterizing the convergence rate of the iterate sequence using a properly defined metric. Within the family of first-order methods, gradient descent (GD) is a fundamental algorithm, widely regarded as the canonical baseline [7]. Momentum-based accelerations—such as Polyak's heavy-ball (HB) method [8], Nesterov's accelerated gradient (NAG) [9], and more recent triple-momentum methods

^{*}The authors can be contacted at: mg1366@rutgers.edu (M. Gürbüzbalaban), yasa.syed@rutgers.edu (Y. Syed), nsa10@psu.edu (N. S. Aybat).

(TMM) [10, 11, 12]—offer faster convergence under convexity and smoothness assumptions when exact gradients are available. In practice, however, gradient information is rarely exact and typically contains stochastic or deterministic errors.

Deterministic errors commonly arise from finite-precision arithmetic in numerical computations. They can also result from approximating gradients by solving auxiliary problems [13, 14], or by using approximation methods based on finite-differences [15]. Moreover, such errors frequently appear in algorithms that cycle through data points, e.g., incremental gradient methods [16, 17]. On the other hand, stochastic errors also naturally occur in large-scale optimization, data science and machine learning settings. These arise commonly, including (i) when stochastic noise is deliberately added to gradient computations to preserve data privacy, as in differentially private optimization [18]—for example, [19] explores such mechanisms in the context of empirical risk minimization; and (ii) when gradients are estimated from mini-batches, i.e., using sample averages over randomly selected data subsets, a standard practice in large-scale or streaming environments, as in stochastic gradient and stochastic approximation methods [20, 21]. Such errors often exhibit Gaussian or sub-Gaussian behavior, particularly when gradient estimates are bounded or when the batch size is sufficiently large to invoke Central Limit Theorem-type arguments [22, 23].

Gradient errors, when they are stochastic, may be unbiased—having zero mean when conditioned on the iterates computed so far [21, 24]—as in the case of uniform sampling of data points with replacement within stochastic gradient descent methods or in differentially private optimization settings where centered noise is added to the gradients for data privacy reasons [2, 18]. However, in many practical scenarios, the errors may be biased containing a drift: (i) when the data points are dependent or when the data points are sampled with techniques that can invoke bias such as without-replacement sampling, random reshuffling, or biased-variance reduction mechanisms [25, 26, 27, 28, 29, 30, 31]; (ii) when the gradients are compressed or quantized [32, 33, 34, 35, 36]; (iii) when the stochastic gradients are clipped or normalized [37, 38, 39, 40]; (iv) in the context of inexact inner solves arising in machine learning applications such as robust learning [41, 42]. reinforcement learning, and meta-learning [43, 44, 45]; (v) finite-precision arithmetic errors or errors due to smoothing of the objective when estimating the gradients [46, 15]; (vi) in adversarial learning settings when deterministic perturbations are added to the data points when computing stochastic gradients that depend on the data points [47, 48]. Because such biased errors accumulate over time. classical analyses that assume unbiased stochastic noise can mispredict performance and fail to quantify robustness of the underlying first-order method to gradient errors.

When gradient errors are persistent or decay slowly, the iterates may fail to converge—oscillating around the optimal solution, deviating significantly before eventually converging, or even diverging entirely [16, 17, 14, 49]. Robustness—understood as sensitivity to gradient errors and quantified by an appropriate solution-accuracy metric—is therefore a critical performance criterion [14, 50]. In particular, while momentum-based methods such as NAG, HB, and TMM are known to converge faster than the standard GD in noise-free settings for convex or strongly convex problems, they are generally less robust to gradient errors [14, 13, 49, 51]. As a result, designing effective algorithm parameters requires a careful understanding of the trade-offs between convergence speed and robustness.

Existing robustness analyses of momentum methods have primarily concentrated on two extremes. On one end, a growing line of work investigates stochastic, unbiased noise, establishing mean-square or high-probability convergence guarantees under light-tailed assumptions (e.g., [52, 53, 54, 55, 56]). On the other end, control-theoretic approaches employ the H_{∞} -norm to characterize worst-case deterministic gradient errors [57], thereby modeling the gradient as deterministically biased. However, H_{∞} -based analyses usually ignore stochastic variability and typically do not provide high-probability guarantees on the iteration complexity for obtaining approximate solutions under stochastically biased gradients.

Only a handful of recent studies have addressed biased stochastic gradient errors in the context of momentum-accelerated methods; however, this line of research remains limited—even for convex and strongly convex optimization problems that are typically easier to analyze compared to non-convex problems. In particular, to the best of our knowledge, no existing work provides non-asymptotic high-probability or large-deviation guarantees for the iterates of momentum methods in the presence of both stochastic and deterministic bias, in the strongly convex setting. To bridge this gap, we focus on the strongly convex and smooth minimization setting, and investigate the robustness of momentum methods to biased gradient errors within a general three-parameter family—step size α and momentum parameters β and ν —which is often referred to in the literature as generalized momentum methods (GMM), see e.g., [58, 57] and the references therein. This framework is broad and expressive: with appropriate parameter choices, it recovers gradient descent (GD) and popular momentum schemes, including heavy-ball (HB), Nesterov's accelerated gradient (NAG), and the triple momentum method (TMM), as special cases.

We consider a general noise model that permits sub-Gaussian gradient errors, which may be biased. This unified formulation is flexible enough to capture bounded deterministic errors, stochastic unbiased errors with sub-Gaussian tails, or combinations of both. We propose the use of the *risk-sensitive index*—a concept from robust control theory [59, 60, 61]—as a robustness measure to assess the impact of bias and stochasticity on algorithmic performance. Given an iteration budget $K \in \mathbb{Z}_+$ and a strongly convex, smooth objective function $f : \mathbb{R}^d \to \mathbb{R}$, we define the risk-sensitive cost $R_K : \mathbb{R} \to \mathbb{R}$ as

$$R_K(\theta) = \frac{2\sigma^2}{\theta(K+1)} \log \left(\mathbb{E} \exp\left[\frac{\theta}{2\sigma^2} S_K\right] \right), \quad S_K = \sum_{k=0}^K (f(x_k) - f_*), \tag{1.1}$$

where $f_* = \min_x f(x)$, σ^2 is the variance proxy of the sub-Gaussian noise, and S_K denotes the cumulative suboptimality of the iterates $\{x_k\}_{k=0}^K$, which depends on the choice of parameters (α, β, ν) . We also consider its stationary analogue, known as the risk-sensitive index, defined as $R(\theta) = \limsup_{K\to\infty} R_K(\theta)$. This metric appears in the literature for the control of dynamical systems driven by Gaussian noise [59, 60, 61]. Ours is a generalization to sub-Gaussian noise settings.

The parameter $\theta > 0$ in the cost $R_K(\theta)$ provides a continuous interpolation between the risk-neutral regime—corresponding to the limit $\theta \to 0$, capturing the average performance $\mathbb{E}\left[\frac{S_K}{K+1}\right]$ —and progressively more risk-averse regimes that place increasing emphasis on tail events for larger positive values of θ , and approximating the worst-case behavior for sufficiently large θ [62]. Conversely, $\theta < 0$ induces a risk-seeking regime that down-weights large suboptimality events and favors variability. Thus, by varying θ , the risk-sensitive cost spans average-case, risk-seeking, and worst-case perspectives with a unified lens. In addition, the risk-sensitive cost $R_K(\theta)$ is a scaled cumulant-generating function, i.e., natural logarithm of the moment generating function, and Chernoff bounds turn $R_K(\theta)$ into explicit exponential tails for suboptimality, yielding high-probability bounds and rate functions that characterize the decay rate for the average suboptimality $\mathbb{P}\left[\frac{S_K}{K+1} > t\right]$. These properties of the risk-sensitive index make it interesting to study in the context of optimization algorithms.

To the best of our knowledge, this work provides the first risk-sensitive analysis of generalized momentum methods. Unlike prior research, which has been predominantly risk-neutral and has typically relied on the assumption of unbiased stochastic gradients, our framework accommodates gradient noise that may be biased, thereby delivering high-probability guarantees that remain valid under biased gradient settings.

Contributions. Our main contributions are built on several pillars. First, we analyze the strongly convex quadratic setting under i.i.d. isotropic Gaussian gradient noise. This case provides a clean and tractable foundation, allowing us to develop explicit characterizations before addressing the more general class of smooth, strongly convex functions subject to potentially biased noise. In the quadratic setting, we investigate how the risk-sensitive index $R(\theta)$ depends on the given algorithm

parameters (α, β, ν) and risk-aversion parameter θ . By modeling the algorithmic class GMM as a linear time-invariant dynamical system and leveraging some existing results from robust control theory, we argue that $R(\theta)$ admits an explicit characterization through solving a discrete-time algebraic Riccati equation (DARE) that depends on the algorithm parameters. However, this is a matrix equation over $2d \times 2d$ matrices, and in general, it entails solving a $4d \times 4d$ generalized eigenvalue problem, which is computationally prohibitive for large d requiring at least $\mathcal{O}(d^3)$ operations. To this end, we establish a dimension-reduction result: for quadratic objectives subject to i.i.d. isotropic Gaussian noise with variance σ^2 , we show that the DARE decomposes into d independent 2×2 Riccati equations. Each such equation can be solved in $\mathcal{O}(1)$ time, allowing the overall solution to be computed in $\mathcal{O}(d)$ operations in parallel. This yields a closed-form expression for the risk-sensitive index in terms of easily solvable 2×2 DAREs. Furthermore, for gradient descent, we can solve the DAREs explicitly and provide an explicit expression for the risk-sensitive index. Building on our characterization of the risk-sensitive index, we then establish a fundamental trade-off between risk (as measured by this index) and convergence rate (quantifying solution speed in the absence of noise) in momentum methods. In particular, parameter choices that slow down convergence speed also reduce the associated risk and enlarge the range of θ values for which the risk remains finite, i.e., improved risk sensitivity and greater flexibility in θ comes at the expense of a reduction in the convergence rate. Specifically, the risk is finite if and only if $\theta > 0$ satisfies $\sqrt{\theta} H_{\infty} < \sqrt{d}$, where H_{∞} denotes the H_{∞} -norm of the dynamical system associated with the GMM iterations—explicitly characterized for quadratic objectives in [57]. Because the H_{∞} -norm quantifies robustness to the worst-case deterministic gradient errors [57], this relation implies that greater robustness, i.e., smaller H_{∞} -norm, permits a wider range of θ for which the risk is finite, thereby linking risk sensitivity (a probabilistic performance measure) to deterministic worst-case robustness in momentum-based methods. While connections between risk sensitivity and the H_{∞} -norm exist in the context of control systems and controlled Markov processes [63, Sec. VI], [61, 64]; what these connections mean in the context of momentum-based optimization algorithms subject to gradient errors is first explored in our work to our knowledge. We then compare momentum methods—HB, NAG, GD, and TMM—across different parameter settings, focusing on their risk profiles, i.e., how their risk sensitivity varies with stepsize and momentum. We find that HB with standard parameters (proposed by Polyak [8]) converges faster than NAG (with standard parameters as in [7]) but incurs higher risk, whereas GD (with the common stepsize $\alpha = 1/L$ where L is the Lipschitz constant of the gradient) is slower yet exhibits a lower risk than both methods. These trade-offs trace a Pareto-optimal frontier over parameter choices, delivering the best attainable risk for a target convergence rate -we illustrate this frontier numerically by leveraging our dimension-reduction framework to compute the risk index.

Second, we establish a large-deviation principle for the average suboptimality $\Delta_K \coloneqq S_K/(K+1)$, quantifying the exponential decay rate of rare-event probabilities for Δ_K in the quadratic setting. This also allows us to control the probability of rare events associated with suboptimality of the ergodic averages of the iterates. We show that the rate function is the Fenchel-Legendre transform of a scaled version of the risk-sensitive index $R(\theta)$. A key challenge to establish such a result is that the summands $f(x_k) - f_*$ that appear in the sum S_K are neither independent nor identically distributed—even when the gradient noise $\{w_{k+1}\}_{k\geq 0}$ is i.i.d.)—so classical results such as Cramér's theorem do not apply. Instead, we verify the hypotheses of the Gärtner–Ellis theorem [65], which accommodates such non-i.i.d. sequences, to identify the rate function. The analysis takes advantage of our characterizations of the risk-sensitive index for momentum methods. These results demonstrate that the rate function and the risk-sensitive index—which govern the tail behavior of suboptimality in the large-iteration limit—are intrinsically linked to the H_{∞} -norm. Moreover, they show that greater robustness to the worst-case deterministic errors (as quantified by the H_{∞} -norm) is associated with a sharper decay of tail probabilities, reflected in a larger rate function.

In our third set of results, we extend the analysis to the minimization of strongly convex and smooth functions. In this setting, explicit characterizations of the risk-sensitive index and the H_{∞} -norm are generally unavailable. While upper bounds \overline{H}_{∞} exist for the H_{∞} -norm [57], no analogous bounds are known for the risk-sensitive cost or the risk-sensitive index. To bridge this gap, we adopt a more general noise model in which gradient errors are sub-Gaussian and may be biased. This model subsumes the Gaussian noise studied in the quadratic case and accommodates stochastic errors with sub-Gaussian tails—including bounded stochastic errors, deterministic errors, and their mixtures. We derive upper bounds on $R_K(\theta)$ at every iteration K, and translate these into finite-time high-probability quarantees and non-asymptotic large-deviation upper bounds for the averaged iterates. Our approach relies on introducing a novel Lyapunov function together with a backward-induction argument, inspired by dynamic programming methods, to iteratively estimate the risk-sensitive cost. Taking the limit as $K \to \infty$, we derive bounds on the risk-sensitive index $R(\theta)$ and associated large-deviation upper bounds. These results can be interpreted as non-asymptotic counterparts of the asymptotic characterizations established in the quadratic case. To the best of our knowledge, such non-asymptotic high-probability and large-deviation bounds for biased gradient estimates in the general class of momentum methods considered here have not previously appeared in the literature. Analogous to the quadratic case, we establish intrinsic trade-offs between risk and convergence rate in the design of first-order accelerated methods. Moreover, we find that the bounds on the H_{∞} norm control the range of θ values for which the risk remains finite. Our bounds connect $R(\theta)$, high-probability guarantees, and large-deviation rates to the H_{∞} -norm, thereby sharpening the link between probabilistic performance and worst-case robustness beyond the quadratic setting as well. They show that greater robustness to deterministic errors (as quantified by the H_{∞} -norm) is associated with sharper tail decay in average suboptimality and reduced bias in the averaged iterates.

Fourth, we provide numerical experiments that illustrate our results. In the strongly convex quadratic setting, our experiments show that a faster convergence rate corresponds to a higher risk sensitivity for each momentum method considered in this paper. We provide Pareto-optimal frontiers for GD, NAG, HB to compare the convergence rate vs. risk trade-offs across these three methods. We also compare large-deviation rate functions across GMMs. Lastly, in the strongly convex setting, we illustrate the behavior of risk-sensitive cost across iterations for HB, RS-HB (a heavy-ball variant more robust to deterministic errors [57]), TMM, NAG, and GD.

2. Related Work

Under a light-tailed (sub-Gaussian) noise assumption, high-probability convergence guarantees for stochastic gradient descent (SGD) and its momentum variants have been established for convex objectives [24, 66, 67, 68, 69, 70, 71, 72] and for non-convex objectives [73, 74, 68]. Beyond this setting, several works relax the light-tailed assumption and instead provide guarantees under bounded variance noise [75, 76] or, for sub-Weibull noise [77]. Unlike our setting, however, these works assume *unbiased* gradient noise and do not extend to the general class of momentum methods (GMM) studied in this paper.

On the other hand, for particular biased gradient noise settings, there is a body of existing work that provides guarantees in expectation, i.e., bounds on the expected suboptimality over the randomness in the noise model, as opposed to high-probability guarantees. These results are obtained under noise models different from ours, typically in more specialized settings and for particular applications. For instance, without-replacement sampling (WRS) in finite-sum problems leads to biased noise, with guarantees established for SGD and Nesterov's accelerated gradient under various WRS schemes [29, 26, 31]. Variance-reduction methods such as SAG and SARAH also yield biased gradient estimates, for which in-expectation guarantees are available [28, 27, 25]. In distributed learning, compression and quantization introduce bias, with guarantees provided in [35, 36, 32, 33, 25]. Gradient clipping and normalization, often used for heavy-tailed noise or

differential privacy, also induce bias [38, 40, 37, 39]. Other sources include low-precision arithmetic [46], non-i.i.d. data in statistical learning [43, 44], and truncated backpropagation strategies for bi-level optimization [45]. Furthermore, there are also few papers that attempt to unify such biased-noise settings, e.g., [78] provides in-expectation guarantees, and [79] establishes almost-sure convergence guarantees for stochastic HB with decaying stepsizes under a biased noise model for general (possibly nonconvex) objectives, where the bias term may grow proportionally with the gradient norm. However, none of these works provides large-deviation bounds; moreover, their analyses rely on decaying step sizes converging to zero and do not apply to the constant step size considered in our work.

Compared to in-expectation guarantees, high-probability guarantees under biased noise are less developed. While in-expectation guarantees can be converted into high-probability guarantees using strategies such as longer runs of the algorithm combined with Chebyshev's inequality, or parallel runs with selection of the best outcome [80, p. 243], [81], these strategies often produce loose complexity bounds with respect to the target probability and desired precision and can be impractical in streaming data settings [82], [56, Remark 13]. Existing high-probability results include random reshuffling for SGD [31, 30] and non-linear SGD variants with heavy-tailed noise where clipping, quantization, or normalization induce bias [83, 68].

The literature on establishing large-deviation principles (LDP) for stochastic GD and its momentum variants is sparse. Previous work on LDP has been mainly on stochastic approximation algorithms, including first- and zeroth-order stochastic gradient methods [84, 85, 86, 87]. However, these papers have a different focus than ours: rather than analyzing suboptimality across iterations under a constant step size, they instead study the vanishing-step-size regime by letting the stepsize go to zero, quantifying deviations of the stochastic dynamics from their mean trajectory (which is determined by the continuous-time gradient flow) and deriving exponential estimates for escape times from neighborhoods of a point when the gradients are subject to unbiased noise or to stationary Markovian noise, i.e., they do not consider the large iteration limit for constant stepsize. More recently, Bajović et al. [88] derive LDP results with matching upper and lower bounds for stochastic GD with a decreasing step size assuming twice continuously differentiable smooth, strongly convex objectives under unbiased gradient noise. For quadratic objectives, they obtain the rate function in closed form in the large iteration limit, showing that higher-order noise moments—not just the variance—govern rare, large errors of the last iterate. On the other hand, in [89] the authors consider *unbiased* heavy-tailed noise, and for SGD with decaying stepsize sequence. they establish an LDP upper bound for the minimum norm-squared of gradients for nonconvex, lower-bounded objectives with Lipschitz-continuous gradients. In the unbiased gradient setting for strongly convex minimization, [90] establishes large-deviation results for the convergence rate of the AC-SA algorithm, strengthening the earlier results of [91]. However, neither of these works considers constant step sizes or the broader class of momentum methods studied here, nor do they address biased gradient noise or the trade-offs between convergence rate and risk sensitivity.

Next, we are going to discuss a related body of work from the risk perspective. Risk sensitivity, and more broadly, entropic risk, has been covered in the literature largely in the control theory context [59, 92, 60, 61]. These works consider centered, independent and identically distributed (i.i.d.) Gaussian noise. In particular, in [61], an exact analysis of $R(\theta)$ is provided in the linear–quadratic control setting. These results are not given in the context of optimization algorithms but rather for general linear dynamical systems. In our work, however, we interpret GMM as a linear dynamical system when the objective is a quadratic and show that their result translates directly into a formula for the risk-sensitive cost of GMM algorithms in this setting. However, computing the risk-sensitivity index via the approach of [61] requires integrating the system's transfer function in the frequency domain, which—using the results of [64], [93, Remark 4.11], and [94, Lemma 3.4]—can be reduced to solving $2d \times 2d$ Riccati equations, entailing at least $\mathcal{O}(d^3)$ computational complexity. By exploiting the special structure of the GMM, we show that it suffices to solve 2×2 Riccati

equations, which involve three unknowns—the entries of a symmetric 2 × 2 matrix—and three corresponding equations; moreover, the approach in [61] applies only to quadratics and does not extend to strongly convex objectives. More recently, in [53] the authors introduced robustness measures related to asymptotic optimality under unbiased gradient errors, analyzing quadratic functions and, more generally, smooth strongly convex functions. In particular, the trade-offs between convergence rate and robustness to gradient errors for GD and NAG have been analyzed in [53]; however, in contrast to ours, the approach in [53] does not extend to biased gradient estimates or deterministic worst-case errors –the rate vs risk trade-off scheme introduced in [53] for first-order optimization methods is later extended in [55] to analyze first-order primal-dual methods for solving strongly convex-strongly concave saddle point problems subject to unbiased gradient errors with finite variance. In a different direction from [53], a more recent work [58] proposes an alternative robustness measure motivated by the entropic risk of the iterates and provides high-probability bounds for GMM in the unbiased sub-Gaussian gradient noise setting. However, their analysis does not accommodate biased gradient estimates, focuses solely on the suboptimality of the last iterate x_K rather than on ergodic averages or cumulative suboptimality S_K , and does not establish large-deviation bounds. Compared to prior work, we treat (i) constant step sizes (not decaying), (ii) biased sub-Gaussian gradient errors (not just unbiased), and (iii) risk-sensitive metrics (RSI/LDP) and their link to H_{∞} -norm in the context of momentum-based optimization algorithms.

Notation. Let \mathbb{Z}_+ and \mathbb{R}_+ denote positive integers and reals including 0, respectively; and $\mathbb{R}_{++} = \mathbb{R}_+ \setminus \{0\}$. A function $f : \mathbb{R}^d \to \mathbb{R}$ is called μ -strongly convex if the function $x \mapsto f(x) - \frac{1}{2}\mu \|x\|^2$ is convex on \mathbb{R}^d for some constant $\mu > 0$. A continuously differentiable function $f : \mathbb{R}^d \to \mathbb{R}$ is L-smooth if its gradient satisfies $\|\nabla f(x) - \nabla f(y)\| \le L\|x - y\|$ for all $x, y \in \mathbb{R}^d$. Let $\mathcal{C}_{\mu}^L(\mathbb{R}^d)$ denote the set of all functions $f : \mathbb{R}^d \to \mathbb{R}$ that are both μ -strongly convex and L-smooth. It can be shown that any $f \in \mathcal{C}_{\mu}^L(\mathbb{R}^d)$ satisfies

$$\frac{\mu}{2} \|x - y\|^2 \le f(x) - f(y) - \nabla f(y)^\top (y - x) \le \frac{L}{2} \|x - y\|^2, \quad \forall \ x, y \in \mathbb{R}^d.$$
 (2.1)

Due to strong convexity, f admits a unique global minimum on \mathbb{R}^d which we will denote by x_* . From (2.1), one has $\mu \leq L$, and we assume $\mu < L$ throughout the paper –otherwise, for $\mu = L$, the class $\mathcal{C}_{\mu}^L(\mathbb{R}^d)$ is trivial, i.e., $f(x) = \frac{\mu}{2} ||x||^2$. Let I_d denote the $d \times d$ identity and let 0_d be the $d \times d$ zero matrix. We drop the subscript d in some cases when it is clear from the context. Given matrix A, let A_{ij} denote the entry on the i-th row and j-th column of A. The spectral radius $\rho(A)$ of a square matrix A is defined as the largest modulus of the eigenvalues of A, and ||A|| denotes the spectral norm of A. We use $\det(A)$ and $\operatorname{trace}(A)$ to denote the determinant and the trace of a matrix A. Throughout the paper, $A \otimes B$ denotes the Kronecker product of the matrices A and B.

3. Preliminaries

Let $f \in \mathcal{C}^L_{\mu}(\mathbb{R}^d)$ be given. We consider the unconstrained problem $f_* := \min_{x \in \mathbb{R}^d} f(x)$. The Generalized Momentum Method (GMM) [58, 57] consists of the following iterations

$$x_{k+1} = x_k - \alpha \nabla f(y_k) + \beta (x_k - x_{k-1}),$$
 (3.1a)

$$y_k = x_k + \nu(x_k - x_{k-1}), \tag{3.1b}$$

starting from an arbitrary initial point $x_0 \in \mathbb{R}^d$ with the convention that $x_{-1} = x_0$. GMM admits three non-negative parameters α, β and ν , where $\alpha > 0$ is the step size, and β and ν are called "momentum parameters". This method generalizes a number of momentum-averaging-based first-order algorithms. If $\nu = 0$, GMM is equivalent to the heavy-ball method (HB) of Polyak [8]. If we choose $\beta = \nu$, GMM recovers Nesterov's accelerated gradient (NAG) method [9]. On the other hand, when $\beta = \nu = 0$, GMM reduces to the gradient descent (GD) method. Finally, the triple

momentum method (TMM) corresponds to the parameter choice $\alpha = \frac{1+\bar{\rho}}{L}$, $\beta = \frac{\bar{\rho}^2}{2-\bar{\rho}}$, $\nu = \frac{\bar{\rho}^2}{(1+\bar{\rho})(2-\bar{\rho})}$, where $\bar{\rho} = 1 - 1/\sqrt{\kappa}$ [10].

A growing body of work has employed control-theoretic tools to analyze the robustness of momentum-based optimization algorithms to noise [53, 57, 12, 95, 96, 55]. To the best of our knowledge, our work is the first to investigate the risk sensitivity of the dynamical systems associated with GMMs, with the aim of characterizing the trade-offs between their sensitivity to gradient noise and their convergence rates. We study the performance of GMM algorithms subject to additive gradient noise, i.e., at each iteration $k \geq 0$, instead of employing the actual gradient $\nabla f(y_k)$, suppose we only have access to its noisy estimate:

$$\tilde{\nabla}f(y_k, w_{k+1}) := \nabla f(y_k) + w_{k+1}, \tag{3.2}$$

where $w_{k+1} \in \mathbb{R}^d$ is the additive gradient noise at y_k . Assumptions on the exact nature of this noise will be provided later. We start with presenting the dynamical system reformulation of (3.1) as a discrete-time dynamical system:

$$\xi_{k+1} = A\xi_k + Bu_{k+1},\tag{3.3a}$$

$$y_k = C\xi_k, \quad u_{k+1} = \tilde{\nabla}f(y_k, w_{k+1}) = \nabla f(y_k) + w_{k+1},$$
 (3.3b)

where A, B and C are system matrices of the form:

$$A = \tilde{A} \otimes \mathsf{I}_d, \quad B = \tilde{B} \otimes \mathsf{I}_d, \quad C = \tilde{C} \otimes \mathsf{I}_d,$$
 (3.4)

with

$$\tilde{A} := \begin{bmatrix} (1+\beta) & -\beta \\ 1 & 0 \end{bmatrix}, \ \tilde{B} := \begin{bmatrix} -\alpha \\ 0 \end{bmatrix}, \ \tilde{C} := \begin{bmatrix} (1+\nu) & -\nu \end{bmatrix}, \tag{3.5}$$

and

$$\xi_k := \begin{bmatrix} x_k \\ x_{k-1} \end{bmatrix}, \tag{3.6}$$

is the *state vector* which is defined by the iterates at step k and the previous iterate at k-1, i.e., x_k and x_{k-1} , respectively. We also define

$$\xi_* := \begin{bmatrix} x_* \\ x_* \end{bmatrix}, \tag{3.7}$$

which consists of two copies of the global optimum x_* concatenated vertically. The vector u_{k+1} is the noisy gradient evaluated at the point y_k . Notice that we can rewrite the noisy GMM iterations (3.3) as

$$\xi_{k+1} = A\xi_k + B\nabla f(C\xi_k) + Bw_{k+1}, \tag{3.8a}$$

$$z_k = F(\xi_k), \tag{3.8b}$$

where z_k is the output of the system that is of interest (defined through an arbitrary map $F: \mathbb{R}^{2d} \to \mathbb{R}^p$ for some $p \ge 1$ and the matrices A, B and C are as in (3.5). Various choices of F are admissible, e.g., setting

$$F(\xi_k) := \overline{w}(f(x_k) - f(x_*)), \tag{3.9}$$

for an increasing scalar function $\overline{w}: \mathbb{R}_+ \to \mathbb{R}_+$ yields a functional that quantifies a weighted measure of suboptimality.

Previous research on the robustness of momentum methods against gradient noise predominantly considered either *stochastic* unbiased noise that is assumed to be Gaussian or light-tailed [52, 53, 58, 97, 98, 55, 99], or deterministic worst-case noise [57, 100, 13]. The existing research on *biased* stochastic gradient methods with momentum to our knowledge is quite limited. In this study,

¹Throughout this paper, we use the terms gradient noise and gradient errors interchangeably.

we expand this scope by considering the case when the gradient noise is light-tailed but is not necessarily unbiased. We first begin our discussion by introducing the necessary filtrations.

GMM generates a sequence of iterates $\{x_k\}_{k\geq 0}$, each situated within a defined filtered probability space $(\Omega, \mathcal{F}, \mathbb{P})$ such that $\mathcal{F}_k \subset \mathcal{F}$ is defined as the σ -algebra generated by the iterates x_0, x_1, \ldots, x_k for all $k \geq 0$. The following assumption says that the noise w_{k+1} at step $k \in \mathbb{Z}_+$ has light tails; but, it is not necessarily unbiased.

Assumption 3.1. Let $\{w_{k+1}\}_{k\geq 0}$ be an adapted process, i.e., w_{k+1} is \mathcal{F}_{k+1} -measurable for $k\geq 0$. The norm $\|w_{k+1}\|$ is sub-Gaussian conditional on \mathcal{F}_k with variance proxy σ^2 , i.e., there exists some $\sigma>0$ such that for all $k\geq 0$ it holds that

$$\mathbb{P}(\|w_{k+1}\| \ge t|\mathcal{F}_k) \le 2e^{-\frac{t^2}{2\sigma^2}}, \quad \forall \ t \ge 0.$$

Remark 3.2. Note that in theorem 3.1, the noise sequence can be biased; i.e., $\mathbb{E}[w_{k+1}|\mathcal{F}_k] = 0$ does not necessarily hold. For example, when $w_{k+1} = \tilde{\zeta}_{k+1} + \tilde{\delta}_k$ where $\tilde{\zeta}_{k+1}$ is i.i.d. sub-Gaussian, independent from \mathcal{F}_k with variance proxy $\tilde{\sigma}^2$ and mean $\mathbb{E}[\tilde{\zeta}_{k+1}|\mathcal{F}_k] = 0$ and $\tilde{\delta}_k$ is a bounded deterministic sequence with the bound $\|\tilde{\delta}_k\|^2 \leq M^2$ for some $M \geq 0$; then, it is easy to see that theorem 3.1 holds for $\sigma^2 = \bar{c}_0(\tilde{\sigma}^2 + M^2)$, for some large enough constant $\bar{c}_0 > 0$, where we did not attempt to optimize the choice of σ . As a special case, if $w := \{w_{k+1}\}_{k \geq 0} \in \ell_2(\mathbb{R}^d)$ —that is, if $\{w_{k+1}\}_{k \geq 0}$ is a deterministic square-summable sequence satisfying $\sum_{k \geq 0} \|w_k\|^2 < \infty$ —then such a finite M exists and theorem 3.1 is satisfied.

Assumption 3.1 encompasses a variety of noise models relevant to practical scenarios. The centered (unbiased) stochastic noise is commonly encountered in differential privacy, where i.i.d. centered noise is added to gradients to protect user data [18]. A similar situation arises in stochastic optimization and statistical learning contexts when the objective takes the form $f(x) := \mathbb{E}_{\xi}[\mathcal{L}(x,\xi)]$ for a loss function \mathcal{L} , and the expectation is approximated via empirical averaging over mini-batches [2, 1]. Under moderate batch sizes, the Central Limit Theorem justifies modeling the resulting gradient noise as Gaussian, a behavior also observed empirically [22, 23]. Consequently, Assumption 3.1 is often satisfied in practice. Light-tail conditions such as this are standard in the analysis of stochastic optimization algorithms, particularly for deriving tail bounds and high-probability guarantees. On the other hand, it is possible that the gradient noise is deterministic, i.e., it contains no stochastic element. This situation is typical in incremental gradient methods or in settings where gradients are approximated by solving subproblems inexactly [13, 100, 99, 101, 102, 6]. Our noise model also captures deterministic corruption of gradients at each iteration, which may arise due to low-precision floating-point arithmetic [103].

3.1. Risk-sensitive cost and the risk-sensitive index. Let $f \in \mathcal{C}^L_{\mu}(\mathbb{R}^d)$ and consider the iterates $\{\xi_k\}_{k\geq 0}$ of the GMM method in (3.8) subject to gradient noise $\{w_{k+1}\}_{k\geq 0}$. Under Assumption 3.1, for a fixed iteration budget K>0, we define our *risk-sensitive cost* as in (1.1), i.e.,

$$R_K(\theta) := \frac{2\sigma^2}{(K+1)\theta} \log \mathbb{E}\left[e^{\frac{\theta}{2\sigma^2}S_K}\right], \quad S_K := \sum_{k=0}^K \left[f(x_k) - f_*\right], \tag{3.10}$$

for a real scalar parameter $\theta > 0$, where the expectation is taken with respect to the entire sequence of noise encountered until K, assuming that the expectation is finite. This type of risk measure appears frequently in the robust control literature [59, 60, 61, 104] for different choices of S_K depending on the dynamics of interest –here, we take the cost function S_K to be cumulative suboptimality over the iterations. By considering the Taylor series expansion of $R_K(\theta)$ with respect to θ , it follows that as $\theta \to 0^+$, the following limit exists:

$$R_K(0) := \lim_{\theta \to 0^+} R_K(\theta) = \mathbb{E}\left(\frac{S_K}{K+1}\right),\tag{3.11}$$

provided that there exists some $\bar{\theta} > 0$ such that $R_K(\theta)$ is finite for $\theta \in (0, \bar{\theta})$. The parameter θ is called the *risk-sensitivity parameter* [92, 62]. The term S_K is a running sum of suboptimality over K iterations; therefore, we see from (3.11) that when $\theta = 0$, the risk-sensitive cost is a measure of average performance $S_K/(K+1)$ in expectation. For $\theta > 0$, as θ gets larger, the risk-sensitive cost $R_K(\theta)$ penalizes large values of S_K more and more due to the exponential term in (3.10) and R_K will be more sensitive to large values of suboptimality. Therefore, in analogy with a risk-averse financial investor that tries to avoid large losses, the case $\theta > 0$ is called the "risk-averse case" (see e.g., [61, 92]). This can also be readily seen from the Taylor expansion of (3.10) around $\theta = 0$, i.e.,

$$R_K(\theta) = R_K(0) + \frac{\theta(K+1)}{4\sigma^2} \operatorname{Var}\left(\frac{S_K}{K+1}\right) + \mathcal{O}(\theta^2). \tag{3.12}$$

We observe that as $\theta > 0$ gets larger, the second term on the right-hand side of (3.12) penalizes the variance of the average suboptimality $S_K/(K+1)$ more and more –note that the variance does not play a role within the $\theta = 0$ case. The risk-sensitive index is then defined as

$$R(\theta) := \limsup_{K \to \infty} R_K(\theta),$$

provided that the limit exists. Risk-sensitive cost is well-studied in the robust control literature and is used to quantify the robustness of dynamical systems to stochastic noise [62, 105, 106, 107]. In some of our results, we will also consider the $\theta < 0$ case, i.e., the risk-seeking scenario.

3.2. H_{∞} -norm. By appropriately choosing the output map $F(\cdot)$ in (3.8), we can obtain different output sequence $\{z_k\}$ that is relevant to the quantity we would like to analyze for GMM. In particular, if F is chosen such that

$$||F(\xi_k)||^2 = f(x_k) - f_*, \tag{3.13}$$

for all $k \geq 0$, then the cumulative cost $S_K = \sum_{k=0}^K \left(f(x_k) - f_* \right)$, can be expressed in terms of the ℓ_2 norm of the sequence $\{z_k\}$, i.e., since $z_k = F(\xi_k)$ for $k \geq 0$, we have $S_K = \sum_{k=0}^K \|z_k\|^2$ -for instance, the condition (3.13) is satisfied when the weighting function in (3.9) is chosen as $\overline{w}(z) = \sqrt{z}$. In this case, when the noise w_{k+1} is deterministic for every $k \geq 0$ and is square-summable; from the limit (3.11), we see that $R_K(0) = \frac{S_K}{K+1}$ is also deterministic and corresponds to the average suboptimality. Given the decaying nature of square-summable noise, a natural relevant question would be whether the deterministic limit $S_\infty := \lim_{K \to \infty} S_K = \sum_{k=0}^\infty \|z_k\|^2$, which captures the cumulative suboptimality over the iterations, exists –with the convention that the limit is $+\infty$ if S_K is not bounded.

The H_{∞} -norm of a dynamical system, defined below, provides tight bounds on the quantity $S_{\infty} = \lim_{K \to \infty} \sum_{k=0}^{K} (f(x_k) - f_*)$ (see [106, 61]), and consequently on the average suboptimality $R_K(0)$ for $K \in \mathbb{Z}_+$ sufficiently large; thereby yielding tight bounds for the suboptimality of the averaged iterates [57]. Roughly speaking, H_{∞} -norm is a measure of how much a dynamical system amplifies deterministic noise in terms of the ℓ_2 -norm (from input noise sequence to output sequence z_k), and is formally defined as follows.

Definition 3.3 ([108, 109, 110, 106, 57]). Consider the purely deterministic setting where the gradient error sequence $w := \{w_{k+1}\}_{k\geq 0}$ is deterministic and square-summable. The GMM system (3.8), with input sequence (gradient noise) $\{w_{k+1}\}_{k\geq 0} \in \ell_2(\mathbb{R}^d)$ and output sequence $\{z_k\}_{k\geq 0}$ satisfying (3.13), has ℓ_2 -gain at most γ if there exists a function $H_{\gamma} : \mathbb{R}^{2d} \to \mathbb{R}_+$, with $H_{\gamma}(\xi_*) = 0$ and such that for every initialization $\xi_0 \in \mathbb{R}^{2d}$ and every input $w \in \ell_2(\mathbb{R}^d)$, it holds that

$$\sum_{k>0} (f(x_k) - f_*) = \sum_{k>0} ||z_k||^2 \le \gamma^2 \sum_{k>0} ||w_{k+1}||^2 + H_{\gamma}(\xi_0).$$
(3.14)

In this context, the function H_{γ} is independent of both the disturbance sequence $\{w_{k+1}\}_{k\geq 0}$ and the initialization ξ_0 , while it may still exhibit dependence on γ . The H_{∞} -norm of the GMM system

is then defined as the minimal such bound, i.e.,

$$H_{\infty} := \inf \left\{ \gamma \in \mathbb{R}_{++} \mid \exists H_{\gamma} \text{ such that } H_{\gamma}(\xi_{*}) = 0 \text{ and } (3.14) \text{ holds for all } w \in \ell_{2}(\mathbb{R}^{d}) \right\}.$$
 (3.15)

This quantity is also referred to as the minimal ℓ_2 -gain of the system (3.8) with output $\{z_k\}_{k\geq 0}$.

The requirement that $H_{\gamma}(\xi_*) = 0$ ensures (3.14) providing tight bounds in the absence of noise. Specifically, if $w_{k+1} = 0$ for all $k \geq 0$ and $\xi_0 = \xi_*$, then $x_0 = x_*$ and since x_* is a fixed point of the GMM iterations, this initialization implies $\sum_{k \geq 0} \left(f(x_k) - f_* \right) = 0$. In this case, the inequality (3.14) reduces to an equality with both sides equal to zero. For linear systems, there exist alternative yet equivalent definitions of the H_{∞} -norm, either based on initialization at a fixed point $\xi_0 = \xi_*$ or stated in the frequency domain [111]. In this work, we adopt a more general definition that applies to both linear and nonlinear systems, since the GMM system can be nonlinear for $f \in \mathcal{C}_{\mu}^L(\mathbb{R}^d)$ that is not a quadratic function.

The H_{∞} -norm quantifies the worst-case deterministic noise amplification of the system in (3.8), i.e., it quantifies how the output behaves in response to the noise input $\{w_{k+1}\}_{k\geq 0}$. A smaller H_{∞} value indicates a more robust system, as the output is less sensitive to worst-case deterministic square-summable input noise; consequently, the cumulative suboptimality over the iterations, i.e., $\sum_{k\geq 0} (f(x_k) - f_*)$, will also be smaller for the same noise level. For GMM, H_{∞} -norm depends on the algorithm parameters (α, β, ν) and the problem parameters L and μ , i.e., smoothness and convexity constants, respectively. For strongly convex quadratics, it is known that H_{∞} -norm can be computed exactly. The following result is a direct consequence of [57, Thm. 4.1] together with [57, eqns. (60)–(61)].

Theorem 3.4 ([57]). Consider a quadratic function $f \in \mathcal{C}^L_{\mu}(\mathbb{R}^d)$ with a Hessian matrix $Q \in \mathbb{R}^{d \times d}$. Suppose that with the given parameters (α, β, ν) , the GMM dynamics exhibit global linear convergence to the unique fixed point of the system ξ_* in the absence of gradient noise, specifically when $w_{k+1} = 0$ in (3.8) for all $k \geq 0$. Under these conditions, the H_{∞} -norm (as given in theorem 3.3) of the GMM is

$$H_{\infty} = \frac{\alpha}{\sqrt{2}} \max_{1 \le i \le d} \frac{\sqrt{\lambda_i}}{\tilde{s}_{\lambda_i}} = \frac{\alpha}{\sqrt{2}} \cdot \max_{\lambda \in \{\mu, L\}} \frac{\sqrt{\lambda}}{\tilde{s}_{\lambda}}, \tag{3.16}$$

where $\mu = \lambda_1 \le \lambda_2 \le ... \lambda_d = L$ are the eigenvalues of Q in a non-decreasing order; moreover,

$$\tilde{s}_{\lambda} := \begin{cases} |1 - \tilde{c}_{\lambda}| \sqrt{1 - \frac{\tilde{b}_{\lambda}^2}{4\tilde{c}_{\lambda}}} & \text{if } \tilde{c}_{\lambda} > 0 \text{ } \text{and } \frac{|\tilde{b}_{\lambda}|(1 + \tilde{c}_{\lambda})}{4\tilde{c}_{\lambda}} < 1, \\ \left| |1 + \tilde{c}_{\lambda}| - |\tilde{b}_{\lambda}| \right| & \text{otherwise}, \end{cases}$$

with

$$\tilde{b}_{\lambda} := \alpha \lambda (1 + \nu) - (1 + \beta), \quad \tilde{c}_{\lambda} := \beta - \alpha \lambda \nu.$$
 (3.17)

Finally, it always holds that $H_{\infty} \geq \frac{1}{\sqrt{2\mu}}$.

For general strongly convex functions that are not quadratic, exact analytical expressions are typically unavailable. Nevertheless, tight upper bounds have been derived in [57] for GD, NAG, and more generally for GMM, by verifying the feasibility of certain 4×4 matrix inequalities. For completeness, we present these bounds in theorem A.1 in the appendix. In the context of stochastic dynamical systems driven by Gaussian noise, it is known that risk sensitivity is closely related to the H_{∞} -norm: specifically, the largest value of $\theta > 0$ for which the risk-sensitive index $R(\theta)$ remains finite depends on the system's H_{∞} -norm [106, 61]. To the best of our knowledge, however, such connections have not been explored in the setting

of optimization algorithms driven by noise models such as those described in theorem 3.1. To investigate this connection further and gain insight via precise analytical formulas, the next section focuses on the special case of strongly convex quadratic objectives subject to unbiased (centered) i.i.d. Gaussian noise. This serves as a foundation before extending the analysis to general smooth strongly convex functions under the broader noise model of theorem 3.1.

4. Exact analysis of $R(\theta)$ for strongly convex quadratics

We now consider the special case with f being a strongly convex quadratic of the form

$$f(x) := \frac{1}{2}x^{\top}Qx + g^{\top}x + h, \tag{4.1}$$

where $Q \in \mathbb{R}^{d \times d}$ is a symmetric positive-definite matrix, $g \in \mathbb{R}^d$ and $h \in \mathbb{R}$. In this case, the system defined in (3.8) reduces to a linear dynamical system which can be studied further by providing some closed form expressions about its dynamics. First, we will rewrite these iterations as a linear dynamical system. For this purpose, we consider the eigenvalue decomposition

$$Q = U\Lambda U^{\top},\tag{4.2}$$

where $\Lambda = \mathbf{diag}(\lambda)$ is a diagonal matrix containing eigenvalues of Q in increasing order, i.e., $\Lambda_{ii} = \lambda_i$ for i = 1, ..., d such that $0 < \mu = \lambda_1 \le \lambda_2 \le ... \le \lambda_d = L$ are the eigenvalues of Q. Note that

$$f(x_k) - f(x_*) = \frac{1}{2} (x_k - x_*)^{\top} Q(x_k - x_*) = \frac{1}{2} (x_k - x_*)^{\top} (U \Lambda U^{\top}) (x_k - x_*); \tag{4.3}$$

hence, we have $\nabla f(x) = Q(x - x_*)$, implying that

$$\nabla f(C\xi_k) = Q(C\xi_k - x_*) = QC\xi_k^c, \quad \text{where} \quad \xi_k^c := \xi_k - \xi_* \quad \text{with} \quad \xi_* = \begin{bmatrix} x_* \\ x_* \end{bmatrix}. \tag{4.4}$$

Here, the superscript "c" is to highlight that these iterates are shifted to be "centered" around the optimal point x_* , i.e., if GMM iterate sequence converges to x_* , then $\xi_k^c \to 0$.

Based on (4.4), we can rewrite (3.8) as

$$\xi_{k+1}^c = A_Q \xi_k^c + B w_{k+1}, (4.5)$$

where $A_Q := A + BQC$; therefore, using the definitions of A, B and C given in (3.4), we have

$$A_Q := \begin{bmatrix} (1+\beta)\mathsf{I}_d - \alpha(1+\nu)Q & -\beta\mathsf{I}_d + \alpha\nuQ \\ \mathsf{I}_d & 0_d \end{bmatrix}. \tag{4.6}$$

For this setting, we set the map F in (3.8) such that $F(\xi_k) := T\xi_k^c$, this leads to the output

$$z_k = T\xi_k^c \quad \text{with} \quad T := \begin{bmatrix} \frac{1}{\sqrt{2}} \Lambda^{1/2} U^\top & 0_d \end{bmatrix};$$
 (4.7)

and, from (4.3), it can be seen that z_k satisfies the identity (3.13). Therefore, based on eq. (3.14), we can talk about the H_{∞} -norm of the GMM system and the H_{∞} formula from theorem 3.4 is applicable. The H_{∞} -norm characterizes robustness in the hypothetical setting where the noise is fully deterministic. In theorem 3.1, we consider a more general noise model; however, if the noise specified therein were further restricted to be deterministic and square-summable, the H_{∞} -norm would quantify robustness with respect to the worst-case impact of such noise.

The GMM dynamics, as defined by (4.5)–(4.7), constitute a linear dynamical system identified by the system matrices (A_Q, B, T) . In this context, in the special case when

the noise sequence $\{w_{k+1}\}_{k\geq 0}$ consists of i.i.d. multivariate Gaussian vectors such that $w_{k+1} \sim \mathcal{N}(0, \frac{\sigma^2}{d} \mathbf{I}_d)$ for some $\sigma > 0$, then the noise variance is σ^2 and theorem 3.1 is satisfied. In this case, it is known that the risk-sensitive index $R(\theta)$ is finite if and only if $\sqrt{\theta} H_{\infty} < \sqrt{d}$ [61]; indeed, a particular form of a discrete-time algebraic Riccati equation (DARE), i.e.,

$$X = A_Q^{\mathsf{T}} X A_Q + A_Q^{\mathsf{T}} X B (\gamma^2 \mathbf{I}_d - B^{\mathsf{T}} X B)^{-1} B^{\mathsf{T}} X A_Q + T^{\mathsf{T}} T, \tag{4.8}$$

admits a positive semi-definite solution $X \succeq 0$ if and only if $\gamma > H_{\infty}$ [112, Corollary 2.1, Prop. 3.7] –thus, $\sqrt{\theta}H_{\infty} < \sqrt{d}$ holds if and only if (4.8) has a positive semi-definite solution for the parameter choice $\gamma = \frac{1}{\sqrt{\theta/d}}$ (see [94, Lemma 3.4] and [61]). To compute a solution $X \in \mathbb{R}^{2d \times 2d}$ for the DARE above, a standard method involves tackling a $4d \times 4d$ generalized eigenvalue problem. More specifically, it necessitates the calculation of the generalized eigenvalues and eigenvectors of the following $4d \times 4d$ matrix pencil:

$$M(\tilde{\lambda}) = \tilde{\lambda} \begin{bmatrix} \mathbf{I}_{2d} & -BB^{\top}/\gamma^2 \\ \mathbf{0}_{2d} & A_Q^{\top} \end{bmatrix} - \begin{bmatrix} A_Q & \mathbf{0}_{2d} \\ -T^{\top}T & \mathbf{I}_{2d} \end{bmatrix}, \tag{4.9}$$

i.e., one needs to compute a pair $(\tilde{\lambda}, \tilde{v})$ such that $M(\tilde{\lambda})\tilde{v} = 0$, and then a solution X to the DARE in (4.8) can be expressed in terms of $\tilde{\lambda}$ and \tilde{v} (see, e.g., [113, eqn. (6)-(8)]). This can be computationally expensive when d is large, requiring at least $\mathcal{O}(d^3)$ operations. However, in the case of GMM methods, the matrices A_Q , B, and T have some special block structure. In the next result, we exploit this structure and provide an explicit formula for the risk-sensitive index $R(\theta)$ in terms of solutions to 2×2 DARE systems when the input noise is i.i.d. Gaussian with covariance $\frac{\sigma^2}{d} \mathbf{I}_d$ for some $\sigma > 0$. With this scaling of the noise covariance matrix, the noise variance is σ^2 and theorem 3.1 is satisfied with variance (proxy) σ^2 . The proof is deferred to the appendix. To establish this result, we first apply a scaling argument by modifying the B matrix in (4.8) to $B\sigma$. We then exploit the block-diagonalizability of the matrix A_Q into 2×2 blocks, together with the uniform block structure of B. The main difficulty lies in proving the existence of solutions to the reduced DARE system and in quantifying how these solutions can be mapped to those of the full $2d \times 2d$ system via suitable permutation matrices and linear transformations.

Theorem 4.1. Let f be a quadratic of the form (4.1). Assume that the gradient noise follows an isotropic Gaussian distribution, i.e., Assumption 3.1 holds for an i.i.d. sequence $\{w_{k+1}\}_{k\geq 0}$ with $w_{k+1} \sim \mathcal{N}(0, \frac{\sigma^2}{d}|_d)$ for some $\sigma > 0$. Let the parameters (α, β, ν) of GMM be such that $\rho(A_Q) < 1$ for A_Q defined in (4.6). For $\lambda > 0$ given, consider the following 2×2 DARE,

$$\tilde{X} = (\tilde{A}^{(\lambda)})^{\top} \tilde{X} \tilde{A}^{(\lambda)} + (\tilde{A}^{(\lambda)})^{\top} \tilde{X} \tilde{B} (\gamma^2 - \tilde{B}^{\top} \tilde{X} \tilde{B})^{-1} \tilde{B}^{\top} \tilde{X} \tilde{A}^{(\lambda)} + \begin{bmatrix} \frac{\lambda}{2} & 0\\ 0 & 0 \end{bmatrix}, \tag{4.10}$$

where $\gamma = \frac{1}{\sqrt{\theta/d}}$, $\tilde{B} \in \mathbb{R}^{2 \times 1}$ is given in (3.5) and

$$\tilde{A}^{(\lambda)} := \begin{bmatrix} 1 + \beta - \alpha(1 + \nu)\lambda & -\beta + \alpha\nu\lambda \\ 1 & 0 \end{bmatrix} \in \mathbb{R}^{2 \times 2}.$$

The risk-sensitive index of the GMM method with risk parameter $\theta > 0$ is given by

$$R(\theta) = \begin{cases} -\frac{\sigma^2}{\theta} \sum_{i=1}^{d} \log(1 - \frac{\theta}{d} \alpha^2 \tilde{X}_{11}^{(\lambda_i)}) & \text{if } \sqrt{\theta} H_{\infty} < \sqrt{d}, \\ \infty & \text{if } \sqrt{\theta} H_{\infty} \ge \sqrt{d}, \end{cases}$$
(4.11)

where $\{\lambda_i\}_{i=1}^d$ are the eigenvalues of Q, H_{∞} is given by (3.16), and $\tilde{X}^{(\lambda_i)} \in \mathbb{R}^{2\times 2}$ is the stabilizing solution to (4.10) for $\lambda = \lambda_i$, i.e., $\tilde{X}^{(\lambda_i)}$ is positive semi-definite solving (4.10) for $\lambda = \lambda_i$ and satisfies $\rho(\tilde{A}^{(\lambda_i)} + \gamma^{-2}\tilde{B}\tilde{B}^{\top}\tilde{X}^{(\lambda_i)}) < 1$.

Proof. The proof is given in section B.

Remark 4.2. Theorem 4.1 relies on Riccati equations for providing a formula for the risk-sensitive index and applies only when $\theta > 0$. Later on, in theorem 4.4 and theorem 4.6, we will provide an alternative approach based on the evaluation of an integral that applies to the $\theta < 0$ case as well.

We note that the solutions to the 2×2 Riccati equations in (4.10) of Theorem 4.1 can be computed by a similar approach to (4.9). For a given parameter $\lambda > 0$, it would suffice to compute the generalized eigenvalues and eigenvectors of the following 4×4 pencil:

$$M^{(\lambda)}(\tilde{\mu}) := \tilde{\mu} \begin{bmatrix} \mathbf{I}_2 & -\tilde{B}\tilde{B}^\top/\gamma^2 \\ \mathbf{0}_2 & (\tilde{A}^{(\lambda)})^\top \end{bmatrix} - \begin{bmatrix} \tilde{A}^{(\lambda)} & \mathbf{0}_2 \\ -\tilde{Q}^{(\lambda)} & \mathbf{I}_2 \end{bmatrix}, \quad \text{where} \quad \tilde{Q}^{(\lambda)} = \begin{bmatrix} \frac{\lambda}{2} & \mathbf{0} \\ \mathbf{0} & \mathbf{0} \end{bmatrix}.$$

That is, given the eigenvalues $\{\lambda_i\}_{i=1}^d$ of Q, one must compute pairs $(\tilde{\mu}_i, \tilde{v}_i)$ satisfying $M^{(\lambda_i)}(\tilde{\mu}_i)\tilde{v}_i = 0$ for all $i = 1, \ldots, d$. Another approach is to solve (4.10) directly, which involves three unknowns—the entries of the symmetric 2×2 matrix—and three polynomial equations in these variables of degree at most four. For instance, the Symbolic Toolbox of MATLAB can be used to express the solutions with an explicit formula. That being said, for gradient descent (GD), we can also compute the solutions explicitly by hand and obtain a formula for the risk-sensitive index which is provided in the next result.

Corollary 4.3. Under the premise of theorem 4.1, given a step size $\alpha \in (0, \frac{2}{L})$, consider the gradient descent method, i.e., $\beta = \nu = 0$, the risk-sensitive index corresponding to the risk parameter $\theta > 0$ is given by

$$R(\theta) = \begin{cases} -\frac{\sigma^2}{\theta} \sum_{i=1}^{d} \log\left(1 - \frac{\theta}{d}\alpha^2 \tilde{a}_i\right) & \text{if } \sqrt{\theta} H_{\infty} < \sqrt{d};\\ \infty & \text{if } \sqrt{\theta} H_{\infty} \ge \sqrt{d}, \end{cases}$$
(4.12)

with

$$H_{\infty} = \begin{cases} \frac{1}{\sqrt{2\mu}} & \text{if } 0 < \alpha \le \frac{2}{L + \sqrt{L\mu}}; \\ \frac{\alpha\sqrt{L}}{\sqrt{2(2 - \alpha L)}} & \text{if } \frac{2}{L + \sqrt{L\mu}} < \alpha < \frac{2}{L}, \end{cases}$$

$$(4.13)$$

and

$$\tilde{a}_i := \frac{1}{2} \left(\frac{\lambda_i}{2} + c_{\text{GD}} \left(1 - (1 - \alpha \lambda_i)^2 \right) - \sqrt{\left(\frac{\lambda_i}{2} + c_{\text{GD}} \left(1 - (1 - \alpha \lambda_i)^2 \right) \right)^2 - 2c_{\text{GD}} \lambda_i} \right),$$

if $1 - \alpha \lambda_i \neq 0$ and $\tilde{a}_i := \frac{\lambda_i}{2}$ if $1 - \alpha \lambda_i = 0$, where $c_{\text{GD}} := \frac{d}{\alpha^2 \theta}$ and $\{\lambda_i\}_{i=1}^d$ are the eigenvalues of Q.

Proof. The proof follows from theorem 4.1 through constructing an explicit solution $\tilde{X}^{(\lambda_i)}$ to the DARE in (4.10) for $\lambda = \lambda_i$ and i = 1, 2, ..., d. Let $i \in \{1, ..., d\}$ be fixed. For gradient descent, we have $\beta = \nu = 0$; hence,

$$\tilde{A}^{(\lambda_i)} = \begin{bmatrix} 1 - \alpha \lambda_i & 0 \\ 1 & 0 \end{bmatrix}, \quad \tilde{B} = \begin{bmatrix} -\alpha \\ 0 \end{bmatrix}.$$

The sparsity structure of $\tilde{A}^{(\lambda_i)}$ implies that the solution $\tilde{X}^{(\lambda_i)}$ has the following form:

$$\tilde{X}^{(\lambda_i)} = \begin{bmatrix} \tilde{a}_i & 0\\ 0 & 0 \end{bmatrix},\tag{4.14}$$

for some non-negative scalar \tilde{a}_i (that may depend on λ_i). It follows after a straightforward computation that such an $\tilde{X}^{(\lambda_i)}$ is a solution to (4.10) for $\gamma = \frac{1}{\sqrt{\theta/d}}$ and $\lambda = \lambda_i$ if \tilde{a}_i satisfies

$$\tilde{a}_i = (1 - \alpha \lambda_i)^2 \tilde{a}_i + (1 - \alpha \lambda_i)^2 \tilde{a}_i^2 \left(\frac{d}{\theta \alpha^2} - \tilde{a}_i\right)^{-1} + \frac{1}{2} \lambda_i.$$

If $1 - \alpha \lambda_i = 0$, then we have $\tilde{a}_i = \frac{1}{2}\lambda_i$; otherwise, if $1 - \alpha \lambda_i \neq 0$, then this is a scalar quadratic equation with solutions of the form:

$$\tilde{a}_{i,\pm} = \frac{1}{2} \left(\frac{\lambda_i}{2} + c_{\text{GD}} \left(1 - (1 - \alpha \lambda_i)^2 \right) \pm \sqrt{\left(\frac{\lambda_i}{2} + c_{\text{GD}} \left(1 - (1 - \alpha \lambda_i)^2 \right) \right)^2 - 2c_{\text{GD}} \lambda_i} \right)$$

where $c_{\text{GD}} = \frac{d}{\alpha^2 \theta}$. Since we are interested in the stabilizing solution of the Riccati equation of (4.10), i.e., the solution $\tilde{X}^{(\lambda_i)}$ that satisfies $\rho(\tilde{A}^{(\lambda_i)} + \gamma^{-2}\tilde{B}\tilde{B}^{\top}\tilde{X}^{(\lambda_i)}) < 1$, we take $\tilde{a}_i = \tilde{a}_{i,-}$. Then, with such choice of \tilde{a}_i , the matrix $\tilde{X}^{(\lambda_i)}$ is a stabilizing solution of the Riccati equation in (4.10), and we conclude from theorem 4.1 that the formula in (4.12) holds with H_{∞} , given in (3.16); moreover, for GD, since we have $\beta = \nu = 0$, the formula in (3.16) simplifies to (4.13), and we conclude.

4.1. Numerical experiments comparing risk, convergence rate, and parameter choice. In this section, we investigate the relationship among risk-sensitive cost, parameter selection, and convergence rate in common parameterizations of GMMs from a numerical perspective. See table 1 for a list of common parameters which covers HB, NAG and GD methods. The last column of this table provides the linear convergence rate $\rho \in (0,1)$ associated with the stated parameters as a function of the condition number $\kappa := L/\mu$ when there is no noise.²

We focus on a simple strongly convex quadratic problem of the form (4.1) with $d=2, L=3, \mu=1, g=[0,\ 0]^{\top}, h=0, Q=\begin{bmatrix} \mu & 0 \\ 0 & L \end{bmatrix}$. We set $\sigma^2=2$, and we conduct the experiments for various values of $\theta>0$ chosen appropriately so that $\sqrt{\theta}H_{\infty}<\sqrt{d}=\sqrt{2}$ –otherwise $R(\theta)$ would be infinite by theorem 4.1.

In fig. 1, we plot $R(\theta)$ for several GMM parameterizations, computed analytically with the DARE-based formula given in theorem 4.1. This formula is valid for $\theta \in \left(0, \frac{d}{H_{\infty}^2}\right)$, and $R(\theta)$ diverges when $\theta \geq \bar{\theta} := \frac{d}{H_{\infty}^2}$; hence, we truncated each curve in fig. 1 around $\bar{\theta}$.

Certain choice of parameters offer more flexibility in θ selection than others, as the H_{∞} -norm depends on these parameters. We observe from fig. 1 that methods achieving the fastest convergence rates (smallest ρ)—such as HB-fastest, GD-fastest, TMM, and NAG-fastest—often exhibit the highest risk and the least flexibility (as they admit a larger H_{∞} -norm).

²If $w_{k+1} = 0$ for every k; then $\rho^2 \in [0,1)$ is such that $f(x_k) - f(x_*) \le \bar{c}_k \rho^{2k} [f(x_0) - f(x_*)]$ where \bar{c}_k has at most polynomial growth, see e.g., [58]. Here, we abuse the notation and use ρ to denote both the spectral radius of a matrix and the convergence rate, similar to the literature [95, 57].

Conv. Rate (ρ) Alg. **Parameters** Comments without noise Popular default choice $\alpha = \frac{1}{L}, \ \beta = \nu = 0$ $1 - \frac{1}{\kappa} [95]$ GD-pop [95].GD-Fastest rate without $\alpha = \frac{2}{L+\mu}, \ \beta = \nu = 0$ $1 - \frac{2}{\kappa + 1}$ [95] fastest noise [95]. Fastest rate while $\alpha = \frac{2}{L + \sqrt{L\mu}}, \ \beta = \nu = 0$ $1 - \frac{2}{\kappa + \sqrt{\kappa}}$ [57] RS-GD achieving optimal H_{∞} [57]. NAG-Popular Nesterov setting $\alpha = \frac{1}{L}, \ \beta = \nu = \frac{1 - 1/\sqrt{\kappa}}{1 + 1/\sqrt{\kappa}}$ $1 - \frac{1}{\sqrt{\kappa}}$ [95] [95].pop NAG-Fastest known rate for $\alpha = \frac{4}{3L+\mu}, \ \beta = \nu = \frac{\sqrt{3\kappa+1}-2}{\sqrt{3\kappa+1}+2}$ $1 - \frac{2}{\sqrt{3\kappa+1}} [95]$ fastest quadratics [95]. Tunable α with matching NAG- $\alpha \in \left(0, \frac{1}{L}\right], \ \beta = \nu = \frac{1 - \sqrt{\alpha \mu}}{1 + \sqrt{\alpha \mu}}$ β optimizing ρ [52, $1 - \sqrt{\alpha \mu} \ [52]$ beta-opt Lemma 2.1]. $\alpha = \frac{1+\rho}{L}, \ \beta = \frac{\rho^2}{2-\rho}, \ \nu = \frac{\rho^2}{(1+\rho)(2-\rho)}$ $\alpha = \frac{4}{(\sqrt{L}+\sqrt{\mu})^2}, \ \beta = \left(\frac{\sqrt{\kappa}-1}{\sqrt{\kappa}+1}\right)^2, \nu = \frac{\rho^2}{(1+\rho)(2-\rho)}$ $1 - \frac{1}{\sqrt{\kappa}} \ [10]$ TMM Proposed in [10]. Fastest rate without $1 - \frac{2}{\sqrt{\kappa} + 1}$ [95] HBnoise [95]. $1 - \frac{\sqrt{2}}{\sqrt{\kappa}} + \mathcal{O}\left(\frac{1}{\kappa\sqrt{\kappa}}\right)$ as $\kappa \to \infty$ [57] $\alpha = \frac{a^2(\kappa)}{L}, \ \beta = \left(1 - \frac{a(\kappa)}{\sqrt{\kappa}}\right)^2, \nu = 0$ RS-HB Proposed in [57].

Table 1. Common parameterizations of GMMs.

For NAG, we compare three step sizes: $\alpha = \frac{4}{3L+\mu}$ (NAG-fastest), $\alpha = \frac{1}{L}$ (NAG-pop), and $\alpha = \frac{1}{2L}$ (NAG-beta-opt) –since $L > \mu$, $\frac{4}{3L+\mu} > \frac{1}{L} > \frac{1}{2L}$, each choice of α is paired with the momentum parameter $\beta = \nu = \frac{1-\sqrt{\alpha\mu}}{1+\sqrt{\alpha\mu}}$ –this choice is in line with NAG-pop and NAG-fastest parameter choice stated in table 1. All variants achieve the accelerated rate $\rho = 1 - \Theta\left(\frac{1}{\sqrt{\kappa}}\right)$, with step size affecting the constant factor. Notably, smaller step sizes yield slower convergence but significantly lower risk, illustrating the trade-off between rate and risk sensitivity. A similar pattern holds for gradient descent (GD), where we compare three step sizes: $\alpha = \frac{2}{L+\mu}$ (GD-fastest), $\alpha = \frac{2}{L+\sqrt{L\mu}}$ (RS-GD), and $\alpha = \frac{1}{L}$ (GD-pop). As the step size decreases, the convergence rate slows, i.e., corresponding ρ value increases, but the corresponding risk sensitivity measured by the risk-sensitive index $R(\theta)$ improves and the $R(\theta)$ is finite for a wider range of $\theta > 0$. This highlights a fundamental trade-off: improved flexibility in choice of θ and lower risk sensitivity come at the expense of slower convergence.

In fig. 2(a), we plot the H_{∞} -norm for GD as a function of the step size based on the formula (4.13). The best robustness in the H_{∞} sense—namely, the minimal achievable H_{∞} -norm of $\frac{1}{\sqrt{2\mu}}$, as implied by (4.13) and theorem 3.4—is attained only when $0 < \alpha \le \alpha_{\rm crit} := \frac{2}{L + \sqrt{L\mu}}$. In particular, RS-GD works with this maximal step size $\alpha_{\rm crit}$ that provides the fastest rate

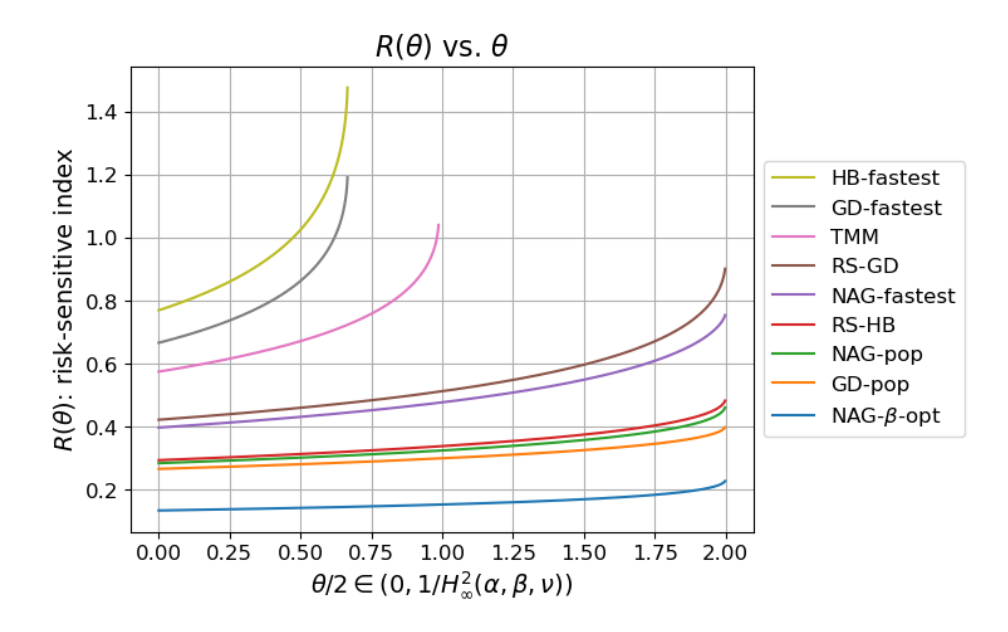


FIGURE 1. Risk sensitivity for common parameterizations of GMM methods; $d=2, L=3, \mu=1, \sigma^2=2$.

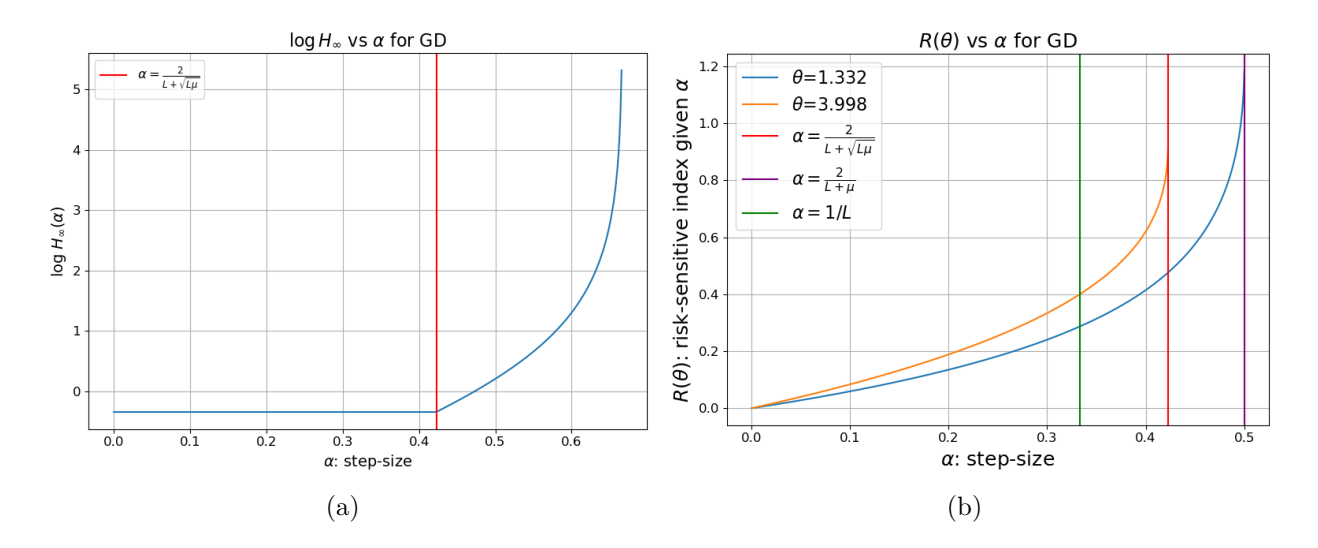


FIGURE 2. (a) H_{∞} as a function of α based on (4.13) in the same problem setting; (b) The risk-sensitive index as a function of GD step-size α for $\theta \approx \{4/3, 4\}$, where the objective is a quadratic with $d = 2, L = 3, \mu = 1$, and $\sigma^2 = 2$.

subject to the best (smallest) H_{∞} -norm.³ For $\alpha > \alpha_{\rm crit}$, H_{∞} -norm increases with α ; therefore, the range of θ for which the risk-sensitive index is finite gets narrower. This is illustrated in fig. 2(b), which plots the risk as a function of the step size for GD with two choices of θ , namely around 4 (orange) and 4/3 (blue). Comparing three step size choices, $\alpha = \frac{1}{L}$ (GD-pop), $\alpha = \frac{2}{L+\mu}$ (GD-fastest), and $\alpha = \alpha_{\rm crit}$ (RS-GD), we observe that the risk becomes infinite for GD-fastest as θ approaches 4/3, whereas for the same θ value, the risk is still

 $^{^3\}mathrm{GD}$ admits the convergence rate $\rho_{\mathrm{GD}}(\alpha) = \max\{|1-\alpha\mu|, |1-\alpha L|\}$ for $\alpha \in (0,\frac{2}{L}),$ see [16].

finite for the other step size choices (that are relatively smaller). Similarly, the risk associated with RS-GD tends to infinite as θ approaches 4 but it is finite for smaller choices of the step size. Basically, faster convergence rates come at the expense of increased risk sensitivity.

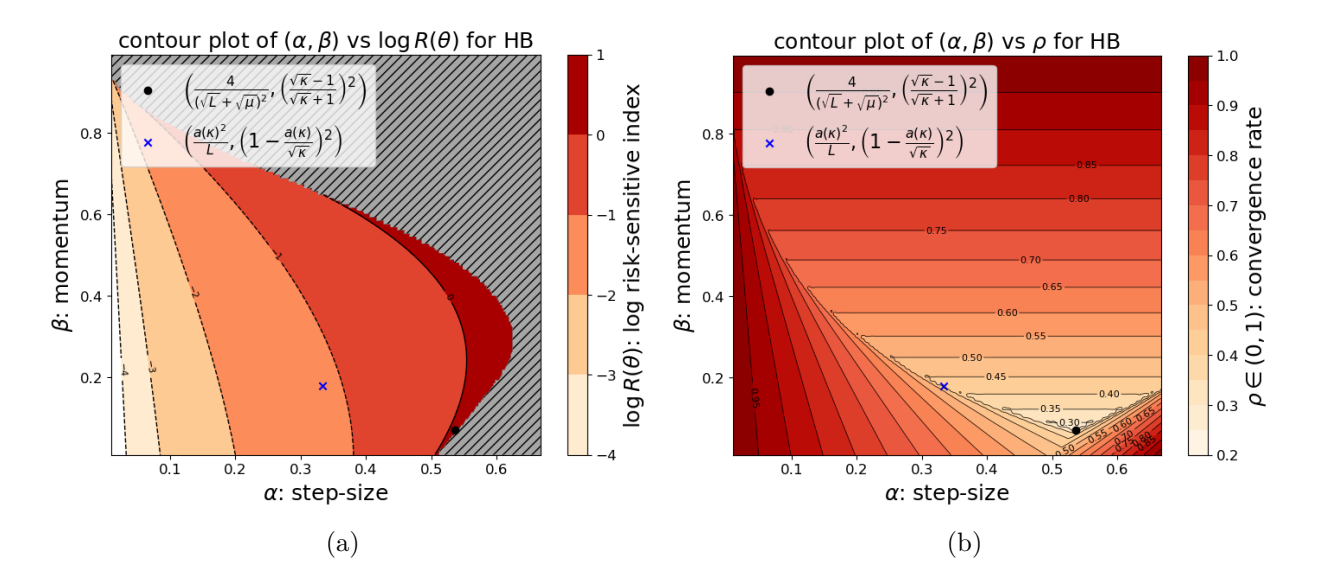


FIGURE 3. (a) Logarithm of the risk-sensitive index $R(\theta)$ as a function of the parameters α, β of HB with $\theta = 1.2$, $\sigma^2 = 2, \nu = 0$. (b) Convergence rate ρ as a function of α, β . The objective is a quadratic with $d = 2, L = 3, \mu = 1$.

In fig. 3, we consider the HB algorithm on a quadratic function with $\mu=1, L=3, d=2, \sigma^2=2, \theta=1.2$ and plot the logarithm of risk-sensitive index (fig. 3(a)) and the convergence rate ρ (fig. 3(b)) as a function of the step size α and momentum parameter β —see [58, Lemma 3.1] for a precise convergence rate characterization of HB for strongly convex quadratics. The black dot indicates the standard HB parameters that yield the fastest convergence rate, while the blue cross represents the parameters of the RS-HB method, which achieve the best known rate while minimizing the H_{∞} -norm [57]. The shaded gray region denotes parameter values for which the risk becomes infinite. As shown in fig. 3, the fastest convergence rate in the noiseless case (black dot) comes at the cost of higher risk, whereas the RS-HB configuration (blue cross), offers improved robustness with a lower risk sensitivity and H_{∞} -norm. Overall, we observe that faster convergence rates (lighter colors in fig. 3(b)) are typically accompanied by higher risk (darker colors in fig. 3(a)).

In fig. 4, we observe a phenomenon similar to the HB case for the NAG algorithm. The parameter setting labeled NAG-fastest (black dot), which achieves the fastest convergence rate in the absence of noise, incurs a higher risk compared to NAG-pop (blue cross), a commonly used parameterization. While NAG-fastest offers faster convergence, it comes at the cost of increased risk. As in GD and HB, the higher risk values are generally associated with faster convergence rates also for NAG.

As demonstrated so far, a faster rate, i.e., smaller $\rho \in (0,1)$, comes often at the expense of an increased risk sensitivity index. To better understand this relationship, fixing the risk parameter $\theta = 0.2$, we examine the Pareto-optimal boundary in Figure 5 for the same simple quadratic problem we used for fig. 1, i.e., $d = 2, L = 3, \mu = 1$, and $\sigma^2 = 2$. In this setting, a point (ρ, R) in the plane of convergence rate $\rho \in (0, 1)$ and risk sensitivity index $R \ge 0$ is said

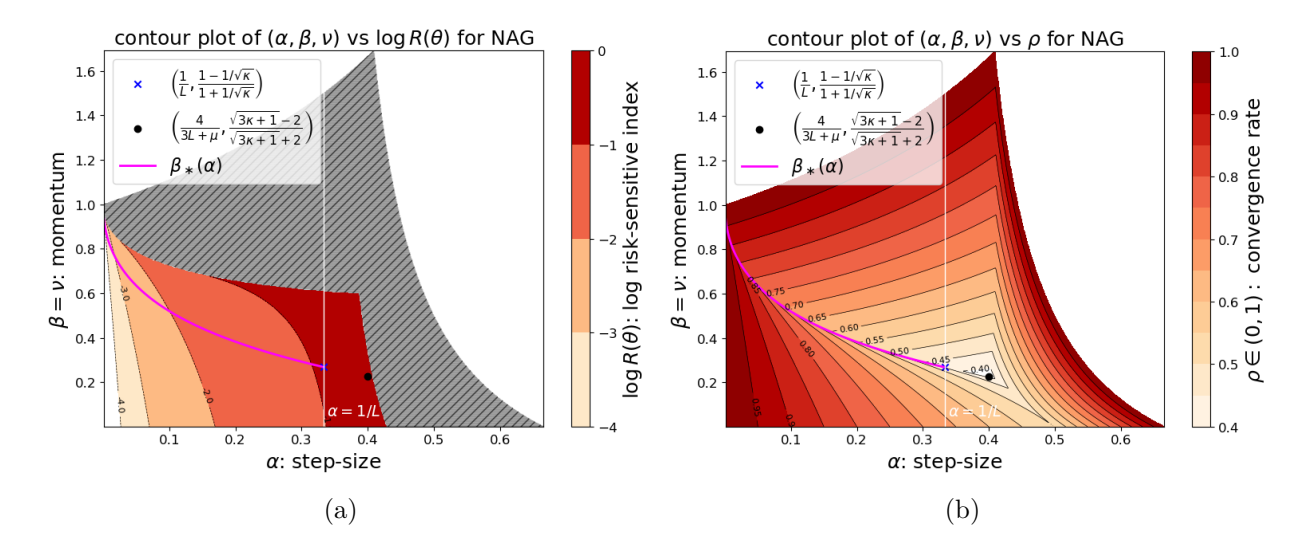


FIGURE 4. (a) Logarithm of the risk-sensitive index $R(\theta)$ as a function of the parameters α, β of NAG with $\theta = 3.7$, $\sigma^2 = 2, \nu = \beta$. (b) Convergence rate ρ as a function of α, β , where $\beta_*(\alpha) = \frac{1 - \sqrt{\alpha \mu}}{1 + \sqrt{\alpha \mu}}$ for $\alpha \in [0, \frac{1}{L}]$. The objective is a quadratic with $d = 2, L = 3, \mu = 1$.

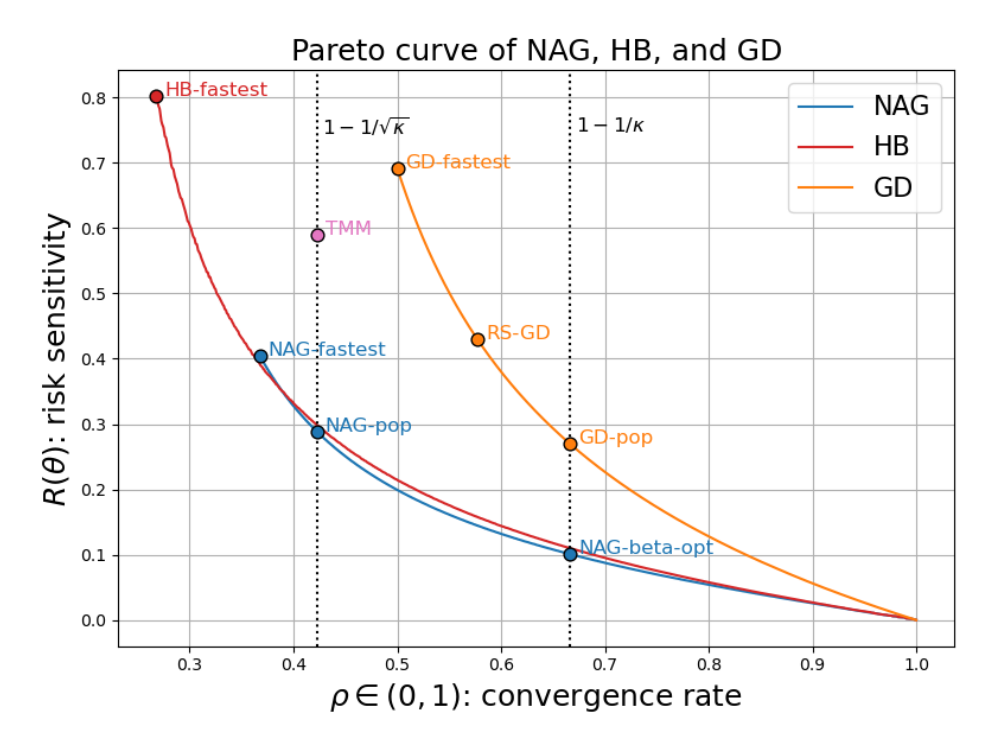


FIGURE 5. Pareto boundary for GD, NAG, HB illustrating the trade-off between risk and rate for a quadratic objective with $d=2, L=3, \mu=1, \sigma^2=2, \theta=0.2$.

to lie on the Pareto-optimal boundary if there is no other achievable pair (ρ', R') with $\rho' < \rho$ and $R' \le R$, or $\rho' \le \rho$ and R' < R. Equivalently, one cannot improve both the rate and the risk

simultaneously beyond a Pareto-optimal point. In fig. 5, each smooth curve corresponds to one algorithm (GD, HB, NAG), parametrized by its step-size α (and momentum parameters β, ν where applicable). As we slide α (and β, ν) within the stability region, we trace out the set of all achievable $(\rho(\alpha, \beta, \nu), R(\alpha, \beta, \nu))$. The Pareto frontier is the upper-left envelope of these curves: it marks the parameters that has the lowest risk R for a given achievable rate ρ for a method. This frontier is numerically estimated via a grid search over the parameter space using the convergence rate formula from [58] and the explicit risk characterization provided in theorem 4.1.

The dashed vertical lines on the right of Figure 5 marks the standard rate $1-\frac{1}{\kappa}$ achieved by gradient descent with common step size $\alpha = 1/L$ while the other line on the left marks the accelerated rate $1 - \frac{1}{\sqrt{\kappa}}$ with the square root dependency to κ ; indeed, $1 - \frac{1}{\kappa} > 1 - \frac{1}{\sqrt{\kappa}}$ here as $\kappa > 1$. Dots label classical parameter choices within the parameter space of each algorithm -see Table 1 for the definitions of these parameter choices. We observe that GD achieves the most *conservative* frontier: its Pareto-optimal curve lies above those of the momentum methods HB and NAG shown here. Although GD-fastest attains the best rate achievable by GD, it remains slower and riskier than NAG-pop and NAG-fastest. For moderate rates $(\rho \approx 0.5-1.0)$, the Pareto-optimal curve of HB shows that HB can achieve lower risk than GD. At very fast rates ($\rho \approx 0.25$ –0.275) which GD cannot achieve, HB's accelerated dynamics come with increased risk sensitivity. NAG's popular tuning, NAG-pop, lies slightly below HB for low-to-moderate rates, achieving a small reduction in risk for the same ρ . NAG-fastest is faster than NAG-pop as expected, but admits a slightly higher risk than what HB can achieve for the same rate. On the other hand, TMM sits clearly above NAG and HB, indicating that while it is able to achieve a faster rate than GD, its risk sensitivity index is more than its counterparts which are able to achieve the same rate (NAG-pop has exactly the same rate) in the quadratic setting. Finally, if the step size, α , is carefully selected, one can achieve the same rate as GD-pop with NAG-beta-opt while simultaneously minimizing risk sensitivity among all competing popular parameterizations –indeed, for Figure 5 we selected $\alpha = \frac{\mu}{L^2}$ for NAG-beta-opt to match GD-pop's convergence rate.

4.2. Large deviations and the risk-sensitive index. It is well-known that averaging iterates can help with optimization performance in inexact gradient settings, see e.g., [57, 99, 100, 24, 114] and the references therein. If we consider the ergodic averages of the iterates

$$\bar{x}_K := \frac{x_0 + x_1 + \dots + x_K}{K + 1},$$

a natural performance metric we want to control is the probability $\mathbb{P}(f(\bar{x}_K) - f_* \geq t)$ that the suboptimality is larger than a given threshold t > 0. Clearly, by convexity, we have the bound

$$\mathbb{P}(f(\bar{x}_K) - f_* \ge t) \le \mathbb{P}\left(\frac{\sum_{j=0}^K \left[f(x_j) - f_*\right]}{K+1} \ge t\right) = \mathbb{P}\left(\frac{S_K}{K+1} \ge t\right). \tag{4.15}$$

The decay rate of this probability as a function of t is related to the large deviation behavior of the sequence of random variables $\Delta_K = S_K/(K+1)$ for $K \ge 0$ [107, 65]. Large deviations aim to quantify the exponential decay rate of the probabilities corresponding to rare events. More

 $^{^4}$ A 3000 × 3000 grid is used for HB and NAG over the interval $(0, \frac{2}{L}) \times (0, 2)$ for (α, β) . For HB we set $\nu = 0$, while for NAG we set $\nu = \beta$. A grid of size 5000 is used for GD over the interval $(0, \alpha^*)$, where $\alpha^* \coloneqq \frac{2}{L+\mu} = \max\{\frac{1}{L}, \frac{2}{L+\mu}, \frac{2}{L+\sqrt{L\mu}}\}$, for which GD achieves the fastest rate.

specifically, given a sequence of random variables $\{\Delta_K\}_{K\geq 0}$, we say that the sequence Δ_K satisfies a large deviation principle (LDP) if there exists a non-negative, lower semi-continuous function $I: \mathbb{R} \to [0, \infty]$ such that for every (Borel) measurable set $E \subset \mathbb{R}$, it holds that

$$-\inf_{s\in E^o} I(s) \le \liminf_{K\to\infty} \frac{1}{K} \log \mathbb{P}(\Delta_K \in E) \le \limsup_{K\to\infty} \frac{1}{K} \log \mathbb{P}(\Delta_K \in E) \le -\inf_{s\in \bar{E}} I(s), \quad (4.16)$$

where E^o and \bar{E} denotes the interior and closure of the set E. If only the (upper-bound) rightmost inequality in (4.16) holds (either for all Borel sets E or for certain classes of sets), then we say that $\{\Delta_K\}$ satisfies an LDP upper bound. The function $I(\cdot)$ is called the rate function. A rate function is called a good rate function if it admits compact level sets; this allows the infimum over I(s) in (4.16) to be attained at some point in the closure of E, i.e., \bar{E} . One difficulty in characterizing a good rate function arises from the fact that the random variables $\{f(x_k) - f_*\}_{k\geq 0}$ are not i.i.d., even when the noise sequence $\{w_{k+1}\}_{k\geq 0}$ is i.i.d. Consequently, standard large deviations results such as Cramér's Theorem do not apply. In the following result, we characterize the rate function by verifying the conditions of the Gärtner–Ellis Theorem [65], which accommodates non-i.i.d. sequences similar to $\{f(x_k) - f_*\}_{k\geq 0}$. This characterization further leverages the risk-sensitive index formula, established in the proof of theorem 4.1, expressed as an integral over the unit circle.

Proposition 4.4. Let f be a quadratic of the form (4.1). Assume that the gradient noise follows an isotropic Gaussian distribution, i.e., Assumption 3.1 holds for an i.i.d. sequence $\{w_{k+1}\}_{k\geq 0}$ with $w_{k+1} \sim \mathcal{N}(0, \frac{\sigma^2}{d} \mathsf{I}_d)$ for some $\sigma > 0$. Let the parameters (α, β, ν) of GMM be such that $\rho(A_Q) < 1$ for A_Q defined in (4.6). Then, the sequence $\{\Delta_K\}_{K\geq 0}$ such that $\Delta_K = S_K/(K+1)$ satisfies an LDP with the following rate function:

$$I(s) = \sup_{-\infty < \theta < \frac{d}{H_{\infty}^2}} \left[\frac{\theta}{2\sigma^2} \left(s - R(\theta) \right) \right], \tag{4.17}$$

which is a good rate function, where H_{∞} satisfies (3.16) and the risk-sensitive index admits the integral representation

$$R(\theta) = \begin{cases} -\frac{\sigma^2}{2\pi\theta} \int_{-\pi}^{\pi} \log \det \left(\mathsf{I}_d - \frac{\theta}{d} G(e^{i\omega}) G(e^{i\omega})^* \right) d\omega, & \text{if } -\infty < \theta < \frac{d}{H_{\infty}^2}; \\ +\infty, & \text{if } \theta \ge \frac{d}{H_{\infty}^2}, \end{cases}$$

$$(4.18)$$

with the convention that the value at $\theta = 0$ is interpreted by continuity as the limit

$$R(0) = \lim_{\theta \to 0} -\frac{\sigma^2}{2\pi \theta} \int_{-\pi}^{\pi} \log \det \left(\mathsf{I}_d - \frac{\theta}{d} G(e^{i\omega}) G(e^{i\omega})^* \right) d\omega \tag{4.19}$$

$$= \frac{\sigma^2}{2\pi d} \int_{-\pi}^{\pi} \operatorname{trace}\left(G(e^{i\omega}) G(e^{i\omega})^*\right) d\omega. \tag{4.20}$$

Here, $G(z) := T(z|_{2d} - A_Q)^{-1}B \in \mathbb{R}^{d \times d}$ for $z \in \mathbb{C} \backslash Spec(A_Q)$ where $Spec(A_Q)$ denotes the set of eigenvalues of A_Q , $G(e^{i\omega})^*$ denotes the Hermitian (conjugate) transpose of $G(e^{i\omega})$, B and T are defined in (3.4) and (4.7), respectively. Furthermore, for any t > 0,

$$\limsup_{K \to \infty} \frac{1}{K} \log \mathbb{P}(f(\bar{x}_K) - f_* > t) \le \lim_{K \to \infty} \frac{1}{K} \log \mathbb{P}\left(\frac{S_K}{K+1} \ge t\right) = -\inf_{s \in [t,\infty)} I(s). \tag{4.21}$$

Proof. The proof is provided in section C.1.

Remark 4.5. Since $R(\theta) < +\infty$ if and only if $\theta H_{\infty}^2 < d$ (cf. (4.18)), the supremum in (4.17) may equivalently be taken over all $\theta \in \mathbb{R}$, i.e., $I(s) = \sup_{\theta \in \mathbb{R}} \frac{\theta}{2\sigma^2} \left(s - R(\theta) \right)$. With the change of variable $\lambda = \theta/(2\sigma^2)$ and $\tilde{\Lambda}(\lambda) = \lambda R(2\sigma^2\lambda)$, we obtain $I(s) = \sup_{\lambda \in \mathbb{R}} \{\lambda s - \tilde{\Lambda}(\lambda)\}$, i.e., I is the Fenchel–Legendre (convex) conjugate of $\tilde{\Lambda}$; hence, $\tilde{\Lambda}$ is simply a scaled version of the risk-sensitive index. See section C.1 (proof of theorem 4.4) for details.

With some additional effort, involving the computation of the matrix $G(e^{i\omega})G^*(e^{i\omega})$ and leveraging its diagonal structure, we can simplify the integral representation (4.18) in the following corollary.

Corollary 4.6. In the setting of theorem 4.4, the formula (4.18) is equivalent to

$$R(\theta) = \begin{cases} -\frac{\sigma^2}{2\pi\theta} \sum_{i=1}^d \int_{-\pi}^{\pi} \log\left(1 - \frac{\theta}{d} h_{\omega}(\lambda_i)\right) d\omega, & if \quad -\infty < \theta < \frac{d}{H_{\infty}^2}; \\ +\infty, & \theta \ge \frac{d}{H_{\infty}^2}, \end{cases}$$
(4.22)

with the convention that the value at $\theta = 0$ is interpreted by continuity as the limit

$$R(0) = \lim_{\theta \to 0} -\frac{\sigma^2}{2\pi\theta} \sum_{i=1}^d \int_{-\pi}^{\pi} \log\left(1 - \frac{\theta}{d} h_{\omega}(\lambda_i)\right) d\omega = \frac{\sigma^2}{2\pi d} \sum_{i=1}^d \int_{-\pi}^{\pi} h_{\omega}(\lambda_i) d\omega.$$

Here, $\{\lambda_i\}_{i=1}^d$ are the eigenvalues of Q,

$$h_{\omega}(\lambda) := \frac{\alpha^2 \lambda}{2\left(1 + \tilde{b}_{\lambda}^2 + \tilde{c}_{\lambda}^2 + 2\left[\tilde{b}_{\lambda}(1 + \tilde{c}_{\lambda})\cos(\omega) + \tilde{c}_{\lambda}\cos(2\omega)\right]\right)},$$

with $\tilde{b}_{\lambda} = \alpha \lambda (1 + \nu) - (1 + \beta)$ and $\tilde{c}_{\lambda} = \beta - \alpha \lambda \nu$ as in (3.17).

Proof. The proof can be found in section C.2.

In fig. 6(a), we illustrate theorem 4.4 for a quadratic objective as in (4.1) in dimension d=2 with parameters $g=[0,0]^{\top},\ h=0,\ \text{and}\ Q=\begin{bmatrix} \mu & 0 \\ 0 & L \end{bmatrix}$ where $\mu=1,\ L=3.$ The figure displays the rate function I(t) corresponding to various methods and parameter choices within the GMM framework, as listed in table 1, using the dual representation (4.17). This entails computing $R(\theta)$, for which we evaluate the integral in (4.18) numerically. For $\theta > 0$, one may alternatively compute $R(\theta)$ based on the alternative representation (4.11). Since I(t) is a good rate function, it has compact level sets, a property that is evident in the plots. Given that the gradient noise is i.i.d. Gaussian, the iterates follow a Gaussian distribution, and the average suboptimality $S_K/(K+1)$ exhibits exponential tails for all K, including in the limit as $K \to \infty$. This behavior results in the linear growth of I(t) in the large-t regime. Notably, in this regime, HB-fastest, the fastest in terms of convergence rate (see table 1), has the smallest values of I(t), which indicates a slower decay of probabilities for large deviations. As seen from formula (4.17), the rate function is, up to scaling, the convex conjugate (Fenchel-Legendre transform) of the risk-sensitive index (see theorem 4.5). Consequently, a similar trade-off between convergence rate and risk arises: faster convergence entails a slower decay of the probabilities of rare events for sufficiently large t. Due to the parabolic shape of I(t), its minimum is attained at the most probable value of t, i.e., smaller or larger values being relatively less likely.

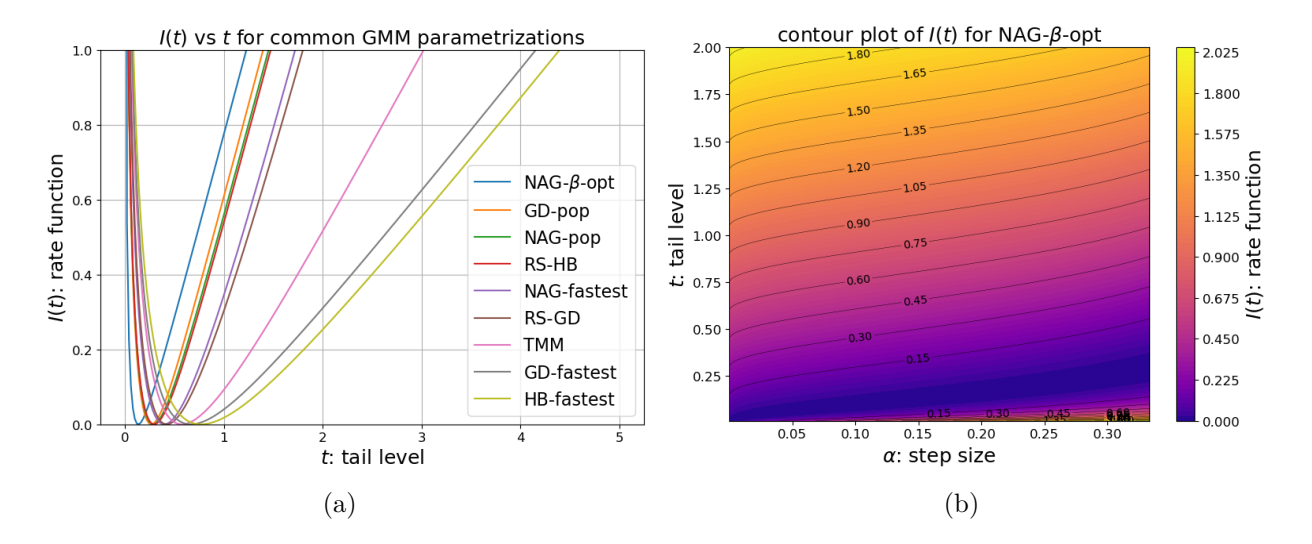


FIGURE 6. (a) The rate function, I(t), for common GMM parameterizations as a function of t, a given suboptimality threshold. (b) The rate function, I(t), for NAG-beta-opt varying step-size α and varying suboptimality threshold, t. The objective is a quadratic with $d=2, L=3, \mu=1, \sigma^2=2$.

In fig. 6(b), we further investigate the NAG-beta-opt method, which exhibits the fastest tail decay for sufficiently large t as seen in fig. 6(a). Specifically, we present a contour plot of the rate function I(t) as a function of α and t under the NAG-beta-opt parameterization, varying the step size $\alpha \in (0, 1/L]$ and the tail threshold t, where $\beta = \frac{1-\sqrt{\alpha\mu}}{1+\sqrt{\alpha\mu}}$. The prominent "purple valley" visible in the plot traces, for each value of α , the corresponding value of t that minimizes I(t)—representing the most probable values achievable at that step size. For a fixed step size, as t increases, I(t) is non-decreasing, as expected, and it governs the decay rate of the probability that the average suboptimality exceeds the threshold t.

5. Main Results for Strongly Convex Objectives

Our analysis in Section 4 focuses on the asymptotic limit of $R_K(\theta)$ as $K \to \infty$ for strongly convex quadratic objectives. In this section, our purpose is to obtain bounds for finite K for more general smooth strongly convex functions $f \in \mathcal{C}^L_\mu(\mathbb{R}^d)$ within our biased noise model.

In general for the class of GMM algorithms, beyond gradient descent, one difficulty is that the squared distance to the optimal solution $||x_k - x_*||^2$ is not necessarily monotonically decreasing [58, Lemma 3.1] even in the absence of noise. This monotonicity issue can be circumvented by analyzing the method using the following more general Lyapunov function:

$$V_{P,c_1}(\xi_k) := c_1 \left(f(x_k) - f(x_*) \right) + \begin{bmatrix} x_k - x_* \\ x_{k-1} - x_* \end{bmatrix}^{\top} P \begin{bmatrix} x_k - x_* \\ x_{k-1} - x_* \end{bmatrix}, \tag{5.1}$$

where $c_1 \geq 0$, $P = \tilde{P} \otimes \mathsf{I}_d$ for some 2×2 symmetric positive semi-definite matrix \tilde{P} . This Lyapunov function has been beneficial in the study of HB, NAG and GMM methods [12, 58, 57, 53, 52] leading to a tight convergence rate analysis without noise (when $w_{k+1} = 0 \ \forall k \geq 0$) for a wide range of parameter values [96]. Indeed, in the absence of noise, it can be certified that GMM iterate sequence linearly converges to x_* with a rate $\rho \in (0,1)$ or better, if ρ and

 \tilde{P} satisfy a 3×3 matrix inequality (MI) [12]. Explicit solutions (ρ, \tilde{P}) that satisfy this MI are known for NAG with the common choice of parameters (NAG-pop, NAG-beta-opt in Table 1), for GD and also for some choices of HB, GMM parameters [58]; however for more general parameters, explicit solutions are not known and they can be computed numerically in an efficient way by solving a 3×3 MI.

When the objective function f is strongly convex and smooth but not quadratic, the dynamical system corresponding to the GMM iterations becomes nonlinear, as the gradients are nonlinear functions of the state. In this setting, although the H_{∞} -norm remains well-defined (as per theorem 3.3), deriving an explicit formula for it does not seem possible, and the proof technique used in theorem 4.1 does not directly apply. Moreover, as observed in section 4, finiteness of the H_{∞} -norm is necessary for the risk $R(\theta)$ to remain finite in a neighborhood of zero, at least for quadratic objectives. Otherwise, $R(\theta)$ can become infinite for any $\theta > 0$. Therefore, to establish finite upper bounds on the risk $R(\theta)$ for general objectives $f \in \mathcal{C}^L_{\mu}(\mathbb{R}^d)$, we must impose conditions on the algorithm parameters that ensure the H_{∞} -norm is finite.

Recent work by [57] establishes a 4×4 MI which, if satisfied, guarantees both a finite upper bound on the H_{∞} -norm and a descent property for the Lyapunov function $V_{P,c_1}(\cdot)$. This result is tight in the sense that, for certain parameter choices, the bound on the H_{∞} -norm matches the corresponding quadratic bounds up to some constants, and in the noiseless case, this MI recovers the rate results implied by the 3×3 MI provided in [12]. We include this result in the appendix (theorem A.1) for completeness, together with its corollaries (theorems A.2 and A.3) that provide explicit bounds \overline{H}_{∞} on the H_{∞} -norm corresponding to GD, NAG-beta-opt and NAG-pop which are obtained by constructing explicit solutions to the MI. In the next result, we show that when the 4×4 MI holds, it also enables us to derive bounds on the risk sensitivity $R_K(\theta)$ for any horizon K and for any $\theta > 0$ satisfying $\sqrt{\theta} \ \overline{H}_{\infty} < 1$. This type of upper bound on θ to guarantee finiteness of H_{∞} is expected; a similar constraint arises in the quadratic case where computations are exact as in (4.12). The proof of this result mirrors the dynamic programming technique employed within the risk-sensitive control [62]. Since the risk metric $R_K(\theta)$ aggregates risk across iterations and the noise sequence $\{w_{k+1}\}_{k>0}$ is conditionally independent from \mathcal{F}_k , we can isolate the contribution of each step via a backward-induction argument while fixing the iteration budget to K. This induction argument makes the critical parameter condition explicit, i.e., $\sqrt{\theta H_{\infty}} < 1$ that guarantees finiteness of the risk for all iteration budgets. The proof relies on a novel Lyapunov function, obtained by modifying $V_{P,c_1}(\xi_k)$ into a weighted form that incorporates convex averages with $V_{P,c_1}(\xi_{k-1})$. Full details are provided in the appendix. This modification allows us to derive tighter bounds.

Theorem 5.1. Consider the noisy GMM iterations stated in (3.8) for minimizing $f \in \mathcal{C}^L_{\mu}(\mathbb{R}^d)$, starting from $x_0 = x_{-1} \in \mathbb{R}^d$ with fixed parameters (α, β, ν) . Let theorem 3.1 hold and consider the risk-sensitive cost in (3.10) for some given arbitrary iteration budget $K \geq 1$ that is fixed. Assume that there exists non-negative scalars $\rho_0, \rho_1, \rho_2, \rho_3 \in [0,1)$, $a,b,c_1,c_0 \geq 0$, and a positive semi-definite matrix $\tilde{P} \in \mathbb{R}^{2 \times 2}$ which satisfies the conditions (i) and (ii) of theorem A.1 so that the H_{∞} -norm of the GMM system admits the finite upper bound

$$\overline{H}_{\infty} := \left(\frac{1}{1 - \left(p + q\right)} \frac{r}{c_1 + \frac{2}{L}\tilde{r}(\tilde{P})}\right)^{1/2} < \infty, \tag{5.2}$$

where

$$p = \rho_0^2 + c_1 \rho_1^2 + \rho_2^2 + \frac{4b(1+\nu)^2 L^2}{\mu} c_1, \quad q = \rho_3^2 + \frac{4b\nu^2 L^2}{\mu} c_1, \quad r := a + \alpha^2 \left(\frac{c_1 L}{2} + \tilde{P}_{11}\right),$$

and

$$\tilde{r}(\tilde{P}) = \begin{cases} \tilde{P}_{11} - \tilde{P}_{12}^2 / \tilde{P}_{22} & \text{if } \tilde{P}_{22} \neq 0, \\ \tilde{P}_{11} & \text{if } \tilde{P}_{22} = 0. \end{cases}$$

Then, given $\theta > 0$, we have the upper bound $R_K(\theta) \leq \overline{R}_K(\theta)$ with

$$\overline{R}_{K}(\theta) := \begin{cases} \frac{1}{\left(c_{1} + \frac{2}{L}\tilde{r}(\tilde{P})\right)(K+1)} \min\left\{\frac{1}{J_{p,q}}\bar{c}\left(K, \frac{\theta}{J_{p,q}}\right), \bar{c}(K+1, \theta)\right\}, & if \sqrt{\theta}\,\overline{H}_{\infty} < 1; \\ +\infty, & otherwise, \end{cases}$$
(5.3)

where
$$\bar{c}(K,\theta) := \left(\frac{1-\lambda_{+}^{K+1}}{1-\lambda_{+}} - 1 + J_{p,q}\right) V_{P,c_{1}}(\xi_{0}) + \hat{c}(K,\theta),$$

$$\lambda_{+} = \frac{p + \sqrt{p^2 + 4q}}{2} \in [0, 1), \quad J_{p,q} = \frac{1}{1 + \lambda_{+} - p} \in (0, 1],$$

$$\hat{c}(K,\theta) := \begin{cases} \frac{2\sigma^2(c_1 + \frac{2}{L}\tilde{r}(\tilde{P}))}{\theta} \sum_{j=1}^K \log\left(\frac{c_1 + \frac{2}{L}\tilde{r}(\tilde{P}) + r \theta a_{j,K}}{c_1 + \frac{2}{L}\tilde{r}(\tilde{P}) - r \theta a_{j,K}}\right), & if \sqrt{\theta} \,\overline{H}_{\infty} < 1, \\ +\infty & else, \end{cases}$$

$$a_{j,K} := \frac{1 - \lambda_+^{K-j+1}}{1 - (p+q)} \quad for \quad j = 1, 2, \dots, K,$$
 (5.4)

and V_{P,c_1} is as in (5.1) with $P = \tilde{P} \otimes I_d$

Proof. The proof is provided in Appendix \mathbb{D} .

As a corollary of this theorem, in the next result, we obtain bounds on the expected suboptimality for the averaged iterates.

Corollary 5.2. Under the premise of theorem 5.1, for any given $K \ge 0$, the expected suboptimality of the averaged iterate $\bar{x}_K := \frac{x_0 + x_1 + \dots + x_K}{K+1}$ satisfies

$$\mathbb{E}[f(\bar{x}_K) - f_*] \leq R_K(0) \tag{5.5}$$

$$\leq \overline{R}_K(0) := \lim_{\theta \downarrow 0} \overline{R}_K(\theta)$$
(5.6)

$$= \frac{\left(c_1 + \frac{2}{L}\tilde{r}(\tilde{P})\right)^{-1}}{K+1} \min\left\{\frac{1}{J_{p,q}}\bar{c}(K,0), \bar{c}(K+1,0)\right\}, \tag{5.7}$$

where

$$\bar{c}(K,0) := \left(\frac{1 - \lambda_{+}^{K+1}}{1 - \lambda_{+}} - 1 + J_{p,q}\right) V_{P,c_{1}}(\xi_{0}) + 4\sigma^{2} r \sum_{j=1}^{K} a_{j,K}.$$

$$(5.8)$$

Proof. From the Taylor expansion of $R_K(\theta)$ around $\theta = 0$, using (3.11) we have:

$$\mathbb{E}[f(\bar{x}_K) - f_*] \le \frac{1}{K+1} \sum_{k=0}^K \mathbb{E}[f(x_k) - f_*] = R_K(0) = \lim_{\theta \downarrow 0} R_K(\theta),$$

where we used the convexity of f in the above inequality. We note that for $\theta > 0$ sufficiently small, $R_K(\theta)$ and $\overline{R}_K(\theta)$ are continuous in θ and they satisfy $R_K(\theta) \leq \overline{R}_K(\theta)$ by theorem 5.1. Furthermore, it is straightforward to check that the limit $\overline{R}_K(0) := \lim_{\theta \downarrow 0} \overline{R}_K(\theta)$ exists and admits the formula in (5.7), which follows from (5.3) and the fact that

$$\lim_{\theta \downarrow 0} \hat{c}(K, \theta) = 4\sigma^2 r \sum_{j=1}^{K} a_{j,K}.$$

Furthermore, $\overline{R}_K(\theta)$ is right-continuous at $\theta = 0$; therefore, it is necessarily the case that $\mathbb{E}[f(\bar{x}_K) - f_*] = R_K(0) \le \overline{R}_K(0) = \lim_{\theta \downarrow 0} \overline{R}_K(\theta)$ and we conclude.

Corollary 5.3. For GD, given any $K \ge 0$ and $\alpha \in (0, \frac{2}{L})$, the risk-sensitive cost admits the following bound:

$$R_K(\theta) \le \min \left\{ \overline{R}_K^{(1)}(\theta), \overline{R}_K^{(2)}(\theta) \right\} \quad \text{for} \quad \theta \in \left(0, \frac{1}{\overline{H}_{\infty}^2}\right)$$

where

$$\overline{H}_{\infty} = \begin{cases} \frac{1}{\sqrt{2\mu}} & \text{if} \quad 0 < \alpha \le \frac{1}{L}, \\ \frac{1}{\sqrt{2\mu}} \frac{\alpha L}{2 - \alpha L} & \text{if} \quad \frac{1}{L} < \alpha \le \frac{2}{L + \sqrt{L\mu}}, \\ \frac{1}{\sqrt{2\mu}} \sqrt{\kappa} & \text{if} \quad \frac{2}{L + \sqrt{L\mu}} < \alpha \le \frac{2}{L + \mu}, \\ \frac{\alpha \sqrt{L}}{\sqrt{2}(2 - \alpha L)} & \text{if} \quad \frac{2}{L + \mu} < \alpha < \frac{2}{L}, \end{cases}$$

$$\overline{R}_{K}^{(1)}(\theta) := \frac{L}{2(K+1)} \left(\frac{1 - [\rho_{GD}(\alpha)]^{K+1}}{1 - \rho_{GD}(\alpha)} \|x_{0} - x_{*}\|^{2} + \frac{4\sigma^{2}}{L\theta} \sum_{j=1}^{K} \log \left(\frac{2 + \frac{\theta L\alpha^{2}}{1 - \rho_{GD}(\alpha)} a_{j,K}^{(1)}}{2 - \frac{\theta L\alpha^{2}}{1 - \theta_{GD}(\alpha)} a_{j,K}^{(1)}} \right) \right),$$

with $a_{j,K}^{(1)} = \frac{1 - [\rho_{GD}(\alpha)]^{K-j+1}}{1 - \rho_{GD}(\alpha)}$ for $j = 1, \dots, K$, $\rho_{GD}(\alpha) = \max\{\|1 - \alpha\mu|, |1 - \alpha L|\}$ and

$$\overline{R}_{K}^{(2)}(\theta) := \frac{1}{K+1} \left[\frac{1 - \left[1 - 2\mu\alpha(1 - \frac{L\alpha}{2}) + \alpha\mu|1 - \alpha L|s_{\text{GD}}\right]^{K+1}}{2\mu\alpha(1 - \frac{L\alpha}{2}) - \alpha\mu|1 - \alpha L|s_{\text{GD}}} [f(x_0) - f_*] \right]$$

$$\left. + \frac{2\sigma^2}{\theta} \sum_{j=1}^K \log \left(\frac{1 + \theta a_{j,K}^{(2)} \alpha \left(\frac{L}{2} \alpha + \frac{|1 - \alpha L|}{2s_{\text{GD}}} \right)}{1 - \theta a_{j,K}^{(2)} \alpha \left(\frac{L}{2} \alpha + \frac{|1 - \alpha L|}{2s_{\text{GD}}} \right)} \right) \right],$$

with
$$a_{j,K}^{(2)} = \frac{1 - \left[1 - 2\mu\alpha(1 - \frac{L\alpha}{2}) + \alpha\mu|1 - \alpha L|s_{\text{GD}}\right]^{K - j + 1}}{2\mu\alpha(1 - \frac{L\alpha}{2}) - \alpha\mu|1 - \alpha L|s_{\text{GD}}}$$
 for $j = 1, ..., K$, $s_{\text{GD}} = 1$ for $\alpha \in [0, \frac{1}{L}]$ and $s_{\text{GD}} = \frac{2 - \alpha L}{\alpha L}$ for $\alpha \in (\frac{1}{L}, \frac{2}{L})$.

Proof. Theorem A.2 shows that the conditions of theorem 5.1 are satisfied for GD with $\alpha \in (0, 2/L)$ if we take

$$p = \rho_{GD}(\alpha) = \max\{|1 - \alpha \mu|, |1 - \alpha L|\}, \quad q = 0, \quad r = \frac{\alpha^2}{1 - \rho_{GD}(\alpha)}, \quad \tilde{P} = \mathbf{I}_2, \quad c_1 = 0,$$

which corresponds to the Lyapunov function $V_{P,c_1}(\xi_k) = ||x_k - x_*||^2$. Then, $\lambda_+ = p$, $J_{p,q} = 1$, $\tilde{r}(\tilde{P}) = 1$ and $\min\{\bar{c}(K,\theta), \bar{c}(K+1,\theta)\} = \bar{c}(K,\theta)$. Invoking theorem 5.1 implies the desired upper bound $\overline{R}_K^{(1)}(\theta)$. Similarly, by theorem A.2, we can also take

$$p = 1 - 2\mu\alpha \left(1 - \frac{L\alpha}{2}\right) + \alpha\mu |1 - \alpha L| s_{\text{GD}}, \ q = 0, \ r = \alpha \left(\frac{L}{2}\alpha + \frac{|1 - \alpha L|}{2s_{\text{GD}}}\right), \ \tilde{P} = 0, \ c_1 = 1,$$

within theorem 5.1, which corresponds to the Lyapunov function $V_{P,c_1}(\xi_k) = f(x_k) - f_*$ and together with $\lambda_+ = p$, $J_{p,q} = 1$ and $\tilde{r}(\tilde{P}) = 0$ leads to the desired upper bound $\overline{R}_K^{(2)}(\theta)$.

Corollary 5.4. For NAG with $\alpha \in (0, 1/L]$ and $\beta = \nu = \frac{1 - \sqrt{\alpha \mu}}{1 + \sqrt{\alpha \mu}}$, the bound (5.3) in theorem 5.1 holds with constants

$$\begin{split} p &= [1 - \sqrt{\alpha \mu}] + \left[\frac{2}{s_1} \left(\frac{\alpha}{4(1 + \sqrt{\alpha \mu})^2}\right)\right] + \left[\frac{2}{\mu} \left(\frac{\alpha^2 \mu^2 + 2\alpha \mu + \alpha \mu (1 - \sqrt{\alpha \mu})}{4(1 + \sqrt{\alpha \mu})^2}\right)\right] + \frac{4L^3 \alpha^2}{2\mu s_2} (1 + \nu)^2 \,, \\ q &= \frac{2}{s_1} \left(\frac{\alpha (1 - \sqrt{\alpha \mu})}{4(1 + \sqrt{\alpha \mu})^2}\right) + \frac{4L^3 \alpha^2 \nu^2}{2\mu s_2} \,, \quad r = a + \alpha^2 \left(\frac{c_1 L}{2} + \tilde{P}_{11}\right) = s_1 + \frac{L\alpha^2 (2 + s_2)}{2s_2} + \frac{\alpha}{2} \,, \\ c_1 &= 1, \quad \tilde{r}(\tilde{P}) = 0 \,, \end{split}$$

where

$$s_1 = \frac{2(5-2\sqrt{\alpha\mu}+\alpha\mu)\sqrt{\alpha}}{\sqrt{\mu}(1+\sqrt{\alpha\mu})^2}, \quad s_2 = \frac{8L^3\alpha\sqrt{\alpha}}{\mu\sqrt{\mu}(1+\sqrt{\alpha\mu})^2}(4+(1-\sqrt{\alpha\mu})^2).$$

Proof. For NAG with this choice of step size α and momentum parameters $\beta = \nu$, by theorem A.3, we observe that the conditions of theorem 5.1 hold for this choice of p, q, r values with $c_1 = 1$ and

$$\tilde{P} = \frac{1}{2\alpha} \begin{bmatrix} 1 \\ -(1 - \sqrt{\alpha \mu}) \end{bmatrix} \begin{bmatrix} 1 & -(1 - \sqrt{\alpha \mu}) \end{bmatrix}.$$

A short computation reveals that for this choice of \tilde{P} , theorem 5.1 is applicable with $\tilde{r}(\tilde{P}) = 0$, and we conclude.

We next leverage theorem 5.1 to bound the risk-sensitive index in the following corollary.

Corollary 5.5. Under the premise of theorem 5.1, for $\theta > 0$ it holds that

$$R(\theta) \leq \overline{R}(\theta) := \limsup_{K \to \infty} \overline{R}_K(\theta) = \begin{cases} \frac{2\sigma^2}{\theta} \log \left(\frac{1 + \theta(\overline{H}_{\infty})^2}{1 - \theta(\overline{H}_{\infty})^2} \right), & \sqrt{\theta} \ \overline{H}_{\infty} < 1, \\ +\infty, & otherwise. \end{cases}$$
(5.9)

Furthermore,

$$\limsup_{K \to \infty} \mathbb{E}[f(\bar{x}_K) - f_*] \le \lim_{\theta \downarrow 0} \overline{R}(\theta) = 4\sigma^2(\overline{H}_\infty)^2.$$
 (5.10)

Proof. By theorem 5.1, for $\theta > 0$ satisfying $\sqrt{\theta} \overline{H}_{\infty} < 1$, we have

$$\limsup_{K \to \infty} \overline{R}_K(\theta) = \frac{1}{c_1 + \frac{2}{L} \tilde{r}(\tilde{P})} \limsup_{K \to \infty} \frac{1}{K+1} \min \left\{ \frac{1}{J_{p,q}} \bar{c}\left(K, \frac{\theta}{J_{p,q}}\right), \bar{c}(K+1, \theta) \right\}$$

$$= \frac{1}{c_1 + \frac{2}{L} \tilde{r}(\tilde{P})} \limsup_{K \to \infty} \frac{1}{K+1} \bar{c}(K+1, \theta)$$
(5.11)

$$= \frac{2\sigma^{2}}{\theta} \limsup_{K \to \infty} \frac{1}{K+1} \sum_{j=1}^{K+1} \log \left(\frac{c_{1} + \frac{2}{L}\tilde{r}(\tilde{P}) + r \, \theta a_{j,K+1}}{c_{1} + \frac{2}{L}\tilde{r}(\tilde{P}) - r \, \theta a_{j,K+1}} \right)$$
(5.13)

$$= \frac{2\sigma^2}{\theta} \limsup_{K \to \infty} \frac{1}{K+1} \sum_{j=1}^{K+1} \log \left(\frac{c_1 + \frac{2}{L} \tilde{r}(\tilde{P}) + r \, \theta a_{1,j}}{c_1 + \frac{2}{L} \tilde{r}(\tilde{P}) - r \, \theta a_{1,j}} \right), \tag{5.14}$$

where we used the definition of $\bar{c}(K+1,\theta)$ and $a_{j,K+1}$ given in theorem 5.1. Since the sequence $\{a_{1,j}\}_{j\geq 1}$ is non-decreasing in j admitting $\lim_{j\to\infty} a_{1,j} = \frac{1}{1-(p+q)}$; the sequence $\ell_j := \log\left(\frac{c_1 + \frac{2}{L}\tilde{r}(\tilde{P}) + r \theta a_{1,j}}{c_1 + \frac{2}{L}\tilde{r}(\tilde{P}) - r \theta a_{1,j}}\right)$ is also non-decreasing and admits the limit

$$\ell_{\infty} := \lim_{j \to \infty} \ell_j = \log \left(\frac{c_1 + \frac{2}{L} \tilde{r}(\tilde{P}) + r \, \theta 1 / (1 - (p + q))}{c_1 + \frac{2}{L} \tilde{r}(\tilde{P}) - r \, \theta 1 / (1 - (p + q))} \right) = \log \left(\frac{1 + \theta (\overline{H}_{\infty})^2}{1 - \theta (\overline{H}_{\infty})^2} \right),$$

using the definition of \overline{H}_{∞} from theorem 5.1. Hence we conclude from (5.14) that

$$\overline{R}(\theta) = \limsup_{K \to \infty} \overline{R}_K(\theta) = \frac{2\sigma^2}{\theta} \ell_{\infty} = \frac{2\sigma^2}{\theta} \log \left(\frac{1 + \theta(\overline{H}_{\infty})^2}{1 - \theta(\overline{H}_{\infty})^2} \right).$$

Since $R(\theta) = \limsup_{K \to \infty} R_K(\theta) \le \limsup_{K \to \infty} \overline{R}_K(\theta)$ and $R_K(\theta) = +\infty$ for $\sqrt{\theta} \overline{H}_{\infty} \ge 1$ for $\forall K$, we obtain (5.9) as desired. With similar computations, taking limit superior on both sides in (5.7) with respect to K and using (5.8), we obtain $\limsup_{K \to \infty} \mathbb{E}[f(\overline{x}_K) - f_*] \le 4\sigma^2(\overline{H}_{\infty})^2$. Finally, the fact that $\lim_{\theta \downarrow 0} \overline{R}(\theta) = 4\sigma^2(\overline{H}_{\infty})^2$ follows simply by taking limit as $\theta \to 0$ in (5.9).

Remark 5.6. For momentum methods with constant step size and unbiased stochastic gradient estimates, ergodic averages converge to a neighborhood controlled by the variance proxy σ^2 . For example, for NAG-beta-opt (using parameters as in table 1) with i.i.d. noise $w_{k+1} \sim \mathcal{N}(0, \frac{\sigma^2}{d})$, [53, Cor. 4.8] gives $\limsup_{K \to \infty} \mathbb{E}[f(\bar{x}_K) - f_*] \leq \sigma^2 \frac{\sqrt{\alpha}}{2\sqrt{\mu}} (1 + \alpha L)$ for $\alpha \in (0, 1/L]$, which vanishes as $\alpha \to 0$. In contrast, under biased noise the neighborhood is generally bounded away from zero, owing to a potentially non-vanishing worst-case drift. From (5.10), the asymptotic error is governed by the bound on H_{∞} -norm. For NAG-beta-opt, under the theorem 3.1, by theorem A.3 in the appendix, we have $\overline{H}_{\infty} = \frac{2\sqrt{5}}{\sqrt{\mu}} + \mathcal{O}(\sqrt{\alpha})$ as $\alpha \to 0$, and by (5.10) this yields $\limsup_{K \to \infty} \mathbb{E}[f(\bar{x}_K) - f_*] \leq \sigma^2 \left(\frac{80}{\mu} + \mathcal{O}(\sqrt{\alpha})\right)$, and the right-hand side remains strictly positive as $\alpha \to 0$. Corollary 5.5 shows that momentum algorithms with smaller bound \overline{H}_{∞} exhibit tighter bounds on the asymptotic (suboptimality) bias, i.e., $\limsup_{K \to \infty} \mathbb{E}[f(\bar{x}_K) - f_*]$. Similar observations can be made for GD, HB or GMM. To our knowledge, this connection to the H_{∞} -norm is entirely new for momentum methods.

For quadratic functions, we obtained large deviation results which obtains both the upper bound and the lower bound in (4.16) through an exact computation of the risk-sensitive index as $K \to \infty$. Beyond quadratics, we have only bounds on the risk-sensitive index. In the following result, we leverage this bound to obtain a large-deviation upper bound and high probability bounds for finite K.

Theorem 5.7. Under the premise of Theorem 5.1, consider the averaged iterates $\bar{x}_K = \frac{\sum_{j=0}^K x_j}{K+1}$. Then, for any $K \ge 1$ given and for any $\theta \in [0, 1/\overline{H}_{\infty}^2)$ and $t \ge 0$, we have

$$\mathbb{P}\left(f(\bar{x}_K) - f_* \ge t\right) \le \mathbb{P}\left(\frac{S_K}{K+1} \ge t\right) \le \exp\left(-(K+1)\frac{\theta}{2\sigma^2}\left(t - \overline{R}_K(\theta)\right)\right). \tag{5.15}$$

Furthermore, for any $t \geq 0$,

$$\mathbb{P}(f(\bar{x}_K) - f_* \ge t) \le \exp\left(-(K+1)\bar{I}_K(t)\right),\tag{5.16}$$

where

$$\bar{I}_{K}(t) := \sup_{0 < \theta < 1/\overline{H}_{\infty}^{2}} \frac{\theta}{2\sigma^{2}} \left(t - \overline{R}_{K}(\theta) \right) \ge \max \left(\check{c}_{K}^{(1)} \Psi \left(\frac{t}{\check{c}_{K}^{(1)}}, \check{a}_{K}^{(1)}, \check{b}_{K}^{(1)} \right), \Psi \left(t, \check{a}_{K}^{(2)}, \check{b}_{K}^{(2)} \right) \right), \tag{5.17}$$

with

$$\check{a}_{K}^{(1)} = \frac{\left(\frac{1-\lambda_{+}^{K+1}}{1-\lambda_{+}} - 1 + J_{p,q}\right)V(\xi_{0})}{\left(c_{1} + \frac{2}{L}\tilde{r}(\tilde{P})\right)K}, \quad \check{b}_{K}^{(1)} = \frac{(1-\lambda_{+}^{K})(\overline{H}_{\infty})^{2}}{J_{p,q}}, \quad \check{c}_{K}^{(1)} = \frac{K}{(K+1)J_{p,q}},$$

$$\check{a}_{K}^{(2)} = \frac{\left(\frac{1-\lambda_{+}^{K+2}}{1-\lambda_{+}} - 1 + J_{p,q}\right)V(\xi_{0})}{\left(c_{1} + \frac{2}{L}\tilde{r}(\tilde{P})\right)(K+1)}, \quad \check{b}_{K}^{(2)} = (1-\lambda_{+}^{K+1})(\overline{H}_{\infty})^{2},$$

and

$$\Psi(t, \check{a}, \check{b}) = \begin{cases} \frac{t - \check{a}}{2\sigma^2 \check{b}} \sqrt{1 - \frac{4\sigma^2 \check{b}}{t - \check{a}}} - \log\left(\frac{1 + \sqrt{1 - \frac{4\sigma^2 \check{b}}{t - \check{a}}}}{1 - \sqrt{1 - \frac{4\sigma^2 \check{b}}{t - \check{a}}}}\right), & if \quad t - \check{a} \ge 4\sigma^2 \check{b}; \\ 0, & if \quad 0 \le t - \check{a} < 4\sigma^2 \check{b}. \end{cases}$$
(5.18)

Proof. The first inequality in (5.15) is a consequence of the convexity of f. The second inequality is trivial for $\theta = 0$, and for $(0, 1/(\overline{H}_{\infty})^2)$ it is simply a Chernoff-type bound. More specifically, for $t \geq 0$, and $\theta \in (0, 1/(\overline{H}_{\infty})^2)$,

$$\mathbb{P}\left(\frac{S_K}{K+1} \ge t\right) = \mathbb{P}\left(\exp\left(\frac{\theta}{2\sigma^2}S_K\right) \ge \exp\left(\frac{\theta}{2\sigma^2}(K+1)t\right)\right) \\
\le \exp\left(-\frac{\theta}{2\sigma^2}(K+1)t\right)\mathbb{E}\left(\exp\left(\frac{\theta}{2\sigma^2}S_K\right)\right) \\
\le \exp\left(-(K+1)\frac{\theta}{2\sigma^2}\left(t-\overline{R}_K(\theta)\right)\right),$$

where we used $\overline{R}_K(\theta) \ge R_K(\theta)$. Then, (5.16) is obtained by taking supremum over θ . Finally, the lower bound on $\overline{I}_K(t)$ given in (5.17) is a consequence of Lemma E.4 in the appendix.

For the large K limit in the previous result, we can obtain the following large deviation bound.

Corollary 5.8. Under the premise of theorem 5.1, it holds that

$$\limsup_{K \to \infty} \frac{1}{K} \log \mathbb{P}(f(\bar{x}_K) - f_* \ge t) \le -\bar{I}(t), \tag{5.19}$$

where

$$\bar{I}(t) := \begin{cases}
\frac{t}{2\sigma^2(\overline{H}_{\infty})^2} \sqrt{1 - \frac{4\sigma^2(\overline{H}_{\infty})^2}{t}} - \log\left(\frac{1 + \sqrt{1 - \frac{4\sigma^2(\overline{H}_{\infty})^2}{t}}}{1 - \sqrt{1 - \frac{4\sigma^2(\overline{H}_{\infty})^2}{t}}}\right), & \text{if } t \ge 4\sigma^2(\overline{H}_{\infty})^2; \\
0, & \text{if } t < 4\sigma^2(\overline{H}_{\infty})^2.
\end{cases} (5.20)$$

Proof. Taking limit superior of both sides in (5.15), for any $\theta \in [0, 1/\overline{H}_{\infty}^2)$,

$$\limsup_{K \to \infty} \frac{1}{K} \log \mathbb{P}(f(\bar{x}_K) - f(x_*) \ge t) = -\frac{\theta}{2\sigma^2} \left(t - \limsup_{K \to \infty} \overline{R}_K(\theta) \right).$$

Finally, taking supremum over θ and using theorem 5.5, we see that (5.19) holds with

$$\bar{I}(t) = \sup_{0 < \theta < 1/\overline{H}_{\infty}^2} \overline{F}(\theta) := \left[\frac{\theta t}{2\sigma^2} - \log \left(\frac{1 + \theta(\overline{H}_{\infty})^2}{1 - \theta(\overline{H}_{\infty})^2} \right) \right].$$

Moreover, $\overline{F}(\cdot)$ is differentiable for $0 < \theta < 1/\overline{H}_{\infty}^2$ with the derivative

$$\overline{F}'(\theta) = \frac{t}{2\sigma^2} - \frac{2(\overline{H}_{\infty})^2}{1 - \left(\theta(\overline{H}_{\infty})^2\right)^2},\tag{5.21}$$

being negative for all $\theta \in (0, 1/\overline{H}_{\infty}^2)$ when $t < 4\sigma^2 \overline{H}_{\infty}^2$ in which case we get $\overline{I}(t) = \overline{F}(0) = 0$. If $t \ge 4\sigma^2(\overline{H}_{\infty})^2$, then $\overline{F}'(\theta) = 0$ when $\theta = \theta_* := \frac{1}{\overline{H}_{\infty}^2} \sqrt{1 - \frac{4\sigma^2 \overline{H}_{\infty}^2}{t}}$. Therefore, we get $\overline{I}(t) = \overline{F}(\theta_*)$ which implies (5.20) as desired.

Remark 5.9. By Corollary 5.5, $\limsup_{K\to\infty} \mathbb{E}[f(\bar{x}_K) - f_*] = \overline{m} := 4\sigma^2(\overline{H}_\infty)^2$. Since this value represents the asymptotic expected suboptimality, the events with suboptimality below \overline{m} are not exponentially unlikely; hence, $\bar{I}(t) = 0$ whenever $t < \overline{m}$, in accordance with (5.20). In contrast, for $t > \overline{m}$, (5.20) shows that $\bar{I}(t)$ is strictly decreasing in \overline{H}_∞ over the region where $\bar{I}(t) > 0$, i.e., when $0 < \overline{H}_\infty < \frac{\sqrt{t}}{2\sigma}$. Therefore, smaller values of \overline{H}_∞ correspond to strictly larger decay rates $\bar{I}(t)$ at the threshold t, provided that t exceeds the critical level $\overline{m} = 4\sigma^2(\overline{H}_\infty)^2$. This shows that a smaller bound on H_∞ -norm—reflecting greater robustness to worst-case deterministic noise—leads to sharper concentration properties and faster decay of the tail probabilities associated with $f(\bar{x}_K) - f_*$. This is broadly consistent with the numerical behavior observed in fig. 6(b) for quadratics: reducing the step size increases the rate function I(t) while simultaneously decreasing the bound on H_∞ -norm for NAG-beta-opt, implied by (A.7) in the appendix.

6. Numerical Experiments

We consider the following strongly convex smooth objective:

$$f(x) := \sum_{i=1}^{p} g_{\lambda}(a_i^{\top} x - b_i) + \frac{\mu}{2} ||x||^2,$$

where $\mu > 0$ is a regularization parameter, $a_i \in \mathbb{R}^d$, $b_i \in \mathbb{R}$ for i = 1, ..., p for some $p \ge 1$ denotes the problem data, and $g_{\lambda}(\cdot)$ denotes the Huber loss defined as

$$g_{\lambda}(x) := \begin{cases} \frac{1}{2}x^2, & |x| \leq \lambda; \\ \lambda\left(|x| - \frac{1}{2}\lambda\right), & |x| > \lambda, \end{cases}$$

with $\lambda > 0$ denoting the smoothing parameter of the Huber-loss. Such objectives arise in regularized formulations of robust linear regression [115]. This objective resembles the heavy-ball counter-example analyzed in [95] and its variations have been studied in the literature [10, 57] to test momentum methods.

In our experiments, for d=10, p=1000, the entries of the data matrix $A=[a_1,a_2,...,a_p] \in \mathbb{R}^{d \times p}$ and the vector $b \in \mathbb{R}^p$ are i.i.d. with a uniform distribution on the interval [-1,1]. We set $\mu=0.005$ and L=20, and scale A so that $||A||=\sqrt{L-\mu}$ –indeed, with these choice of parameters, f is μ -strongly convex and ∇f is Lipschitz with constant L. Finally, the smoothing parameter is set to $\lambda=0.1$.

In this experiment we consider RS-HB, HB-fastest, GD-pop, NAG-beta-opt, and TMM (using the parameters provided in table 1 for each method). On the left plot of fig. 7, we consider unbiased stochastic noise setting, where batching is used with batch size b < p to construct an unbiased estimator of the gradient, i.e., the gradients are estimated with $\tilde{\nabla} f(y_k) := \frac{p}{b} \sum_{t=1}^b g_{\lambda}(a_{i_t}^{\top} y_k + b_{i_t}) + \mu y_k$, using $i_1, ..., i_b$ that are sampled with replacement from $\{1, ..., p\}$ independently at step k. This type of estimation is common in the context of stochastic gradient descent and momentum methods [52, 116, 117]. For each method, we run n = 100 sample paths, i.e., for every run ℓ , $\{x_j^{(\ell)}\}_{j=0}^K$ is a simulated trajectory and each $\ell \in \{1, 2, ..., n\}$ corresponds to an independent run where we execute the algorithm in consideration with the iteration budget of K = 1000 iterations. We estimate the sensitive cost sequence $\{R_k(\theta)\}_k$ numerically by considering the sample averages, i.e.,

$$\hat{R}_k(\theta) := \frac{2\hat{\sigma}^2}{\theta(k+1)} \log \left(\frac{1}{n} \sum_{\ell=1}^n \exp \left(\frac{\theta}{2\hat{\sigma}^2} \sum_{j=0}^k \left[f\left(x_j^{(\ell)}\right) - f_* \right] \right) \right), \quad 0 \le k \le K.$$

where $\hat{\sigma}^2$ is an estimate of the variance proxy σ^2 using the empirical variance of stochastic gradients.⁵ On the left plot of fig. 7, we illustrate $\hat{R}_k(\theta)$ for $\theta \in \{0.001, 1000\}$ in a logarithmic scale. We observe that GD-pop begins with a higher risk-sensitive cost than its momentum-based competitors, but after 1500 iterations this cost begins to fall below the competitors' costs. This phenomenon reflects the trade-off between convergence rate and risk, as discussed in section 4. While GD-pop converges more slowly, it can exhibit greater robustness to noise, since the impact of noise accumulates more gradually over iterations than the others. Furthermore, both HB-fastest and its robustly-stable variant (RS-HB) converge to higher risk levels than TMM and NAG-beta-opt, with NAG-beta-opt achieving the lowest risk among the momentum-based methods we compared. This behavior is consistent with the patterns observed in the quadratic case, shown in fig. 5.

On the right plot of fig. 7, we retain the same experimental setup as in the left plot except for one key difference: we introduce a bias term into the stochastic gradients. Specifically, at each iteration k, we add an adversarial (bias) component to the previously unbiased stochastic gradients. To construct this bias, for every iteration k, we sample 50 points from a δ -ball centered at $\nabla f(y_k)$ with $\delta = 2.5$. This value of δ is chosen to clearly illustrate the contrast between the non-adversarial and adversarial noise scenarios. Among the sampled points, we select the one that maximizes the suboptimality $f(x_{k+1}) - f_*$. This form of adversarial

⁵At iteration k, we compute the empirical variance, emp var_k, using 100 samples of the gradient evaluated at y_k , each of batch size 64. The final variance proxy estimate is $\hat{\sigma}^2 := \frac{1}{4} \max_{1 \le k \le K} \exp \operatorname{var}_k$ –the scaling by $\frac{1}{4}$ is from the fact for a σ^2 -subGaussian random variable, X, $\operatorname{Var}[X] \le 4\sigma^2$. This can be seen from the intermediary moment calculation in theorem E.1 by taking $\tilde{p} = 2$.

perturbation is inspired by techniques from adversarial learning [47]. We plot the risk for both $\theta \in \{0.001, 1000\}$. On the right plot, we observe the hierarchy in the performance of the algorithms; moreover, GD notably settles below its momentum-based competitors earlier (at around 750 iterations) than in the case with no adversarial noise.

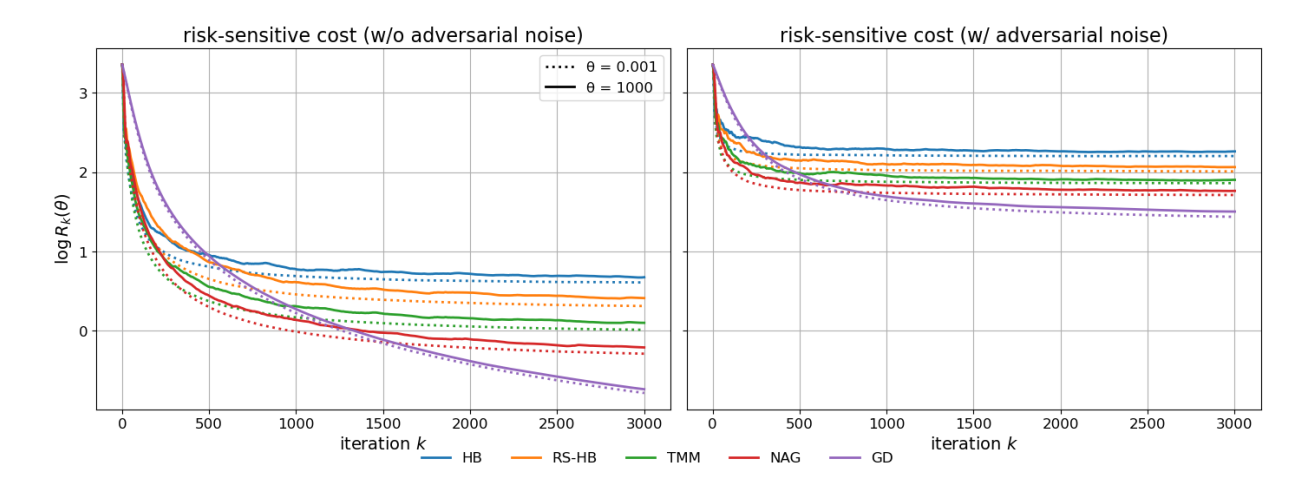


FIGURE 7. The risk-sensitive cost for GD settles the lowest among its popular competitors, HB, RS-HB, GD, and NAG in the case where there is pure stochastic noise and mixed stochastic and adversarial noise; $d = 10, p = 1000, \mu = 0.005, L = 20, \theta = \{0.001, 1000\}.$

7. Conclusion

We analyzed the trade-off between convergence rate and robustness to gradient errors in generalized momentum methods (GMMs), encompassing Nesterov's accelerated gradient, heavy-ball, and gradient descent methods. Using the concept of risk sensitivity index (RSI) from robust control, we characterized robustness under stochastic, potentially biased, additive gradient errors. For quadratic objectives with isotropic Gaussian noise, we derived closed-form RSI expressions via Riccati equations and identified a Pareto frontier between convergence rate and the robustness. We further established a large-deviation principle that connects the rate function characterizing the associated large-deviation principle to RSI and the H_{∞} -norm, thus bridging robustness to stochastic biased noise with robustness to deterministic worst-case errors. Extending our results to strongly convex smooth objectives, beyond quadratics, we provided finite-time RSI bounds under biased sub-Gaussian errors, yielding high-probability and non-asymptotic guarantees, and highlighted similar robustness—convergence trade-offs. To our knowledge, this is the first risk-sensitive, non-asymptotic analysis of GMMs with biased gradients. We provided numerical experiments on robust regression to illustrate our results.

References

- [1] L. Bottou, Large-scale machine learning with stochastic gradient descent, in: Y. Lechevallier, G. Saporta (Eds.), Proceedings of COMPSTAT'2010, Physica-Verlag HD, Heidelberg, 2010, pp. 177–186.
- [2] L. Bottou, F. E. Curtis, J. Nocedal, Optimization methods for large-scale machine learning, SIAM Review 60 (2) (2018) 223–311.

- [3] A. Beck, M. Teboulle, A fast iterative shrinkage-thresholding algorithm for linear inverse problems, SIAM Journal on Imaging Sciences 2 (1) (2009) 183–202.
- [4] N. S. Aybat, G. Iyengar, A first-order smoothed penalty method for compressed sensing, SIAM Journal on Optimization 21 (1) (2011) 287–313.
- [5] N. S. Aybat, G. Iyengar, A first-order augmented Lagrangian method for compressed sensing, SIAM Journal on Optimization 22 (2) (2012) 429–459.
- [6] M. Gurbuzbalaban, A. Ozdaglar, P. A. Parrilo, Convergence rate of incremental gradient and incremental Newton methods, SIAM Journal on Optimization 29 (4) (2019) 2542–2565.
- [7] Y. Nesterov, Lectures on Convex Optimization, 2nd Edition, Vol. 137, Springer, 2018.
- [8] B. T. Polyak, Introduction to optimization, Optimization Software, Inc, New York (1987).
- [9] Y. E. Nesterov, A method of solving a convex programming problem with convergence rate O(1/k²), Doklady Akademii Nauk SSSR 269 (3) (1983) 543–547, in Russian; English transl. in Soviet Mathematics Doklady 27(2):372–376, 1983.
- [10] B. Van Scoy, R. A. Freeman, K. M. Lynch, The fastest known globally convergent first-order method for minimizing strongly convex functions, IEEE Control Systems Letters 2 (1) (2018) 49–54.
- [11] S. Cyrus, B. Hu, B. Van Scoy, L. Lessard, A robust accelerated optimization algorithm for strongly convex functions, in: 2018 Annual American Control Conference (ACC), IEEE, 2018, pp. 1376–1381.
- [12] B. Hu, L. Lessard, Dissipativity theory for Nesterov's accelerated method, in: Proceedings of the 34th International Conference on Machine Learning, Vol. 70 of Proceedings of Machine Learning Research, PMLR, International Convention Centre, Sydney, Australia, 2017, pp. 1549–1557.
- [13] A. d'Aspremont, Smooth optimization with approximate gradient, SIAM Journal on Optimization 19 (3) (2008) 1171–1183.
- [14] O. Devolder, F. Glineur, Y. Nesterov, First-order methods of smooth convex optimization with inexact oracle, Mathematical Programming 146 (1-2) (2014) 37–75.
- [15] K. Scheinberg, Finite difference gradient approximation: To randomize or not?, INFORMS Journal on Computing 34 (5) (2022) 2384–2388.
- [16] D. P. Bertsekas, Nonlinear Programming, 2nd Edition, Athena Scientific, Belmont, MA, 2002.
- [17] D. P. Bertsekas, Incremental gradient, subgradient, and proximal methods for convex optimization: A survey, in: Optimization for Machine Learning, The MIT Press, 2011.
- [18] N. Kuru, I. S. Birbil, M. Gürbüzbalaban, S. Yildirim, Differentially private accelerated optimization algorithms, SIAM Journal on Optimization 32 (2) (2022) 795–821.
- [19] A. Rajkumar, S. Agarwal, A differentially private stochastic gradient descent algorithm for multiparty classification, in: N. D. Lawrence, M. Girolami (Eds.), Proceedings of the Fifteenth International Conference on Artificial Intelligence and Statistics, Vol. 22 of Proceedings of Machine Learning Research, PMLR, La Palma, Canary Islands, 2012, pp. 933–941.
- [20] B. T. Polyak, A. B. Juditsky, Acceleration of stochastic approximation by averaging, SIAM Journal on Control and Optimization 30 (4) (1992) 838–855.
- [21] H. Robbins, S. Monro, A stochastic approximation method, Annals of Mathematical Statistics 22 (1951) 400–407.
- [22] J. Bernstein, Y.-X. Wang, K. Azizzadenesheli, A. Anandkumar, SignSGD: Compressed optimisation for non-convex problems, in: International Conference on Machine Learning, PMLR, 2018, pp. 560–569.
- [23] J. Bernstein, J. Zhao, K. Azizzadenesheli, A. Anandkumar, SignSGD with majority vote is communication efficient and fault tolerant, in: International Conference on Learning Representations, 2019. URL https://openreview.net/forum?id=BJxhijAcY7
- [24] A. Nemirovski, A. Juditsky, G. Lan, A. Shapiro, Robust stochastic approximation approach to stochastic programming, SIAM Journal on Optimization 19 (4) (2009) 1574–1609.
- [25] M. Even, Stochastic gradient descent under Markovian sampling schemes, in: A. Krause, E. Brunskill, K. Cho, B. Engelhardt, S. Sabato, J. Scarlett (Eds.), Proceedings of the 40th International Conference on Machine Learning, Vol. 202 of Proceedings of Machine Learning Research, PMLR, 2023, pp. 9412–9439.
- [26] O. Shamir, Without-replacement sampling for stochastic gradient methods, in: D. Lee, M. Sugiyama, U. Luxburg, I. Guyon, R. Garnett (Eds.), Advances in Neural Information Processing Systems, Vol. 29, Curran Associates, Inc., 2016, pp. 46–54.
- [27] L. M. Nguyen, J. Liu, K. Scheinberg, M. Takáč, SARAH: A novel method for machine learning problems using stochastic recursive gradient, in: D. Precup, Y. W. Teh (Eds.), Proceedings of the 34th

- International Conference on Machine Learning, Vol. 70 of Proceedings of Machine Learning Research, PMLR, 2017, pp. 2613–2621.
- [28] D. Driggs, J. Liang, C.-B. Schönlieb, On biased stochastic gradient estimation, Journal of Machine Learning Research 23 (24) (2022) 1–43.
- [29] T. H. Tran, K. Scheinberg, L. M. Nguyen, Nesterov accelerated shuffling gradient method for convex optimization, in: K. Chaudhuri, S. Jegelka, L. Song, C. Szepesvari, G. Niu, S. Sabato (Eds.), Proceedings of the 39th International Conference on Machine Learning, Vol. 162 of Proceedings of Machine Learning Research, PMLR, 2022, pp. 21703–21732.
- [30] H. Yu, X. Li, High probability guarantees for random reshuffling, arXiv preprint at arXiv:2311.11841 (2025).
- [31] M. Gürbüzbalaban, A. Özdaglar, P. A. Parrilo, Why random reshuffling beats stochastic gradient descent, Mathematical Programming 186 (1) (2021) 49–84.
- [32] A. Beznosikov, S. Horvath, P. Richtarik, M. Safaryan, On biased compression for distributed learning, Journal of Machine Learning Research 24 (276) (2023) 1–50.
- [33] S. U. Stich, S. P. Karimireddy, The error-feedback framework: SGD with delayed gradients, Journal of Machine Learning Research 21 (237) (2020) 1–36.
- [34] A. F. Aji, K. Heafield, Sparse communication for distributed gradient descent, in: Proceedings of the 2017 Conference on Empirical Methods in Natural Language Processing, Association for Computational Linguistics, 2017, pp. 440–445.
- [35] A. Beikmohammadi, S. Khirirat, S. Magnússon, Parallel momentum methods under biased gradient estimations, IEEE Transactions on Control of Network Systems 12 (2) (2025) 1721–1732.
- [36] S. P. Karimireddy, Q. Rebjock, S. Stich, M. Jaggi, Error feedback fixes SignSGD and other gradient compression schemes, in: K. Chaudhuri, R. Salakhutdinov (Eds.), Proceedings of the 36th International Conference on Machine Learning, Vol. 97 of Proceedings of Machine Learning Research, PMLR, 2019, pp. 3252–3261.
- [37] A. Koloskova, H. Hendrikx, S. U. Stich, Revisiting gradient clipping: Stochastic bias and tight convergence guarantees, in: A. Krause, E. Brunskill, K. Cho, B. Engelhardt, S. Sabato, J. Scarlett (Eds.), Proceedings of the 40th International Conference on Machine Learning, Vol. 202 of Proceedings of Machine Learning Research, PMLR, 2023, pp. 17343–17363.
- [38] X. Chen, S. Z. Wu, M. Hong, Understanding gradient clipping in private SGD: A geometric perspective, in: H. Larochelle, M. Ranzato, R. Hadsell, M. Balcan, H. Lin (Eds.), Advances in Neural Information Processing Systems, Vol. 33, Curran Associates, Inc., 2020, pp. 13773–13782.
- [39] V. V. Mai, M. Johansson, Stability and convergence of stochastic gradient clipping: Beyond lipschitz continuity and smoothness, in: M. Meila, T. Zhang (Eds.), Proceedings of the 38th International Conference on Machine Learning, Vol. 139 of Proceedings of Machine Learning Research, PMLR, 2021, pp. 7325–7335.
- [40] H. Xiao, Z. Xiang, D. Wang, S. Devadas, A theory to instruct differentially-private learning via clipping bias reduction, in: 2023 IEEE Symposium on Security and Privacy (SP), 2023, pp. 2170–2189.
- [41] L. Zhu, M. Gürbüzbalaban, A. Ruszczyński, Mean–semideviation–based distributionally robust learning with weakly convex losses: convergence rates and finite-sample guarantees, Mathematical Programming (2025) 1–31.
- [42] M. Gürbüzbalaban, A. Ruszczyński, L. Zhu, A stochastic subgradient method for distributionally robust non-convex and non-smooth learning, Journal of Optimization Theory and Applications 194 (3) (2022) 1014–1041.
- [43] Y. F. Wu, W. Zhang, P. Xu, Q. Gu, A finite-time analysis of two time-scale actor-critic methods, in: H. Larochelle, M. Ranzato, R. Hadsell, M. Balcan, H. Lin (Eds.), Advances in Neural Information Processing Systems, Vol. 33, Curran Associates, Inc., 2020, pp. 17617–17628.
- [44] J. Bhandari, D. Russo, R. Singal, A finite time analysis of temporal difference learning with linear function approximation, in: S. Bubeck, V. Perchet, P. Rigollet (Eds.), Proceedings of the 31st Conference On Learning Theory, Vol. 75 of Proceedings of Machine Learning Research, PMLR, 2018, pp. 1691–1692.
- [45] A. Shaban, C.-A. Cheng, N. Hatch, B. Boots, Truncated back-propagation for bilevel optimization, in: K. Chaudhuri, M. Sugiyama (Eds.), Proceedings of the Twenty-Second International Conference on Artificial Intelligence and Statistics, Vol. 89 of Proceedings of Machine Learning Research, PMLR, 2019, pp. 1723–1732.

- [46] L. Xia, S. Massei, M. E. Hochstenbach, B. Koren, On the influence of stochastic roundoff errors and their bias on the convergence of the gradient descent method with low-precision floating-point computation, arXiv preprint at arXiv:2202.12276 (2023).
- [47] A. Madry, A. Makelov, L. Schmidt, D. Tsipras, A. Vladu, Towards deep learning models resistant to adversarial attacks, in: International Conference on Learning Representations, 2018. URL https://openreview.net/forum?id=rJzIBfZAb
- [48] H. Gu, X. Guo, X. Li, Adversarial training for gradient descent: Analysis through its continuous-time approximation, arXiv preprint at arXiv:2105.08037 (2023).
- [49] N. Flammarion, F. Bach, From averaging to acceleration, there is only a step-size, in: P. Grünwald, E. Hazan, S. Kale (Eds.), Proceedings of The 28th Conference on Learning Theory, Vol. 40 of Proceedings of Machine Learning Research, PMLR, Paris, France, 2015, pp. 658–695.
- [50] M. Hardt, Robustness versus acceleration (Aug. 2014). URL http://blog.mrtz.org/2014/08/18/robustness-versus-acceleration
- [51] M. Schmidt, N. Roux, F. Bach, Convergence rates of inexact proximal-gradient methods for convex optimization, in: J. Shawe-Taylor, R. Zemel, P. Bartlett, F. Pereira, K. Weinberger (Eds.), Advances in Neural Information Processing Systems, Vol. 24, Curran Associates, Inc., 2011, pp. 1458–1466.
- [52] N. S. Aybat, A. Fallah, M. Gürbüzbalaban, A. Ozdaglar, A universally optimal multistage accelerated stochastic gradient method, in: H. Wallach, H. Larochelle, A. Beygelzimer, F. d'Alché-Buc, E. Fox, R. Garnett (Eds.), Advances in Neural Information Processing Systems, Vol. 32, Curran Associates, Inc., 2019, pp. 8525–8536.
- [53] N. S. Aybat, A. Fallah, M. Gürbüzbalaban, A. Ozdaglar, Robust accelerated gradient methods for smooth strongly convex functions, SIAM Journal on Optimization 30 (1) (2020) 717–751.
- [54] A. Fallah, M. Gürbüzbalaban, A. Ozdaglar, U. Şimşekli, L. Zhu, Robust distributed accelerated stochastic gradient methods for multi-agent networks, Journal of Machine Learning Research 23 (1) (2022) 9893–9988.
- [55] X. Zhang, N. S. Aybat, M. Gürbüzbalaban, Robust accelerated primal-dual methods for computing saddle points, SIAM Journal on Optimization 34 (1) (2024) 1097–1130.
- [56] Y. Laguel, N. S. Aybat, M. Gürbüzbalaban, High probability and risk-averse guarantees for a stochastic accelerated primal-dual method, Journal of Machine Learning Research 25 (421) (2024) 1–56.
- [57] M. Gürbüzbalaban, Robustly stable accelerated momentum methods with a near-optimal L_2 gain and H_{∞} performance, To Appear in Math. of Operations Research. arXiv preprint at arXiv:2309.11481v5, (2023).
 - URL https://arxiv.org/abs/2309.11481v5
- [58] B. Can, M. Gürbüzbalaban, Entropic risk-averse generalized momentum methods, To Appear in Optimization Methods and Software, arXiv preprint at arXiv:2204.11292 (2022).
- [59] D. Jacobson, Optimal stochastic linear systems with exponential performance criteria and their relation to deterministic differential games, IEEE Transactions on Automatic Control 18 (2) (1973) 124–131.
- [60] P. Whittle, Risk-sensitive linear/quadratic/Gaussian control, Advances in Applied Probability 13 (4) (1981) 764–777.
- [61] K. Glover, J. C. Doyle, State-space formulae for all stabilizing controllers that satisfy an H_{∞} -norm bound and relations to risk sensitivity, Systems & Control Letters 11 (3) (1988) 167–172.
- [62] P. Whittle, Risk sensitivity, a strangely pervasive concept, Macroeconomic Dynamics 6 (1) (2002) 5–18.
- [63] W. H. Fleming, H. M. Soner, Controlled Markov processes and viscosity solutions, Vol. 25, Springer Science & Business Media, 2006.
- [64] P. A. Iglesias, M. A. Peters, An entropy formula for nonlinear systems, Journal of the Franklin Institute 337 (7) (2000) 859–874.
- [65] A. Dembo, O. Zeitouni, Large deviations techniques and applications, 2nd Edition, Vol. 38, Springer Science & Business Media, 2009.
- [66] E. Hazan, S. Kale, Beyond the regret minimization barrier: Optimal algorithms for stochastic stronglyconvex optimization, Journal of Machine Learning Research 15 (71) (2014) 2489–2512.
- [67] N. J. A. Harvey, C. Liaw, Y. Plan, S. Randhawa, Tight analyses for non-smooth stochastic gradient descent, in: A. Beygelzimer, D. Hsu (Eds.), Proceedings of the Thirty-Second Conference on Learning Theory, Vol. 99 of Proceedings of Machine Learning Research, PMLR, 2019, pp. 1579–1613.

- [68] A. Armacki, S. Yu, P. Sharma, G. Joshi, D. Bajovic, D. Jakovetic, S. Kar, High-probability convergence bounds for online nonlinear stochastic gradient descent under heavy-tailed noise, in: Proceedings of The 28th International Conference on Artificial Intelligence and Statistics, PMLR, 2025, pp. 1774–1782.
- [69] S. M. Kakade, A. Tewari, On the generalization ability of online strongly convex programming algorithms, in: D. Koller, D. Schuurmans, Y. Bengio, L. Bottou (Eds.), Advances in Neural Information Processing Systems, Vol. 21, Curran Associates, Inc., 2008, pp. 801–808.
- [70] A. Rakhlin, O. Shamir, K. Sridharan, Making gradient descent optimal for strongly convex stochastic optimization, arXiv preprint at arXiv:1109.5647 (2012).
- [71] D. Davis, D. Drusvyatskiy, L. Xiao, J. Zhang, From low probability to high confidence in stochastic convex optimization, Journal of Machine Learning Research 22 (49) (2021) 1–38.
- [72] P. Jain, D. M. Nagaraj, P. Netrapalli, Making the last iterate of SGD information theoretically optimal, SIAM Journal on Optimization 31 (2) (2021) 1108–1130.
- [73] S. Ghadimi, G. Lan, Stochastic first- and zeroth-order methods for nonconvex stochastic programming, SIAM Journal on Optimization 23 (4) (2013) 2341–2368.
- [74] X. Li, F. Orabona, A high probability analysis of adaptive SGD with momentum, arXiv preprint at arXiv:2007.14294 (2020).
- [75] E. Gorbunov, M. Danilova, A. Gasnikov, Stochastic optimization with heavy-tailed noise via accelerated gradient clipping, in: H. Larochelle, M. Ranzato, R. Hadsell, M. Balcan, H. Lin (Eds.), Advances in Neural Information Processing Systems, Vol. 33, Curran Associates, Inc., 2020, pp. 15042–15053.
- [76] E. Gorbunov, M. Danilova, I. Shibaev, P. Dvurechensky, A. Gasnikov, High probability complexity bounds for non-smooth stochastic optimization with heavy-tailed noise, arXiv preprint at arXiv:2106.05958 (2024).
- [77] S. Li, Y. Liu, High probability guarantees for nonconvex stochastic gradient descent with heavy tails, in: K. Chaudhuri, S. Jegelka, L. Song, C. Szepesvari, G. Niu, S. Sabato (Eds.), Proceedings of the 39th International Conference on Machine Learning, Vol. 162 of Proceedings of Machine Learning Research, PMLR, 2022, pp. 12931–12963.
- [78] Y. Demidovich, G. Malinovsky, I. Sokolov, P. Richtarik, A guide through the zoo of biased SGD, in: A. Oh, T. Naumann, A. Globerson, K. Saenko, M. Hardt, S. Levine (Eds.), Advances in Neural Information Processing Systems, Vol. 36, Curran Associates, Inc., 2023, pp. 23158–23171.
- [79] U. K. R. Tadipatri, M. Vidyasagar, Convergence of the stochastic heavy ball method with approximate gradients and/or block updating, arXiv preprint at arXiv:2303.16241 (2025).
- [80] A. S. Nemirovsky, D. B. Yudin, Problem Complexity and Method Efficiency in Optimization, Wiley-Interscience Series in Discrete Mathematics, John Wiley & Sons, Inc., New York, 1983, translated from the Russian and with a preface by E. R. Dawson.
- [81] D. Hsu, S. Sabato, Loss minimization and parameter estimation with heavy tails, Journal of Machine Learning Research 17 (18) (2016) 1–40.
- [82] E. Gorbunov, A. Sadiev, M. Danilova, S. Horváth, G. Gidel, P. Dvurechensky, A. Gasnikov, P. Richtárik, High-probability convergence for composite and distributed stochastic minimization and variational inequalities with heavy-tailed noise, in: R. Salakhutdinov, Z. Kolter, K. Heller, A. Weller, N. Oliver, J. Scarlett, F. Berkenkamp (Eds.), Proceedings of the 41st International Conference on Machine Learning, Vol. 235 of Proceedings of Machine Learning Research, PMLR, 2024, pp. 15951–16070.
- [83] A. Cutkosky, H. Mehta, High-probability bounds for non-convex stochastic optimization with heavy tails, in: M. Ranzato, A. Beygelzimer, Y. Dauphin, P. Liang, J. W. Vaughan (Eds.), Advances in Neural Information Processing Systems, Vol. 34, Curran Associates, Inc., 2021, pp. 4883–4895.
- [84] P. Dupuis, H. J. Kushner, Stochastic approximations via large deviations: Asymptotic properties, SIAM Journal on Control and Optimization 23 (5) (1985) 675–696.
- [85] P. Dupuis, H. J. Kushner, Asymptotic behavior of constrained stochastic approximations via the theory of large deviations, Probability Theory and Related Fields 75 (2) (1987) 223–244.
- [86] P. Dupuis, Large deviations analysis of some recursive algorithms with state dependent noise, The Annals of Probability 16 (4) (1988) 1509–1536.
- [87] H. Hult, A. Lindhe, P. Nyquist, G.-J. Wu, A weak convergence approach to large deviations for stochastic approximations, arXiv preprint at arXiv:2502.02529 (2025).
- [88] D. Bajovic, D. Jakovetic, S. Kar, Large deviations rates for stochastic gradient descent with strongly convex functions, in: F. Ruiz, J. Dy, J.-W. van de Meent (Eds.), Proceedings of The 26th International

- Conference on Artificial Intelligence and Statistics, Vol. 206 of Proceedings of Machine Learning Research, PMLR, 2023, pp. 10095–10111.
- [89] A. Armacki, S. Yu, D. Bajovic, D. Jakovetic, S. Kar, Large deviation upper bounds and improved MSE rates of nonlinear SGD: Heavy-tailed noise and power of symmetry, arXiv preprint at arXiv:2410.15637 (2025).
- [90] S. Ghadimi, G. Lan, Optimal stochastic approximation algorithms for strongly convex stochastic composite optimization II: shrinking procedures and optimal algorithms, SIAM Journal on Optimization 23 (4) (2013) 2061–2089.
- [91] S. Ghadimi, G. Lan, Optimal stochastic approximation algorithms for strongly convex stochastic composite optimization I: A generic algorithmic framework, SIAM Journal on Optimization 22 (4) (2012) 1469–1492.
- [92] P. Whittle, Risk-sensitivity, large deviations and stochastic control, European Journal of Operational Research 73 (2) (1994) 295–303.
- [93] M. A. Peters, P. Iglesias, Minimum Entropy Control for Time-Varying Systems, Springer Science & Business Media, 1997.
- [94] A. Stoorvogel, J. Ludlage, The discrete time minimum entropy H_{∞} control problem, Memorandum COSOR, Technische Universiteit Eindhoven, 1993.
- [95] L. Lessard, B. Recht, A. Packard, Analysis and design of optimization algorithms via integral quadratic constraints, SIAM Journal on Optimization 26 (1) (2016) 57–95.
- [96] B. Can, M. Gurbuzbalaban, L. Zhu, Accelerated linear convergence of stochastic momentum methods in Wasserstein distances, in: K. Chaudhuri, R. Salakhutdinov (Eds.), Proceedings of the 36th International Conference on Machine Learning, Vol. 97 of Proceedings of Machine Learning Research, PMLR, 2019, pp. 891–901.
- [97] H. Mohammadi, M. Razaviyayn, M. R. Jovanović, Robustness of accelerated first-order algorithms for strongly convex optimization problems, IEEE Transactions on Automatic Control 66 (6) (2021) 2480–2495.
- [98] B. Van Scoy, L. Lessard, The speed-robustness trade-off for first-order methods with additive gradient noise, arXiv preprint at arXiv:2109.05059 (2021).
- [99] X. Zhang, N. S. Aybat, M. Gürbüzbalaban, SAPD+: An accelerated stochastic method for nonconvex-concave minimax problems, in: S. Koyejo, S. Mohamed, A. Agarwal, D. Belgrave, K. Cho, A. Oh (Eds.), Advances in Neural Information Processing Systems, Vol. 35, Curran Associates, Inc., 2022, pp. 21668–21681.
- [100] O. Devolder, Exactness, inexactness and stochasticity in first-order methods for large-scale convex optimization, Ph.D. thesis, CORE UCLouvain Louvain-la-Neuve, Belgium (2013).
- [101] M. Gürbüzbalaban, A. Ozdaglar, P. Parrilo, A globally convergent incremental Newton method, Mathematical Programming 151 (1) (2015) 283–313.
- [102] M. Gürbüzbalaban, A. Ozdaglar, P. A. Parrilo, On the convergence rate of incremental aggregated gradient algorithms, SIAM Journal on Optimization 27 (2) (2017) 1035–1048.
- [103] T. Sun, K. Tang, D. Li, Gradient descent learning with floats, IEEE Transactions on Cybernetics 52 (3) (2022) 1763–1771.
- [104] A. J. Shaiju, I. R. Petersen, Formulas for discrete time LQR, LQG, LEQG and minimax LQG optimal control problems, IFAC Proceedings Volumes 41 (2008) 8773–8778.
- [105] P. Dupuis, M. R. James, I. Petersen, Robust properties of risk-sensitive control, Mathematics of Control, Signals and Systems 13 (4) (2000) 318–332.
- [106] W. H. Fleming, M. R. James, The risk-sensitive index and the H_2 and H_{∞} norms for nonlinear systems, Mathematics of Control, Signals and Systems 8 (3) (1995) 199–221.
- [107] H. Pham, A risk-sensitive control dual approach to a large deviations control problem, Systems & Control Letters 49 (4) (2003) 295–309.
- [108] D. N. Tran, C. M. Kellett, P. M. Dower, Qualitative equivalences of ISS and ℓ_p -gain stability properties for discrete-time nonlinear systems, Automatica 77 (C) (2017) 360–369.
- [109] W. Lin, C. I. Byrnes, H_{∞} -control of discrete-time nonlinear systems, IEEE Transactions on Automatic Control 41 (4) (1996) 494–510.
- [110] A. van der Schaft, L_2 -Gain and Passivity Techniques in Nonlinear Control, 3rd Edition, Springer Publishing Company, Incorporated, 2018.

- [111] K. Zhou, J. Doyle, K. Glover, Robust and Optimal Control, Prentice Hall, NJ, 1996.
- [112] D. Hinrichsen, N. K. Son, Stability radii of linear discrete-time systems and symplectic pencils, International Journal of Robust and Nonlinear Control 1 (2) (1991) 79–97.
- [113] W. F. Arnold, A. J. Laub, Generalized eigenproblem algorithms and software for algebraic Riccati equations, Proceedings of the IEEE 72 (12) (1984) 1746–1754.
- [114] A. Dieuleveut, A. Durmus, F. Bach, Bridging the gap between constant step size stochastic gradient descent and Markov Chains, Annals of Statistics 48 (3) (2020) 1348–1382.
- [115] P. Filzmoser, K. Nordhausen, Robust linear regression for high-dimensional data: An overview, WIREs Comput. Stat. 13 (4) (2021). URL https://wires.onlinelibrary.wiley.com/doi/10.1002/wics.1524
- [116] M. Gürbüzbalaban, Y. Hu, Fractional moment-preserving initialization schemes for training deep neural networks, in: A. Banerjee, K. Fukumizu (Eds.), Proceedings of The 24th International Conference on Artificial Intelligence and Statistics, Vol. 130 of Proceedings of Machine Learning Research, PMLR, 2021, pp. 2233–2241.
- [117] M. Gürbüzbalaban, U. Simsekli, L. Zhu, The heavy-tail phenomenon in SGD, in: M. Meila, T. Zhang (Eds.), Proceedings of the 38th International Conference on Machine Learning, Vol. 139 of Proceedings of Machine Learning Research, PMLR, 2021, pp. 3964–3975.
- [118] V. Ionescu, M. Weiss, On computing the stabilizing solution of the discrete-time Riccati equation, Linear Algebra and its Applications 174 (1992) 229–238.

Appendix A. Existing bounds on the H_{∞} -norm for $f \in \mathcal{C}^{L}_{\mu}(\mathbb{R}^{d})$

Theorem A.1 ([57]). Consider the inexact GMM dynamics in (3.8) for minimizing $f \in \mathcal{C}^L_{\mu}(\mathbb{R}^d)$ with fixed parameters (α, β, ν) where $\alpha > 0$, and $\beta, \nu \geq 0$, when the gradient at step k, $\nabla f(y_k)$, is subject to additive gradient error w_{k+1} resulting in $\tilde{\nabla} f(y_k, w_{k+1})$. Assume that there exists non-negative scalars $\rho_0, \rho_1, \rho_2, \rho_3 \in [0, 1), a, b, c_0, c_1 \geq 0$ and a positive semi-definite matrix $\tilde{P} \in \mathbb{R}^{2 \times 2}$ such that the following conditions hold:

(i) p+q<1, where

$$p := \rho_0^2 + c_1 \rho_1^2 + \rho_2^2 + \frac{4b(1+\nu)^2 L^2}{\mu} c_1, \qquad q := \rho_3^2 + \frac{4b\nu^2 L^2}{\mu} c_1; \tag{A.1}$$

(ii)
$$c_1 + \frac{2}{L}\tilde{r}(\tilde{P}) > 0$$
 and $c_1 + \tilde{P}_{11} > 0$ such that

$$\tilde{M}_2(\tilde{P}, a) + c_1 \tilde{M}_1 + c_0 \tilde{M}_0 \succeq 0, \tag{A.2}$$

where \tilde{M}_0, \tilde{M}_1 and $\tilde{M}_2(\tilde{P}, a)$ are 4×4 real symmetric matrices defined as

$$\tilde{M}_0 = \begin{bmatrix} 2\mu L\tilde{C}^\top \tilde{C} & -(\mu+L)\tilde{C}^\top & 0_{2\times 1} \\ -(\mu+L)\tilde{C} & 2 & 0 \\ 0_{1\times 2} & 0 & 0 \end{bmatrix}, \quad \tilde{M}_1 = \begin{bmatrix} \tilde{X} + \tilde{Z} & \left| \frac{L\alpha(\beta-\nu)}{2}\tilde{M}_3^\top \right| \\ \frac{L\alpha(\beta-\nu)}{2}\tilde{M}_3 & \frac{\alpha(1-L\alpha)}{2} \right| \\ \frac{L\alpha(\beta-\nu)}{2}\tilde{M}_3 & \frac{\alpha(1-L\alpha)}{2} & 0 \end{bmatrix},$$

$$\tilde{M}_2(\tilde{P},a) = \begin{bmatrix} -\tilde{A}^\top \tilde{P}\tilde{A} + \rho_0^2 \tilde{P} & -\tilde{A}^\top \tilde{P}\tilde{B} & -\tilde{A}^\top \tilde{P}\tilde{B} \\ -\tilde{B}^\top \tilde{P}\tilde{A} & -\tilde{B}^\top \tilde{P}\tilde{B} + bc_1 & -\tilde{B}^\top \tilde{P}\tilde{B} \\ -\tilde{B}^\top \tilde{P}\tilde{A} & -\tilde{B}^\top \tilde{P}\tilde{B} & a \end{bmatrix},$$

with

$$\tilde{M}_3 := \begin{bmatrix} 1 & -1 \end{bmatrix}, \qquad \tilde{Z} = \begin{bmatrix} \rho_1^2 P_{11} + \frac{\mu}{2} \rho_2^2 & \rho_1^2 P_{12} & 0 \\ \rho_1^2 P_{12} & \rho_1^2 P_{22} + \frac{\mu}{2} \rho_3^2 & 0 \\ 0 & 0 & 0 \end{bmatrix},$$

$$\tilde{X} = \tilde{X}_1 + \rho_0^2 \tilde{X}_2 + (1 - \rho_0^2) \tilde{X}_3, \qquad \tilde{X}_1 = \frac{1}{2} \begin{bmatrix} -L\tilde{\Delta}^2 & L\tilde{\Delta}^2 & -(1 - \alpha L)\tilde{\Delta} \\ L\tilde{\Delta}^2 & -L\tilde{\Delta}^2 & (1 - L\alpha)\tilde{\Delta} \\ -(1 - \alpha L)\tilde{\Delta} & (1 - L\alpha)\tilde{\Delta} & \alpha(2 - L\alpha) \end{bmatrix}, (A.3)$$

$$\tilde{X}_2 = \frac{1}{2} \begin{bmatrix} \nu^2 \mu & -\nu^2 \mu & -\nu \\ -\nu^2 \mu & \nu^2 \mu & \nu \\ -\nu & \nu & 0 \end{bmatrix}, \qquad \tilde{X}_3 = \frac{1}{2} \begin{bmatrix} (1+\nu)^2 \mu & -\nu(1+\nu)\mu & -(1+\nu) \\ -\nu(1+\nu)\mu & \nu^2 \mu & \nu \\ -(1+\nu) & \nu & 0 \end{bmatrix},$$

and $\tilde{\Delta} := \beta - \nu$; moreover, $\tilde{A}, \tilde{B}, \tilde{C}$ matrices are as in (3.5) and

$$\tilde{r}(\tilde{P}) = \begin{cases} \tilde{P}_{11} - \tilde{P}_{12}^2 / \tilde{P}_{22} & if \quad \tilde{P}_{22} \neq 0, \\ \tilde{P}_{11} & if \quad \tilde{P}_{22} = 0. \end{cases}$$
(A.4)

Then, the Lyapunov function V_{P,c_1} defined in (5.1) with $P = \tilde{P} \times I_d$ satisfies the decay property

$$V_{P,c_1}(\xi_{k+1}) \le pV_{P,c_1}(\xi_k) + qV_{P,c_1}(\xi_{k-1}) + r\|w_{k+1}\|^2, \tag{A.5}$$

for all $k \ge 0$ along the GMM iterates where p,q are as in (A.1), and $r := a + \alpha^2 \left(\frac{c_1 L}{2} + \tilde{P}_{11}\right)$ with the convention that $\xi_{-1} := \xi_0$. Furthermore, in the special case when the sequence $\{w_{k+1}\}_{k\ge 0}$ is deterministic and square-summable, the H_{∞} -norm of the GMM defined in (3.3) is finite and admits the bound

$$H_{\infty} \le \overline{H}_{\infty} := \left(\frac{1}{1 - \left(p + q\right)} \frac{r}{c_1 + \frac{2}{L}\tilde{r}(\tilde{P})}\right)^{1/2}.$$
(A.6)

More specifically, it satisfies (3.14) for $\gamma = \overline{H}_{\infty}$ with

$$H_{\gamma}(\xi_0) = \frac{1 + \frac{4b\nu^2 L^2}{\mu} c_1 + \rho_3^2}{1 - (p + q)} \left(\frac{4\|\tilde{P}\|}{\mu} + c_1 \right) \frac{1}{c_1 + \frac{2}{L}\tilde{r}(\tilde{P})} (f(x_0) - f_*).$$

Proof. The result follows directly from Theorem 5.6 and the inequalities (47)-(48) in [57]. \square

The following results are corollaries of the previous theorem, providing explicit bounds on the H_{∞} -norm for GD and NAG.

Corollary A.2 ([57]). For GD with step size with $\alpha \in (0, 2/L)$, the descent property (A.5) and the bound (A.6) holds with

$$p = \rho_{GD}(\alpha) := \max\{|1 - \alpha \mu|, |1 - \alpha L|\}, \quad q = 0, \quad r = \frac{\alpha^2}{1 - \rho_{GD}(\alpha)}, \quad \tilde{P} = \mathbf{I}_2, \quad c_1 = 0.$$

In addition, (A.5) and (A.6) also hold with an alternative set of parameters:

$$p=1-2\mu\alpha(1-\frac{L\alpha}{2})+\alpha\mu|1-\alpha L|s_{\text{GD}},\quad q=0,\quad r=\alpha\left(\frac{L}{2}\alpha+\frac{|1-\alpha L|}{2s_{\text{GD}}}\right),\quad \tilde{P}=0,\quad c_1=1,$$

where $s_{\rm GD}=1$ when $\alpha \leq \frac{1}{L}$ and $s_{\rm GD}=\frac{2-\alpha L}{\alpha L}$ for $\alpha \in (1/L,2/L)$. Therefore, theorem A.1 implies

$$H_{\infty} \leq \overline{H}_{\infty} = \begin{cases} \frac{1}{\sqrt{2\mu}} & \text{if} \quad 0 < \alpha \leq \frac{1}{L}, \\ \frac{1}{\sqrt{2\mu}} \frac{\alpha L}{2 - \alpha L} & \text{if} \quad \frac{1}{L} < \alpha \leq \frac{2}{L + \sqrt{L\mu}}, \\ \frac{1}{\sqrt{2\mu}} \sqrt{\kappa} & \text{if} \quad \frac{2}{L + \sqrt{L\mu}} < \alpha \leq \frac{2}{L + \mu}, \\ \frac{\alpha \sqrt{L}}{\sqrt{2}(2 - \alpha L)} & \text{if} \quad \frac{2}{L + \mu} < \alpha < \frac{2}{L}. \end{cases}$$

Proof. See [57, Section 5] for details.

Corollary A.3 ([57]). For NAG with $\alpha \in (0, 1/L]$ and $\beta = \nu = \frac{1 - \sqrt{\alpha \mu}}{1 + \sqrt{\alpha \mu}}$, the descent property (A.5) and the bound (A.6) holds for

$$p = \rho_{NAG}^{2} + \frac{8\alpha\sqrt{\alpha}L^{3}}{\mu(1+\sqrt{\alpha\mu})^{2}\hat{s}_{2}} + \frac{\sqrt{\alpha}(4-\sqrt{\alpha\mu}+\alpha\mu)}{2\hat{s}_{1}(1+\sqrt{\alpha\mu})^{2}},$$

$$q = \frac{\sqrt{\alpha}(1-\sqrt{\alpha\mu})}{2\hat{s}_{1}(1+\sqrt{\alpha\mu})^{2}} + \frac{2\alpha\sqrt{\alpha}L^{3}\beta^{2}}{\hat{s}_{2}\mu}, \quad r = \frac{\alpha(1+\alpha L)}{2} + \sqrt{\alpha}\hat{s}_{1} + \frac{\alpha^{2}\sqrt{\alpha}L}{2}\hat{s}_{2},$$

$$c_{1} = 1, \quad \tilde{P} = \frac{1}{2\alpha} \begin{bmatrix} 1 \\ -(1-\sqrt{\alpha\mu}) \end{bmatrix} \begin{bmatrix} 1 & -(1-\sqrt{\alpha\mu}) \end{bmatrix},$$

where

$$\hat{s}_1 = \frac{2(5 - 2\sqrt{\alpha\mu} + \alpha\mu)}{\sqrt{\mu}(1 + \sqrt{\alpha\mu})^2}, \quad \hat{s}_2 = \frac{8L^3\alpha}{\mu\sqrt{\mu}(1 + \sqrt{\alpha\mu})^2}(4 + (1 - \sqrt{\alpha\mu})^2),$$

and $\rho_{NAG}^2 := 1 - \sqrt{\alpha \mu}$. Therefore, theorem A.1 provides the bound

$$H_{\infty} \leq \overline{H}_{\infty} = \sqrt{\frac{4(5 - 2\sqrt{\alpha\mu} + \alpha\mu)}{\mu(1 + \sqrt{\alpha\mu})^2} + \frac{\sqrt{\alpha}(1 + \alpha L)}{\sqrt{\mu}} + \frac{8\alpha^3 L^4 \left(4 + (1 - \sqrt{\alpha\mu})^2\right)}{\mu^2(1 + \sqrt{\alpha\mu})^2}}.$$
 (A.7)

Proof. See [57, Section 5] for details.

Appendix B. Proof of Theorem 4.1

We first present a lemma that characterizes the risk-sensitive index in terms of the solutions to the $d \times d$ DARE in (4.8).

Lemma B.1. In the setting of theorem 4.1, the risk-sensitive index of the GMM algorithm in (3.1) for a given risk parameter $\theta > 0$ admits the formula,

$$R(\theta) = \begin{cases} -\frac{\sigma^2}{\theta} \log \det(\mathbf{I}_d - \frac{\theta}{d} B^{\top} X B) & \text{if } \sqrt{\theta} H_{\infty} < \sqrt{d}, \\ +\infty & \text{if } \sqrt{\theta} H_{\infty} \ge \sqrt{d}, \end{cases}$$

where H_{∞} is given by (3.16), and X is the "stabilizing solution" of the DARE in (4.8) for $\gamma = \frac{1}{\sqrt{\theta/d}}$, i.e., X is a solution and has the property that $\rho(A_Q + \gamma^{-2}BB^{\top}X) < 1$ for $\gamma = \frac{1}{\sqrt{\theta/d}}$.

Proof. Since f is a quadratic, the GMM system (4.5)–(4.7) is a linear dynamic system described by the system matrices (A_Q, B, T) . For linear systems, it is well-known that the H_{∞} -norm admits the frequency domain characterization

$$H_{\infty} = \|G\|_{\infty} := \max_{\{z \in \mathbb{C}: \|z\| = 1\}} \|G(z)\|,$$
 (B.1)

(see e.g., [57]); where G is the transfer matrix of the system (A_Q, B, T) defined as $G(z) := T(z|_{2d} - A_Q)^{-1}B$ for $z \in \mathbb{C}\backslash \operatorname{Spec}(A_Q)$ with $\operatorname{Spec}(A_Q) := \bigcup_i \{\lambda_i\}$ denoting the set of eigenvalues of A_Q . Thus, we can conclude that $||G||_{\infty} = H_{\infty}$ and H_{∞} is given by (3.16).

On the other hand, by scaling the gradient noise, we can rewrite the GMM system (4.5)-(4.7):

$$\xi_{k+1}^c = A_O \xi_k^c + B_\sigma \zeta_{k+1}, \quad z_k = T \xi_k^c,$$
 (B.2)

where $B_{\sigma} = \frac{\sigma}{\sqrt{d}}B$ and $\zeta_k \sim \mathcal{N}(0, \mathsf{I}_d)$ is a normal random vector with zero mean and unit variance. Glover and Doyle showed that the risk-sensitive index of this system with the system matrices (A_O, B_{σ}, T) can be represented by the following integral

$$R(\theta) = -\frac{\sigma^2}{2\pi\theta} \int_{-\pi}^{\pi} \log \det \left(\mathbf{I}_d - \frac{\theta}{\sigma^2} G_{\sigma}(e^{i\omega}) G_{\sigma}^*(e^{i\omega}) \right) d\omega, \tag{B.3}$$

for $\theta \in \mathbb{R}$ such that $\theta \|G_{\sigma}\|_{\infty}^{2} < \sigma^{2}$; otherwise, $R(\theta) = +\infty$ (see [61, Section 3])⁶ where G_{σ} is the transfer matrix of the system $(A_{Q}, B_{\sigma}, T)^{7}$ and $B_{\sigma} = \frac{\sigma}{\sqrt{d}}B$ –with the convention that the integral (B.3) for $\theta = 0$ is to be interpreted by continuity according to

$$R(0) := \lim_{\theta \downarrow 0} -\frac{\sigma^2}{2\pi\theta} \int_{-\pi}^{\pi} \log \det \left(\mathsf{I}_d - \frac{\theta}{\sigma^2} G_\sigma(e^{i\omega}) G_\sigma^*(e^{i\omega}) \right) d\omega = \frac{1}{2\pi} \int_{-\pi}^{\pi} \operatorname{trace} \left(G_\sigma(e^{i\omega}) G_\sigma^*(e^{i\omega}) \right) d\omega.$$

Since $G_{\sigma} = \frac{\sigma}{\sqrt{d}}G$, for $\theta \|G\|_{\infty}^2 < d$, it holds that

$$R(\theta) = -\frac{\sigma^2}{2\pi\theta} \int_{-\pi}^{\pi} \log \det \left(\mathsf{I}_d - \frac{\theta}{d} G(e^{i\omega}) G^*(e^{i\omega}) \right) d\omega, \tag{B.4}$$

with the convention that $R(0) = \frac{\sigma^2}{2\pi d} \int_{-\pi}^{\pi} \operatorname{trace} \left(G(e^{i\omega}) G^*(e^{i\omega}) \right) d\omega$ and $R(\theta) = +\infty$ for $\theta > 0$ such that $\sqrt{\theta} \|G\|_{\infty} \ge \sqrt{d}$. Indeed, more compactly we can write

$$R(\theta) = \frac{\sigma^2}{d} \operatorname{Ent}\left(G, \frac{1}{\sqrt{\theta/d}}\right),$$
 (B.5)

where $\operatorname{Ent}(G, \gamma)$ denotes the entropy integral of the transfer matrix G with respect to the parameter $\gamma > 0$ [94], i.e.,

$$\operatorname{Ent}(G,\gamma) := -\frac{\gamma^2}{2\pi} \int_{-\pi}^{\pi} \log \det(\mathbf{I}_d - \gamma^{-2} G(e^{i\omega}) G^*(e^{i\omega})) d\omega, \tag{B.6}$$

which can be computed as follows:

$$\operatorname{Ent}(G,\gamma) = \begin{cases} -\gamma^2 \log \det(\mathsf{I}_d - \gamma^{-2} B^\top X B) & \text{if} \quad ||G||_{\infty} < \gamma, \\ \infty & \text{if} \quad ||G||_{\infty} \ge \gamma, \end{cases}$$
(B.7)

where X is the stabilizing solution to the discrete-time Riccati equation (4.8), i.e., X solves (4.8) and satisfies $\rho(A_Q + \gamma^{-2}BB^\top X) < 1$ (see e.g., [64], [93, Remark 4.11], [94, Lemma 3.4]). Applying this formula to (B.5) and using $||G||_{\infty} = H_{\infty}$, we conclude.

We next present a lemma that establishes a connection between the 2×2 solutions of the DARE given in (4.10) and the $2d \times 2d$ solutions of the larger DARE provided in (4.8).

⁶While [61] primarily focuses on the case $\theta > 0$, the discussion and the formula for the risk-sensitive index in [61, Section 3] also apply when $\theta \le 0$, since they are derived from [61, Lemmas 3.1 and 3.2], whose validity extends to all $\theta \le 0$.

⁷Here, $A_Q := A + BQC$ where B is not scaled by σ , as A_Q is our iteration matrix from (4.6).

Lemma B.2. In the setting of theorem 4.1, consider the $2d \times 2d$ DARE in (4.8), i.e.,

$$X = A_Q^{\top} X A_Q + A_Q^{\top} X B (\gamma^2 \mathbf{I}_d - B^{\top} X B)^{-1} B^{\top} X A_Q + T^{\top} T,$$

for $\gamma = \frac{1}{\sqrt{\theta/d}}$ where the matrices A_Q, B and T are defined in (4.6), (3.4) and (4.7), respectively.

Assume that the parameter θ satisfies $\sqrt{\theta}H_{\infty} < \sqrt{d}$ where H_{∞} is as in (3.16). Then, the stabilizing solution $\overline{X} \in \mathbb{R}^{2d \times 2d}$ to this $2d \times 2d$ DARE is unique and is given by

$$\overline{X} := Y \underset{i=1,\dots,d}{Diag} (\tilde{X}^{(\lambda_i})) Y^{\top} \in \mathbb{R}^{2d \times 2d} \,,$$

where $\tilde{X}^{(\lambda_i)} \in \mathbb{R}^{2 \times 2}$ is the stabilizing solution to (4.10) for $\gamma = \frac{1}{\sqrt{\theta/d}}$ and $\lambda = \lambda_i$, and $Y = V\Sigma \in \mathbb{R}^{2d \times 2d}$ is an orthonormal matrix with V := Diag(U,U) and U is the orthonormal matrix defined in (4.2), and $\Sigma \in \mathbb{R}^{2d \times 2d}$ is the permutation matrix corresponding to the permutation π over the set $\{1,2,\ldots,2d\}$ that satisfies $\pi(i)=2i-1$ for $1 \le i \le d$ and $\pi(i)=2(i-d)$ for $d+1 \le i \le 2d$, i.e., Σ is such that $\Sigma_{ij}=1$ if $j=\pi(i)$; otherwise, $\Sigma_{ij}=0$.

Proof. We first consider the 2×2 DARE in (4.10), i.e.,

$$\tilde{X} := (\tilde{A}^{(\lambda_i)})^\top \tilde{X} \tilde{A}^{(\lambda_i)} + (\tilde{A}^{\lambda_i})^\top \tilde{X} \tilde{B} (\gamma^2 - \tilde{B}^\top \tilde{X} \tilde{B})^{-1} \tilde{B}^\top \tilde{X} \tilde{A}^{(\lambda_i)} + \tilde{Q}^{(\lambda_i)}, \tag{B.8}$$

for i = 1, ..., d, where

$$\tilde{Q}^{(\lambda_i)} = \begin{bmatrix} \frac{\lambda_i}{2} & 0 \\ 0 & 0 \end{bmatrix} = (\tilde{T}^{(\lambda_i)})^{\top} \tilde{T}^{(\lambda_i)} \quad \text{with} \quad \tilde{T}^{(\lambda_i)} := \begin{bmatrix} \frac{\sqrt{\lambda_i}}{\sqrt{2}} & 0 \\ 0 & 0 \end{bmatrix}.$$

We will first argue that a stabilizing solution $\tilde{X}^{(\lambda_i)}$ exists and is unique. For any $i \in \{1, 2, ..., d\}$, the existence of a solution to the DARE in (B.8) can be inferred from the transfer matrix of the system $(\tilde{A}^{(\lambda_i)}, \tilde{B}, T^{(\lambda_i)})$, defined as $G^{(\lambda_i)}(z) := T^{(\lambda_i)}(z | -\tilde{A}^{(\lambda_i)})^{-1}\tilde{B}$. More specifically, it is known that a stabilizing solution exists and it is unique if and only if

$$\gamma > \|G^{(\lambda_i)}\|_{\infty} = \max_{\{z \in \mathbb{C}: \|z\| = 1\}} \|G^{(\lambda_i)}(z)\|, \tag{B.9}$$

(see [112, Corollary 2.1, Prop. 3.7], [94, Lemma 3.4]) where we also know $||G^{(\lambda_i)}||_{\infty}$ equals the H_{∞} -norm of the corresponding system $(\tilde{A}^{(\lambda_i)}, \tilde{B}, T^{(\lambda_i)})$ (see (B.1)). This system subject to a given deterministic noise input $\{\tilde{\delta}_k\}_{k\geq 0}$ admits the state-space representation

$$\tilde{\xi}_{k+1} = \tilde{A}^{(\lambda_i)} \tilde{\xi}_k + \tilde{B} \tilde{\delta}_k \quad \text{where} \quad \tilde{\xi}_k = \begin{bmatrix} \tilde{x}_k \\ \tilde{x}_{k-1} \end{bmatrix} \in \mathbb{R}^2,$$

with the output $\tilde{z}_k = T^{(\lambda_i)}\tilde{\xi}_k$ for $k \geq 0$, which is equivalent to the recursion:

$$\tilde{x}_{k+1} = \tilde{x}_k - \alpha(\tilde{f}'_i(\tilde{y}_k) + \tilde{\delta}_k) + \beta(\tilde{x}_k - \tilde{x}_{k-1}), \quad \tilde{y}_k = \tilde{x}_k + \nu(\tilde{x}_k - \tilde{x}_{k-1}),$$
 (B.10)

$$\tilde{z}_k = \frac{\sqrt{\lambda_i}}{\sqrt{2}}\tilde{x}_k, \quad |\tilde{z}_k|^2 = \frac{\lambda_i}{2}(\tilde{x}_k)^2,$$
(B.11)

where the auxillary function $\tilde{f}_i: \mathbb{R} \to \mathbb{R}$ defined as $\tilde{f}(\tilde{x}) := \frac{1}{2}\lambda_i\tilde{x}^2$ and \tilde{f}'_i represents the derivative of \tilde{f}_i . This recursion is equivalent to GMM with inexact gradients for minimizing \tilde{f}_i in dimension one; therefore, applying Theorem 3.4 to \tilde{f}_i with d=1, $\mu=L=\lambda_i$, it follows that

$$||G^{(\lambda_i)}||_{\infty} = \frac{\alpha}{\sqrt{2}} \frac{\sqrt{\lambda_i}}{\tilde{s}_{\lambda_i}}.$$

Then, by our choice of θ and $\gamma = \frac{1}{\sqrt{\theta/d}}$, we have $\gamma > H_{\infty} = \max_{1 \leq i \leq d} \frac{\alpha}{\sqrt{2}} \frac{\sqrt{\lambda_i}}{\hat{s}_{\lambda_i}} \geq \|G^{(\lambda_i)}\|_{\infty}$ for every $i = 1, 2, \dots, d$, where in the last equality we used theorem 3.4. Therefore, the condition (B.9) holds, and we conclude that the stabilizing solution $\tilde{X}^{(\lambda_i)}$ exists and is unique for every $i = 1, 2, \dots, d$. Next, we introduce the square matrix

$$\hat{X} := \underset{i=1,\dots,n}{\operatorname{Diag}} (\tilde{X}^{(\lambda_i)}) \in \mathbb{R}^{2d \times 2d}, \tag{B.12}$$

as well as the block diagonal matrices $\hat{B} \in \mathbb{R}^{2d \times d}$ with $\hat{B} = \text{Diag}(\tilde{B}, \tilde{B}, \dots, \tilde{B})$ with $\tilde{B} = \begin{bmatrix} -\alpha & 0 \end{bmatrix}^{\top}$, $\hat{Q} = \begin{bmatrix} \text{Diag}(\tilde{Q}^{(\lambda_i)}) \in \mathbb{R}^{2d \times 2d}, \ \hat{A} = \begin{bmatrix} \text{Diag}(\tilde{A}^{(\lambda_i)}) \in \mathbb{R}^{2d \times 2d}. \ \text{Then, } \hat{X} \text{ satisfies} \end{bmatrix}$

$$\hat{X} = \hat{A}^{\top} \hat{X} \hat{A} + \hat{A}^{\top} \hat{X} \hat{B} (\gamma^2 \mathbf{I}_d - \hat{B}^{\top} \hat{X} \hat{B})^{-1} \hat{B}^{\top} \hat{X} \hat{A} + \hat{Q}, \tag{B.13}$$

where we used the fact that $\tilde{X}^{(\lambda_i)} \in \mathbb{R}^{2 \times 2}$ is a solution to (4.10). Since $\tilde{X}^{(\lambda_i)}$ is a stabilizing solution, it also satisfies $\rho(\tilde{A}^{(\lambda_i)} + \gamma^{-2}\tilde{B}\tilde{B}^{\top}\tilde{X}^{(\lambda_i)}) < 1$ for every i. Therefore, \hat{X} is a stabilizing solution of (B.13) satisfying

$$\rho(\hat{A} + \gamma^{-2}\hat{B}\hat{B}^{\top}\hat{X}) = \max_{1 \le i \le d} \rho(\tilde{A}^{(\lambda_i)} + \gamma^{-2}\tilde{B}\tilde{B}^{\top}\tilde{X}^{(\lambda_i)}) < 1.$$
(B.14)

Note that $Q = U\Lambda U^{\top} = U\left(\underset{i=1,...,d}{\operatorname{Diag}}(\lambda_i)\right)U^{\top}$ and we have

$$V^{\top}A_{Q}V = \begin{bmatrix} (1+\beta)\mathbf{I}_{d} - \alpha(1+\nu)\Lambda & -\beta\mathbf{I}_{d} + \alpha\nu\Lambda \\ \mathbf{I}_{d} & 0_{d} \end{bmatrix} = \Sigma\hat{A}\Sigma^{\top},$$

where A_Q is as in (4.6). By similar computations, it also follows that

$$Y\hat{A}Y^{\top} = A_Q, \quad Y\hat{Q}Y^{\top} = T^{\top}T.$$
 (B.15)

If we multiply the equation (B.13) with Y from left and with Y^{\top} from right, using the fact that $Y^{\top}Y = I$, we obtain from (B.15) that $\overline{X} := Y \hat{X} Y^{\top}$ solves the matrix equation

$$X = A_O^{\top} X A_O + A_O^{\top} X M A_O^{\top} X + T^{\top} T$$
(B.16)

with

$$M := Y \hat{B} (\gamma^2 \mathbf{I}_d - \hat{B}^\top \hat{X} \hat{B})^{-1} \hat{B}^\top Y^\top.$$

Note that, by the definition of \hat{B} , it follows that

$$\hat{B}(\gamma^2 \mathbf{I}_d - \hat{B}^\top \hat{X} \hat{B})^{-1} \hat{B}^\top = \underset{i=1,\dots,d}{\operatorname{Diag}} (\hat{Z}^{(i)}), \quad \hat{Z}^{(i)} := \begin{bmatrix} (\frac{\gamma^2}{\alpha^2} - \hat{X}_{2i-1,2i-1})^{-1} & 0 \\ 0 & 0 \end{bmatrix}.$$

Multiplying this equality from left by Σ and from right by Σ^{\top} further, we obtain

$$\Sigma \hat{B}(\gamma^2 \mathbf{I}_{2d} - \hat{B}^\top \hat{X} \hat{B})^{-1} \hat{B}^\top \Sigma^\top = \begin{bmatrix} Z & 0_d \\ 0_d & 0_d \end{bmatrix}, \quad Z = \underset{i=1,\dots,d}{\operatorname{Diag}} \left((\frac{\gamma^2}{\alpha^2} - \hat{X}_{2i-1,2i-1})^{-1} \right).$$

Multiplying this equality with V from left and with V^{\top} from right, we obtain

$$M = \begin{bmatrix} UZU^\top & 0_d \\ 0_d & 0_d \end{bmatrix}.$$

On the other hand, after a similar computation, we have

$$\overline{X} = Y \hat{X} Y^{\top} = \begin{bmatrix} U \operatorname{Diag}_{i=1,\dots,d} \begin{pmatrix} \hat{X}_{2i-1,2i-1} \end{pmatrix} U^{\top} & 0_d \\ 0_d & 0_d \end{bmatrix}.$$
 (B.17)

Then, using the definition of the matrices B and Z,

$$B(\gamma^{2} \mathbf{I}_{d} - B^{\top} \overline{X} B)^{-1} B^{\top} = B \left(\gamma^{2} \mathbf{I}_{d} - \alpha^{2} U \underset{i=1,\dots,d}{\operatorname{Diag}} \left(\hat{X}_{2i-1,2i-1} \right) U^{\top} \right)^{-1} B^{\top}$$
$$= \begin{bmatrix} U Z U^{\top} & 0_{d} \\ 0_{d} & 0_{d} \end{bmatrix} = M. \tag{B.18}$$

Plugging this expression into (B.16), we conclude that \overline{X} satisfies the Riccati equation (4.8) as claimed. Furthermore, using $Y \hat{A} Y^{\top} = A_Q$ and $Y Y^{\top} = I$,

$$\rho(A_Q + \gamma^{-2}BB^{\top}\overline{X}) = \rho\left(Y(\hat{A} + \gamma^{-2}Y^{\top}BB^{\top}\overline{X}Y)Y^{\top}\right)$$
(B.19)

$$= \rho \left(\hat{A} + \gamma^{-2} Y^{\top} B B^{\top} \overline{X} Y \right) \tag{B.20}$$

$$= \rho \left(\hat{A} + \gamma^{-2} Y^{\top} B B^{\top} Y \hat{X} \right) \tag{B.21}$$

$$= \rho \left(\hat{A} + \gamma^{-2} \hat{B} \hat{B}^{\top} \hat{X} \right) < 1, \tag{B.22}$$

where in the second equality we used the fact that Y is orthogonal, in the third equality we used $\overline{X} = Y \hat{X} Y^{\top}$ and in the last equality we used the fact that $Y^{\top}BB^{\top}Y = \hat{B}\hat{B}^{\top}$ and (B.14). We conclude from (B.22) that \overline{X} is a stabilizing solution to (4.8). Finally, if the stabilizing solution exists then it is unique, see [118], [94, Lemma 3.4]. This completes the proof.

Now, the stage is set to complete the proof of theorem 4.1, where we will build on theorem B.2 and theorem B.1. Let $\gamma = \frac{1}{\sqrt{\theta/d}}$. According to theorem B.2, $\overline{X} = Y$ Diag $(\tilde{X}^{(\lambda_i)})Y^{\top} \in \mathbb{R}$

 $\mathbb{R}^{2d\times 2d}$ is a solution to (4.8) satisfying $\rho(A_Q + \gamma^{-2}BB^{\top}\overline{X}) < 1$. Therefore, from theorem B.1,

$$R(\theta) = \begin{cases} -\frac{\sigma^2}{\theta} \log \det(\mathsf{I}_d - \frac{\theta}{d} B^\top Y \underset{i=1,\dots,d}{\operatorname{Diag}} (\tilde{X}^{(\lambda_i)}) Y^\top B) & \text{if } \sqrt{\theta} H_\infty < \sqrt{d}, \\ \infty & \text{if } \sqrt{\theta} H_\infty \ge \sqrt{d}, \end{cases}$$
(B.23)

From the definitions of $B := \tilde{B} \otimes \mathsf{I}_d$ and $Y := V\Sigma$, we obtain

$$B^{\top}Y \underset{i=1,\dots,d}{\operatorname{Diag}} (\tilde{X}^{(\lambda_i)})Y^{\top}B = \alpha^2 U \operatorname{Diag}(\tilde{X}_{11}^{(\lambda_i)})U^{\top}.$$

Consequently,

$$\begin{split} \log \det \left(\mathbf{I}_d - \frac{\theta}{d} B^\top Y \underset{i=1,\dots,d}{\operatorname{Diag}} (\tilde{X}^{(\lambda_i)}) Y^\top B \right) &= & \log \det \left(U \left(\mathbf{I}_d - \frac{\theta}{d} \alpha^2 \underset{i=1,\dots,d}{\operatorname{Diag}} (\tilde{X}^{(\lambda_i)}_{11}) \right) U^\top \right) \\ &= & \sum_{i=1}^d \log \left(1 - \frac{\theta}{d} \alpha^2 \tilde{X}^{(\lambda_i)}_{11} \right). \end{split}$$

Inserting this expression into (B.23), we conclude.

APPENDIX C. PROOFS OF THEOREM 4.4 AND THEOREM 4.6

C.1. **Proof of theorem 4.4.** From (B.4), we recall that for $\theta/d < 1/H_{\infty}^2$, we have

$$R(\theta) = -\frac{\sigma^2}{2\pi\theta} \int_{-\pi}^{\pi} \log \det \left(\mathbf{I}_d - \frac{\theta}{d} G(e^{i\omega}) G^*(e^{i\omega}) \right) d\omega < \infty, \tag{C.1}$$

with the convention that $R(0) = \frac{\sigma^2}{2\pi d} \int_{-\pi}^{\pi} \operatorname{trace} \left(G(e^{i\omega}) G^*(e^{i\omega}) \right) d\omega$ where $H_{\infty} = \max_{\omega} \|G(e^{i\omega})\|$; and $R(\theta) = +\infty$ if $\theta/d \ge 1/H_{\infty}^2$. We conclude that

$$R(\theta) < \infty$$
 when $\theta \in (-\infty, \frac{d}{H_{\infty}^2})$, and $R(\theta) = +\infty$ otherwise. (C.2)

Next, we consider the following logarithmic moment generating function:

$$\tilde{\Lambda}_K(\lambda) := \log \mathbb{E}\left[e^{\lambda \tilde{S}_K}\right], \text{ where } \tilde{S}_K = \frac{S_K}{K+1}.$$

It is known that the function $\tilde{\Lambda}_K(\lambda)$ is convex in λ in its domain for every $K.^9$ Recall that the risk-sensitive index is given by: $R(\theta) = \lim_{K \to \infty} \frac{2\sigma^2}{\theta(K+1)} \log \mathbb{E}\left[e^{\frac{\theta}{2\sigma^2}S_K}\right]$. Therefore, taking $\tilde{S}_K := \frac{1}{K+1}S_K$ and $\lambda = \frac{\theta}{2\sigma^2}$, we observe that the limit,

$$\tilde{\Lambda}(\lambda) := \lim_{K \to \infty} \frac{1}{K+1} \log \mathbb{E}\left[e^{\lambda(K+1)\tilde{S}_K}\right] = \lambda R(2\sigma^2 \lambda), \tag{C.3}$$

exists as an extended number for any $\lambda \in \mathbb{R}$, i.e., the limit is a real number or $+\infty$. In addition, $\tilde{\Lambda}$ admits the domain

$$\operatorname{dom}(\tilde{\Lambda}) := \{\lambda : \tilde{\Lambda}(\lambda) < \infty\} = \left(-\infty, \frac{d}{2\sigma^2 H_{\infty}^2}\right), \tag{C.4}$$

where we used (C.2) and (C.3). Furthermore, $\tilde{\Lambda}$ is a convex function of λ as it is the pointwise limit of convex functions $\frac{1}{K+1}\tilde{\Lambda}_K(\lambda)$. Gärtner-Ellis theorem [65, Section 2] says that if

- (I) 0 in the interior of the domain of $\tilde{\Lambda}$, i.e., $0 \in (\text{dom}(\tilde{\Lambda}))^o$,
- (II) $\tilde{\Lambda}$ is lower semi-continuous,
- (III) $\tilde{\Lambda}$ is essentially smooth, i.e., it satisfies the following properties:
 - (i) The interior of the domain of $\tilde{\Lambda}(\lambda)$ is non-empty,
 - (ii) $\Lambda(\lambda)$ is differentiable in the interior of its domain,
 - (iii) $|\tilde{\Lambda}'(\lambda_n)| \to +\infty$ for all $\lambda_n \to \lambda^*$ where λ^* is in the boundary of the interior of the domain,

then the LDP holds with the good rate function

$$I(s) := \sup_{\lambda \in \text{dom}(\tilde{\Lambda})} [\lambda s - \tilde{\Lambda}(\lambda)] = \sup_{-\infty < \theta < \frac{d}{H_{\infty}^2}} \left[\frac{\theta}{2\sigma^2} \left(s - R(\theta) \right) \right],$$

 $^{{}^8}R(\theta) < \infty$ for $\theta \in (0, \frac{d}{H_\infty^2})$ also follows from theorem 4.1; however, that result does not apply to the $\theta < 0$ regime.

⁹Indeed, for any $\bar{\lambda}_1, \bar{\lambda}_2 \in \text{dom}(\Lambda_k) := \{\lambda : \Lambda_k(\lambda) < \infty\}$, and $\omega \in [0,1]$, we have $\tilde{\Lambda}_K(\omega \bar{\lambda}_1 + (1-\omega)\bar{\lambda}_2) = \log \mathbb{E}[e^{\omega \bar{\lambda}_1 \tilde{S}_K} e^{(1-\omega)\bar{\lambda}_2 \tilde{S}_K}] \leq \log \left(\mathbb{E}[e^{\bar{\lambda}_1 \tilde{S}_K}]^{\omega} \mathbb{E}[e^{\bar{\lambda}_2 \tilde{S}_K}]^{1-\omega}\right) = \omega \tilde{\Lambda}_K(\bar{\lambda}_1) + (1-\omega)\tilde{\Lambda}_K(\bar{\lambda}_2)$ where the inequality is due to Hölder's inequality. Thus, $\tilde{\Lambda}_K(\lambda)$ is convex in λ .

which implies (4.17) as desired. In the rest of the proof, we will argue that these conditions hold. By the assumption $\rho(A_Q) < 1$, theorem 3.4 applies and $H_{\infty} < \infty$. Using this fact and (C.4), we conclude that condition (I) and condition (i) holds. From the representation (C.1), we observe that $R(\theta)$ is continuous and differentiable in its domain; therefore, using (C.3), we conclude that $\tilde{\Lambda}$ is continuous and differentiable on its domain. Hence, conditions (II) and (ii) both also hold. It suffices to argue that condition (iii) holds. Note that $\lambda_* = \frac{d}{2\sigma^2 H_{\infty}^2}$ is the only boundary point for the domain of $\tilde{\Lambda}$ and

$$\tilde{\Lambda}'(\lambda) = R(2\sigma^2\lambda) + 2\sigma^2\lambda \frac{dR_{\sigma^2}(\theta)}{d\theta} \bigg|_{\theta = 2\sigma^2\lambda}.$$
(C.5)

Let λ_n be a sequence with $\lambda_n \to \lambda_*$. First of all, for $\theta \in [0, d/H_\infty^2)$, differentiating (C.1) under the integral sign, we obtain

$$\frac{dR}{d\theta}(\theta) = \frac{\sigma^2}{2\pi} \sum_{k=1}^{\infty} \int_{-\pi}^{\pi} \frac{\theta^{k-1}}{k} \operatorname{trace}(\Theta(\omega)^k) d\omega \ge 0, \tag{C.6}$$

with $\Theta(\omega) = G(e^{i\omega})G^*(e^{i\omega})/d \succeq 0$, where we used the Taylor series

$$-\frac{\log \det(I - \theta X)}{\theta} = \sum_{k=1}^{\infty} \frac{\theta^{k-1}}{k} \operatorname{trace}(X^k) \quad \text{when} \quad \|\theta X\| < 1,$$

for $X = \Theta(\omega)$, noting that $H_{\infty} = \max_{\omega} \|G(e^{i\omega})\|$ and $\|\theta\Theta(\omega)\| \le \theta H_{\infty}^2/d < 1$. Similarly, differentiating (C.6) again, for $\theta \in [0, d/H_{\infty}^2)$,

$$R''(\theta) = \frac{d^2}{d^2\theta}R(\theta) = \frac{\sigma^2}{2\pi} \sum_{k=2}^{\infty} \int_{-\pi}^{\pi} \frac{(k-1)\theta^{k-2}}{k} \operatorname{trace}(\Theta(\omega)^k) d\omega \ge 0.$$
 (C.7)

With the non-negativity of the second derivative, we conclude that $R(\theta)$ is a non-decreasing convex function of θ when $\theta \in [0, \theta_*)$ where $\theta_* := d/H_\infty^2 > 0$. If we consider $\theta_n := 2\sigma^2 \lambda_n$, then $\theta_n \uparrow \theta_*$. Consider $R_{max} := \sup_n R(\theta_n)$. If R_{max} is finite, then by continuity of the function $R(\theta)$ in θ , we would have $R(\theta_*) = R_{max}$ and this would conflict with $R(\theta_*) = +\infty$. Therefore, we have necessarily $R_{max} = +\infty$ and

$$R(\theta_n) = \tilde{\Lambda}(\lambda_n) \to +\infty.$$
 (C.8)

Similarly, for $\theta \in [0, \theta_*)$, by differentiating (C.7) again, we can observe the third derivative $R'''(\theta) \geq 0$ and we conclude $R'(\theta)$ is a non-decreasing convex function of θ . Similarly, if $R'_{\max} := \sup_n R'(\theta_n) < \infty$, then by the continuity and monotonicity of $R'(\theta)$, we have $R'(\theta_*) := R'_{\max}$ and this would imply $R(\theta_*) \leq R(0) + R'_{\max}\theta_*$ which would contradict with the fact $R(\theta_*) = +\infty$. Hence, we necessarily have

$$R'(\theta_n) \to +\infty.$$
 (C.9)

Therefore, combining (C.5), (C.9) and (C.8), we obtain $\tilde{\Lambda}'(\lambda_n) = R(\theta_n) + 2\sigma^2\lambda R'(\theta_n) \to \infty$, and this proves (iii) as desired and the LDP follows from the Gärtner-Ellis Theorem. To prove (4.21), note that by the Gaussian noise assumption, the density of $S_K/(K+1)$ is positive and continuous at any point $s \in (0, \infty)$; therefore, $I(s) < +\infty$ for any s > 0 (see [65, Ex. 2.2.39]. Thus, the rate function I, as the dual of $\tilde{\Lambda}$, is continuous on its domain which includes $(0, \infty)$, and we conclude that for the set $E = [t, \infty]$ with t > 0,

$$\inf_{s\in E^o}I(s)=\inf_{s\in \bar{E}}I(s)=\inf_{s\in [t,\infty]}I(s),$$

and based on the LDP for $S_K/(K+1)$, this implies the equality in (4.21). The inequality in (4.21) is a consequence of (4.15).

C.2. **Proof of theorem 4.6.** For momentum methods, [57, eqn. (59)] shows that the transfer matrix $G(e^{i\omega})$ admits the explicit representation

$$G(e^{i\omega}) = \frac{1}{\sqrt{2}} \underset{j=1,\dots,d}{\text{Diag}} \left[\frac{-\alpha\sqrt{\lambda_j}}{e^{i\omega} - (1+\beta - \beta e^{-i\omega}) + \alpha\lambda_j(1+\nu - \nu e^{-i\omega})} \right] U^T, \tag{C.10}$$

as a diagonal matrix where $\{\lambda_j\}_{j=1}^d$ are the eigenvalues of Q, where we have the eigenvalue decomposition $Q = U\Lambda U^{\top}$ with Λ diagonal satisfying $\Lambda_{jj} = \lambda_j$ and U is a real orthogonal matrix satisfying $U^{\top}U = \mathsf{I}_d$. Thus, with some further straightforward computations, it can be seen that

$$G(e^{i\omega})G^*(e^{i\omega}) = \operatorname{Diag}_{j=1,\dots,d} \left[\frac{\alpha^2 \lambda_j}{2\|e^{i\omega} - (1+\beta - \beta e^{-i\omega}) + \alpha \lambda_j (1+\nu - \nu e^{-i\omega})\|^2} \right] = \operatorname{Diag}_{j=1,\dots,d} [h_\omega(\lambda_j)].$$

Then, by exploiting the diagonal structure of $G(e^{i\omega})G^*(e^{i\omega})$, we obtain the equalities

$$\begin{split} \int_{-\pi}^{\pi} \log \det \left(\mathbf{I}_{d} - \frac{\theta}{d} G(e^{i\omega}) G^{*}(e^{i\omega}) \right) d\omega &= \sum_{j=1}^{d} \int_{-\pi}^{\pi} \log \left(1 - \frac{\theta}{d} h_{\omega}(\lambda_{j}) \right) d\omega, \\ \int_{-\pi}^{\pi} \operatorname{trace} \left(G(e^{i\omega}) G^{*}(e^{i\omega}) \right) d\omega &= \sum_{j=1}^{d} \int_{-\pi}^{\pi} h_{\omega}(\lambda_{i}) d\omega, \end{split}$$

showing that (4.18) is equivalent to (4.22). This completes the proof.

APPENDIX D. PROOF OF THEOREM 5.1

Let $\theta > 0$ be given such that $\sqrt{\theta}\overline{H}_{\infty} < 1$. For the GMM iterate sequence, consider the partial sum sequence defined as

$$\bar{S}_{k,K} = \sum_{j=k}^{K} \left[J_{p,q} V(\xi_j) + (1 - J_{p,q}) V(\xi_{j-1}) \right] \quad \text{for} \quad 0 \le k \le K,$$
 (D.1)

where here and in the rest of the proof, we drop the subscripts c_1, P in the Lyapunov function for notational simplicity, and we use the convention that $\xi_{-1} := \xi_0$. The sum (D.1) is based on a modified Lyapunov function that takes convex averages with $V(\xi_{j-1})$ at time k. Note that when $\tilde{P}_{22} > 0$, by a Schur complement argument, we can write

$$\tilde{P} = \begin{bmatrix} \tilde{P}_{11} - \frac{\tilde{P}_{12}^2}{\tilde{P}_{22}} & 0 \\ 0 & 0 \end{bmatrix} + \begin{bmatrix} \tilde{P}_{12}^2 / \tilde{P}_{22} & \tilde{P}_{12} \\ \tilde{P}_{12} & \tilde{P}_{22} \end{bmatrix} \succeq \begin{bmatrix} \tilde{P}_{11} - \frac{\tilde{P}_{12}^2}{\tilde{P}_{22}} & 0 \\ 0 & 0 \end{bmatrix} = \begin{bmatrix} \tilde{r}(\tilde{P}) & 0 \\ 0 & 0 \end{bmatrix},$$

and when $\tilde{P}_{22} = 0$, we have $\tilde{P}_{12} = 0$ since $\tilde{P} \succeq 0$. Therefore, using $P = \tilde{P} \otimes I_d$, for any $j \geq 0$,

$$V(\xi_{j}) = c_{1}[f(x_{j}) - f(x_{*})] + \begin{bmatrix} x_{j} - x_{*} \\ x_{j-1} - x_{*} \end{bmatrix}^{\top} P \begin{bmatrix} x_{j} - x_{*} \\ x_{j-1} - x_{*} \end{bmatrix} \geq c_{1}[f(x_{j}) - f(x_{*})] + \tilde{r}(\tilde{P}) \|x_{j} - x_{*}\|^{2}$$

$$\geq (c_{1} + \frac{2}{L}\tilde{r}(\tilde{P}))[f(x_{j}) - f(x_{*})],$$

where the last inequality follows from the L-Lipschitzness of ∇f . Hence, by the definition of S_K given in (3.10), we get

$$\frac{\bar{S}_{0,K} - (1 - J_{p,q})V(\xi_0)}{c_1 + \frac{2}{L}\tilde{r}(\tilde{P})} \ge (S_{K-1} + J_{p,q}[f(x_K) - f(x_*)]) \ge J_{p,q}S_K. \tag{D.2}$$

Let $x^+, x, x^- \in \mathbb{R}^d$ be given arbitrary vectors. We consider the 2d-dimensional vectors,

$$\xi^+ := \begin{bmatrix} x^+ \\ x \end{bmatrix}, \quad \xi := \begin{bmatrix} x \\ x^- \end{bmatrix},$$
 (D.3)

and for $0 \le k \le K$, we introduce the deterministic functions $\mathcal{V}_{k,K}$ defined as

$$\mathcal{V}_{k,K}(\xi^+,\xi;\bar{\theta}) \coloneqq \frac{1}{\bar{\theta}} \log \mathbb{E} \left[e^{\bar{\theta}\bar{S}_{k,K}} \mid \xi_k = \xi^+, \xi_{k-1} = \xi \right] \quad \text{where} \quad \bar{\theta} \coloneqq \frac{\theta}{2\sigma^2 \left(c_1 + \frac{2}{L} \tilde{r}(\tilde{P}) \right)}.$$

Since $\theta \in \left(0, \frac{1}{(\overline{H}_{\infty})^2}\right)$, we notice that

$$\bar{\theta} \in (0, \bar{\theta}^{ub}) \quad \text{with} \quad \bar{\theta}^{ub} := \frac{1}{(\overline{H}_{\infty})^2 2\sigma^2 \left(c_1 + \frac{2}{L}\tilde{r}(\tilde{P})\right)}.$$
 (D.4)

From (D.2) and the definition of the risk-sensitive cost, we can infer that 10

$$R_{K}(\theta) \leq \frac{1}{J_{p,q}} \frac{1}{\left(c_{1} + \frac{2}{L}\tilde{r}(\tilde{P})\right)(K+1)} \left[\mathcal{V}_{0,K}\left(\xi_{0}, \xi_{-1}; \frac{\bar{\theta}}{J_{p,q}}\right) - (1 - J_{p,q})V(\xi_{0}) \right], \quad (D.5)$$

$$R_{K-1}(\theta) \leq \frac{1}{\left(c_1 + \frac{2}{L}\tilde{r}(\tilde{P})\right)K} \left[\mathcal{V}_{0,K}\left(\xi_0, \xi_{-1}; \bar{\theta}\right) - (1 - J_{p,q})V(\xi_0) \right]. \tag{D.6}$$

In the rest of the proof, we will obtain bounds for the function $\mathcal{V}_{k,K}$ with a backwards induction over $k \in \{0, 1, ..., K\}$ and build on the last two inequalities. More specifically, we will show that for every $0 \le k \le K$, and for any choice of the vectors $x^+, x, x^- \in \mathbb{R}^d$, we have

$$\mathcal{V}_{k,K}(\xi^+, \xi; \bar{\theta}) \le a_{k,K} V(\xi^+) + b_{k,K} V(\xi) + c_{k,K}(\bar{\theta}),$$
 (D.7)

for suitably chosen scalars $a_{k,K}, b_{k,K}$ and $c_{k,K}$ (that may depend on the choice of $\bar{\theta}$) where ξ^+ and ξ are as in (D.3). Clearly, such a bound holds for k = K with $a_{K,K} = J_{p,q}, b_{K,K} = 1 - J_{p,q}$ and $c_{K,K}(\bar{\theta}) = 0$. Next, we consider k < K, and introduce the next GMM iterate starting from $\xi_k = \xi^+$:

$$\xi^{++} := A\xi^{+} + B\nabla f(C\xi^{+}) + Bw_{k+1}.$$

Note that by the definition of $\mathcal{V}_{k,K}$,

$$e^{\bar{\theta}\mathcal{V}_{k,K}(\xi^{+},\xi;\bar{\theta})} = \mathbb{E}\left[e^{\bar{\theta}\left[\left\{J_{p,q}V(\xi^{+}) + (1-J_{p,q})V(\xi)\right\} + \mathcal{V}_{k+1}(\xi^{++},\xi^{+};\bar{\theta})\right]} \mid \xi_{k} = \xi^{+}, \xi_{k-1} = \xi\right],$$

where the expectation is taken with respect to randomness introduced by the noise w_{k+1} , and, by Theorem A.1, we have

$$V(\xi_{k+1}) \le pV(\xi_k) + qV(\xi_{k-1}) + r||w_{k+1}||^2, \tag{D.8}$$

¹⁰We use the convention that the right-hand side of (D.5) is $+\infty$, when $\frac{\bar{\theta}}{J_{p,q}} \geq \bar{\theta}^{ub}$; in which case the bound (D.5) is trivial.

holding almost surely where p,q,r are as in (A.5). We then invoke the inductive hypothesis, where we assume (D.7) holds at step k+1, and use the previous inequality:

$$\mathcal{V}_{k+1,K}(\xi^{++},\xi^{+};\bar{\theta}) \leq a_{k+1,K}V(\xi^{++}) + b_{k+1,K}V(\xi^{+}) + c_{k+1,K}(\bar{\theta})
\leq a_{k+1,K}[pV(\xi^{+}) + qV(\xi) + r||w_{k+1}||^{2}] + b_{k+1,K}V(\xi^{+}) + c_{k+1,K}(\bar{\theta})
\leq (a_{k+1,K}p + b_{k+1,K})V(\xi^{+}) + a_{k+1,K}qV(\xi) + a_{k+1,K}r||w_{k+1}||^{2} + c_{k+1,K}(\bar{\theta}).$$

This leads to

$$\begin{split} e^{\bar{\theta}\mathcal{V}_{k,K}(\xi^{+},\xi;\bar{\theta})} &= \mathbb{E}\left[\exp\left\{\bar{\theta}\left[\left\{J_{p,q}V(\xi^{+}) + (1-J_{p,q})V(\xi)\right\} + \mathcal{V}_{k+1,K}(\xi^{++},\xi^{+};\bar{\theta})\right]\right\} \Big| \xi_{k} = \xi^{+}, \xi_{k-1} = \xi\right] \\ &\leq \mathbb{E}\left[\exp\left\{\bar{\theta}\left[\left\{J_{p,q}V(\xi^{+}) + (1-J_{p,q})V(\xi)\right\} + ((a_{k+1,K}p + b_{k+1,K})V(\xi^{+}) + a_{k+1,K}qV(\xi) + a_{k+1,K}r\|w_{k+1}\|^{2} + c_{k+1,K}(\bar{\theta})\right]\right\} \Big| \xi_{k} = \xi^{+}, \xi_{k-1} = \xi\right] \\ &= \mathbb{E}\left[\exp\left\{\bar{\theta}\left[\left(J_{p,q} + a_{k+1,K}p + b_{k+1,K}\right)V(\xi^{+}) + (1-J_{p,q} + a_{k+1,K}q)V(\xi) + a_{k+1,K}r\|w_{k+1}\|^{2} + c_{k+1,K}(\bar{\theta})\right]\right\} \Big| \xi_{k} = \xi^{+}, \xi_{k-1} = \xi\right] \\ &= \exp\left\{\bar{\theta}\left[\left(J_{p,q} + a_{k+1,K}p + b_{k+1,K}\right)V(\xi^{+}) + (1-J_{p,q} + a_{k+1,K}q)V(\xi)\right]\right\} \\ &\times \exp\left\{\bar{\theta}\left[c_{k+1,K}(\bar{\theta}) + \frac{1}{\bar{\theta}}\log\mathbb{E}\left[e^{\frac{\bar{t}_{k+1,K}\|w_{k+1}\|^{2}}{2\sigma^{2}}} \Big| \xi_{k} = \xi^{+}, \xi_{k-1} = \xi\right]\right]\right\} \\ &\leq \exp\left\{\bar{\theta}\left[\left(J_{p,q} + a_{k+1,K}p + b_{k+1,K}\right)V(\xi^{+}) + (1-J_{p,q} + a_{k+1,K}q)V(\xi)\right]\right\} \\ &\times \exp\left\{\bar{\theta}\left[c_{k+1,K}(\bar{\theta}) + \frac{1}{\bar{\theta}}\log\left(\frac{1 + \bar{t}_{k+1,K}}{1 - \bar{t}_{k+1,K}}\right)\right]\right\}, \end{split}$$

where $\tilde{t}_{k+1,K} := 2\sigma^2 \bar{\theta} a_{k+1,K} r$, provided that $0 \leq \tilde{t}_{k+1,K} < 1$. In the last inequality, we used (E.1). This implies that (D.7) indeed holds for $a_{k,K}, b_{k,K}, c_{k,K}$ values that satisfy the following backwards recursion

$$a_{k,K} = J_{p,q} + a_{k+1,K}p + b_{k+1,K}, \quad b_{k,K} = 1 - J_{p,q} + a_{k+1,K}q,$$
 (D.9)

$$c_{k,K}(\bar{\theta}) = c_{k+1,K}(\bar{\theta}) + \frac{1}{\bar{\theta}} \log \left(\frac{1 + \tilde{t}_{k+1,K}}{1 - \tilde{t}_{k+1,K}} \right),$$
 (D.10)

for $0 \le k \le K-1$ with the boundary condition $a_{K,K} = J_{p,q}, b_{K,K} = 1 - J_{p,q}, c_{K,K}(\bar{\theta}) = 0$; as long as the condition

$$0 \le \tilde{t}_{k+1,K} < 1 \quad \text{for every} \quad 0 \le k \le K - 1, \tag{D.11}$$

holds. Indeed, by theorem E.2, if we choose $J_{p,q} = \frac{1}{1+(\lambda_+-p)}$, then the solution $a_{k,K}$ to the recurrence (D.9) satisfies $a_{k,K} \leq \frac{1}{1-(p+q)}$ for all $0 \leq k \leq K$. Using this inequality, the bound (D.4) and the formula (A.6), for $0 \leq k \leq K-1$, we have

$$\tilde{t}_{k+1,K} = 2\sigma^2 \bar{\theta} a_{k+1,K} r < \frac{1}{\left(c_1 + \frac{2}{L}\tilde{r}(\tilde{P})\right) (\overline{H}_{\infty})^2 [1 - (p+q)]} r = 1.$$
 (D.12)

Therefore, the condition (D.11) indeed holds. From (E.3) which implies that $a_{0,K} + b_{0,K} = \frac{1-\lambda_+^{K+1}}{1-\lambda_+}$, the $c_{k,K}$ update rule (D.10) and the fact that $\xi_{-1} = \xi_0$, we can conclude that

$$\mathcal{V}_{0,K}(\xi_0, \xi_{-1}; \bar{\theta}) \leq a_{0,K}V(\xi_0) + b_{0,K}V(\xi_0) + c_{0,K}(\bar{\theta})$$
 (D.13)

$$= \left(\frac{1 - \lambda_{+}^{K+1}}{1 - \lambda_{+}}\right) V(\xi_{0}) + \hat{c}(K, \theta), \tag{D.14}$$

with

$$\hat{c}(K,\theta) \coloneqq c_{0,K}(\bar{\theta}) = \frac{2\sigma^2 \left(c_1 + \frac{2}{L}\tilde{r}(\tilde{P})\right)}{\theta} \sum_{j=0}^{K-1} \log \left(\frac{\left(c_1 + \frac{2}{L}\tilde{r}(\tilde{P})\right) + \theta a_{j+1,K}r}{\left(c_1 + \frac{2}{L}\tilde{r}(\tilde{P})\right) - \theta a_{j+1,K}r}\right). \tag{D.15}$$

Combining this inequality with (D.5)-(D.6), we finally obtain the bound (5.3). This completes the proof.

APPENDIX E. SUPPORTING LEMMAS

Lemma E.1. Under theorem 3.1, for every $k \ge 0$, we have the almost sure bound

$$\log \mathbb{E}\left[e^{\frac{t\|w_{k+1}\|^2}{2\sigma^2}} \mid \mathcal{F}_k\right] \le \log\left(\frac{1+t}{1-t}\right) \quad for \quad 0 \le t < t_* := 1.$$
 (E.1)

Proof. Under theorem 3.1, for any $\tilde{p} \geq 1$,

$$\mathbb{E}\left[\|w_{k+1}\|^{\tilde{p}} \mid \mathcal{F}_{k}\right] = \int_{0}^{\infty} \mathbb{P}(\|w_{k+1}\|^{\tilde{p}} \geq t \mid \mathcal{F}_{k}) dt = \int_{0}^{\infty} \mathbb{P}(\|w_{k+1}\| \geq t^{1/\tilde{p}} \mid \mathcal{F}_{k}) dt \\ \leq \int_{0}^{\infty} 2 \exp\left(\frac{-t^{2/\tilde{p}}}{2\sigma^{2}}\right) dt = (2\sigma^{2})^{\tilde{p}/2} \tilde{p} \int_{0}^{\infty} e^{-s} s^{\tilde{p}/2 - 1} ds = (2\sigma^{2})^{\tilde{p}/2} \tilde{p} \Gamma(\tilde{p}/2),$$

where in the second equality we used the change of variables $s := \frac{t^{2/\bar{p}}}{2\sigma^2}$, and the third equality follows from the definition of $\Gamma(\cdot)$ function. Thus, by the dominated convergence theorem,

$$\mathbb{E}\left[e^{\frac{t\|w_{k+1}\|^2}{2\sigma^2}} \mid \mathcal{F}_k\right] = \mathbb{E}\left[1 + \sum_{\tilde{p}=1}^{\infty} \frac{(t\|w_{k+1}\|^2)^{\tilde{p}}}{(2\sigma^2)^{\tilde{p}}\tilde{p}!} \mid \mathcal{F}_k\right] = 1 + \sum_{\tilde{p}=1}^{\infty} \frac{t^{\tilde{p}}\mathbb{E}\left[\|w_{k+1}\|^{2\tilde{p}} \mid \mathcal{F}_k\right]}{(2\sigma^2)^{\tilde{p}}\tilde{p}!}$$

$$\leq 1 + \sum_{\tilde{p}=1}^{\infty} \frac{2(2t\sigma^2)^{\tilde{p}}\tilde{p}!}{(2\sigma^2)^{\tilde{p}}\tilde{p}!} = 2\sum_{\tilde{p}=0}^{\infty} t^{\tilde{p}} - 1 = \frac{2}{1-t} - 1 = \frac{1+t}{1-t},$$

provided |t| < 1, this implies (E.1) and we conclude.

Lemma E.2. Let $K \ge 1$ be a given positive integer that is fixed. Consider the backwards recurrence (D.9) where the scalars $a_{k,K} \in \mathbb{R}$ and $b_{k,K} \in \mathbb{R}$ satisfy

$$a_{k,K} = J_{p,q} + a_{k+1,K}p + b_{k+1,K}, \quad b_{k,K} = 1 - J_{p,q} + a_{k+1,K}q,$$
 (E.2)

for $0 \le k \le K$ with $a_{K,K} = J_{p,q}$, $b_{K,K} = 1 - J_{p,q}$ where p,q are non-negative scalars as in (A.1) satisfying p+q < 1. Then, for any $0 \le k \le K$,

$$\begin{bmatrix} a_{k,K} \\ b_{k,K} \end{bmatrix} = \begin{pmatrix} \sum_{j=0}^{K-k} \overline{M}^j \end{pmatrix} v_{p,q} \quad where \qquad v_{p,q} = \begin{bmatrix} J_{p,q} \\ 1 - J_{p,q} \end{bmatrix}, \quad and \quad \overline{M} = \begin{bmatrix} p & 1 \\ q & 0 \end{bmatrix}.$$

The eigenvalues of \overline{M} are $\lambda_{+,-} = \frac{p \pm \sqrt{p^2 + 4q}}{2}$ with the largest eigenvalue $\lambda_+ \in [0,1)$. Furthermore, if we set $J_{p,q} = \frac{1}{1 + (\lambda_+ - p)}$, then $v_{p,q}$ is an eigenvector of \overline{M} satisfying $\overline{M}v_{p,q} = \lambda_+ v_{p,q}$ and,

$$\begin{bmatrix} a_{k,K} \\ b_{k,K} \end{bmatrix} = \frac{1 - \lambda_{+}^{K-k+1}}{1 - \lambda_{+}} \begin{bmatrix} \frac{1}{1 + (\lambda_{+} - p)} \\ \frac{\lambda_{+} - p}{1 + (\lambda_{+} - p)} \end{bmatrix} = \frac{1}{1 - (p+q)} (1 - \lambda_{+}^{K-k+1}) \begin{bmatrix} 1 \\ \lambda_{+} - p \end{bmatrix}, \tag{E.3}$$

for any $0 \le k \le K$. Furthermore, we have

$$a_{K,K} \le a_{K-1,K} \le \dots \le a_{1,K} \le a_{0,K} \le \frac{1}{1 - (p+q)}.$$
 (E.4)

Proof. For K fixed, the backwards recursion over k for $a_{k,K}$ and $b_{k,K}$ is equivalent to

$$\begin{bmatrix} a_{k,K} \\ b_{k,K} \end{bmatrix} = \overline{M} \begin{bmatrix} a_{k+1,K} \\ b_{k+1,K} \end{bmatrix} + v_{p,q} \quad \text{for} \quad 0 \le k \le K - 1,$$

subject to boundary conditions $\begin{bmatrix} a_{K,K} & b_{K,K} \end{bmatrix}^T = v_{p,q}$. It can be seen that the solution is simply

$$\begin{bmatrix} a_{k,K} \\ b_{k,K} \end{bmatrix} = \left(\sum_{j=0}^{K-k} \overline{M}^j \right) v_{p,q} \quad \text{for} \quad 0 \le k \le K - 1.$$
 (E.5)

The characteristic equation $\det(\overline{M} - \lambda I) = \lambda^2 - p\lambda - q$ admits the roots λ_{\pm} as the eigenvalues of \overline{M} . The fact that $\lambda_{+} \in [0,1)$ is a consequence of the inequalities $p,q \geq 0$ and p+q < 1. For the choice of $J_{p,q} = \frac{1}{1+(\lambda_{+}-p)}$, it is easy to check that $\overline{M}v_{p,q} = \lambda_{+}v_{p,q}$. In this case, using (E.5),

$$\begin{bmatrix} a_{k,K} \\ b_{k,K} \end{bmatrix} = \left(\sum_{j=0}^{K-k} \lambda_+^j \right) v_{p,q} = \frac{1 - \lambda_+^{K-k+1}}{1 - \lambda_+} v_{p,q} \,,$$

and the formula (E.3) follows noting $(1 - \lambda_+)(1 + (\lambda_+ - p)) = 1 - (p + q)$. Finally, note that by (E.3) and the fact that $\lambda_+ \in [0,1)$, for any k < K, we have

$$a_{k+1,K} - a_{k,K} = \frac{1}{1 - (p+q)} (\lambda_+^{K-k+1} - \lambda_+^{K-k}) \le 0.$$

This implies (E.4), together with the fact that $a_{0,K} = \frac{1-\lambda_+^{K+1}}{1-(p+q)} \le \frac{1}{1-(p+q)}$.

Lemma E.3. Consider the function $\phi : \mathbb{R} \times \mathbb{R}_+ \times \mathbb{R}_+ \to \mathbb{R} \cup \{+\infty\}$ defined as

$$\phi(\theta, \check{a}, \check{b}) = \begin{cases} \check{a} + 4\sigma^2 \check{b} & \text{if} \quad \theta = 0, \\ \check{a} + \frac{2\sigma^2}{\theta} \log \left(\frac{1 + \theta \check{b}}{1 - \theta \check{b}} \right) & \text{if} \quad 0 < \theta < 1/\check{b}, \\ +\infty & \text{if} \quad \theta \ge 1/\check{b} \text{ or } \theta < 0, \end{cases}$$

for $\sigma > 0$ given and fixed. Then, for any $t \geq 0$,

$$\Psi(t, \check{a}, \check{b}) := \sup_{\theta \in \mathbb{R}} \frac{\theta}{2\sigma^2} (t - \phi(\theta, \check{a}, \check{b})) = \sup_{0 \le \theta < \frac{1}{\check{b}}} \frac{\theta}{2\sigma^2} (t - \phi(\theta, \check{a}, \check{b}))$$
 (E.6)

$$= \begin{cases} \frac{t - \check{a}}{2\sigma^{2}\check{b}} \sqrt{1 - \frac{4\sigma^{2}\check{b}}{t - \check{a}}} - \log\left(\frac{1 + \sqrt{1 - \frac{4\sigma^{2}\check{b}}{t - \check{a}}}}{1 - \sqrt{1 - \frac{4\sigma^{2}\check{b}}{t - \check{a}}}}\right), & if \quad t - \check{a} \ge 4\sigma^{2}\check{b}, \\ 0, & if \quad 0 \le t - \check{a} < 4\sigma^{2}\check{b}. \end{cases}$$
(E.7)

Also, for any $\check{c} > 0$,

$$\sup_{\theta \in \mathbb{R}} \frac{\theta}{2\sigma^2} (t - \check{c}\phi(\theta, \check{a}, \check{b})) = \check{c}\Psi\left(\frac{t}{\check{c}}, \check{a}, \check{b}\right). \tag{E.8}$$

Proof. By the definition of $\phi(\theta, \check{a}, \check{b})$, we have

$$\Psi(t,\check{a},\check{b}) = \sup_{0 < \theta < \frac{1}{\check{b}}} F(\theta,t,\check{a},\check{b}) := \frac{\theta}{2\sigma^2} \left(t - \check{a} - \frac{2\sigma^2}{\theta} \log \left(\frac{1 + \theta \check{b}}{1 - \theta \check{b}} \right) \right).$$

The derivative

$$\frac{d}{d\theta}F(\theta,t,\check{a},\check{b}) = \frac{t-\check{a}}{2\sigma^2} - \frac{2\check{b}}{1-\left(\theta\check{b}\right)^2},$$

is negative for $0 \le t - a < 4\sigma^2 \check{b}$ and $0 < \theta < 1/\check{b}$ in which case we obtain

$$\Psi(t,\check{a},\check{b}) = F(0,t,\check{a},\check{b}) := \lim_{\theta \downarrow 0} F(\theta,t,\check{a},\check{b}) = 0;$$

whereas for $t-a>4\sigma^2\check{b}$, the derivative is zero at $\theta=\theta_*:=\sqrt{1-\frac{4\sigma^2\check{b}}{t-\check{a}}}/\check{b}>0$, in which case, we get $\Psi(t,\check{a},\check{b})=F(\theta_*,t,\check{a},\check{b})$ which implies (E.7) as desired. The equality (E.8) is obtained by a simple scaling argument. Indeed, by the positivity of \check{c} ,

$$\sup_{\theta \in \mathbb{R}} \frac{\theta}{2\sigma^2} (t - \check{c}\phi(\theta, \check{a}, \check{b})) = \check{c}\sup_{\theta \in \mathbb{R}} \frac{\theta}{2\sigma^2} \left(\frac{t}{\check{c}} - \phi(\theta, \check{a}, \check{b}) \right) = \check{c}\Psi \left(\frac{t}{\check{c}}, \check{a}, \check{b} \right).$$

Lemma E.4. In the setting of theorem 5.7, the lower bound (5.17) holds.

Proof. Because $a_{j+1,K}$ is non-increasing for $j \in \{0, \dots, K-1\}$, note that the function sequence

$$\hat{\phi}_{j}(\theta) := \begin{cases} \frac{2\sigma^{2}}{\theta} \log \left(\frac{\left(c_{1} + \frac{2}{L}\tilde{r}(\tilde{P})\right) + \theta a_{j+1,K}r}{\left(c_{1} + \frac{2}{L}\tilde{r}(\tilde{P})\right) - \theta a_{j+1,K}r} \right), & \text{if } 0 \leq \theta (\overline{H}_{\infty})^{2} < 1, \\ +\infty & \text{else,} \end{cases}$$

with the convention

$$\hat{\phi}_{j}(0) = \lim_{\theta \downarrow 0} \frac{2\sigma^{2}}{\theta} \log \left(\frac{\left(c_{1} + \frac{2}{L}\tilde{r}(\tilde{P})\right) + \theta a_{j+1,K}r}{\left(c_{1} + \frac{2}{L}\tilde{r}(\tilde{P})\right) - \theta a_{j+1,K}r} \right) = 4\sigma^{2} a_{j+1,K}r,$$

is non-increasing, i.e., $\hat{\phi}_{j_1}(\theta) \ge \hat{\phi}_{j_2}(\theta)$ for every θ whenever $0 \le j_1 \le j_2 \le K - 1$. Therefore, in the setting of theorem 5.1, we have

$$\hat{c}(K,\theta) \le K\left(c_1 + \frac{2}{L}\tilde{r}(\tilde{P})\right)\hat{\phi}_0(\theta),$$

and thus from theorem 5.1, we obtain

$$\overline{R}_K(\theta) \le \min \left(\check{c}_K^{(1)}\phi(\theta, \check{a}_K^{(1)}, \check{b}_K^{(1)}), \phi(\theta, \check{a}_K^{(2)}, \check{b}_K^{(2)})\right),$$

where we used $a_{1,K} = \frac{1-\lambda_+^K}{1-(p+q)}$ implied by (E.3) and the formula (A.6) with $\phi(\theta,\cdot,\cdot)$ defined as in theorem E.3. Then, using theorem E.3, we conclude that

$$\begin{split} \bar{I}_K(t) &= \sup_{0 \leq \theta < \frac{1}{(\overline{H}_\infty)^2}} \frac{\theta}{2\sigma^2} \left(t - \overline{R}_K(\theta) \right) \\ &\geq \max \left\{ \sup_{0 \leq \theta < \frac{1}{(\overline{H}_\infty)^2}} \frac{\theta}{2\sigma^2} \left(t - \check{c}_K^{(1)} \phi(\theta, \check{a}_K^{(1)}, \check{b}_K^{(1)}) \right), \\ &\qquad \qquad \sup_{0 \leq \theta < \frac{1}{(\overline{H}_\infty)^2}} \frac{\theta}{2\sigma^2} \left(t - \phi(\theta, \check{a}_K^{(2)}, \check{b}_K^{(2)}) \right) \right\} \\ &= \max \left\{ \check{c}_K^{(1)} \Psi \left(\frac{t}{\check{c}_K^{(1)}}, \check{a}_K^{(1)}, \check{b}_K^{(1)} \right), \Psi \left(t, \check{a}_K^{(2)}, \check{b}_K^{(2)} \right) \right\}. \end{split}$$

Acknowledgments This research was supported in part by the Office of Naval Research under award number N00014-24-1-2628 and N00014-24-1-2666.